

Landscape Control of Thunderstorm Development  
in Interior Alaska.

A  
Thesis

Presented to the Faculty  
of the University of Alaska Fairbanks  
in Partial Fulfillment of the Requirements  
for the Degree of

DOCTOR OF PHILOSOPHY

By

Dorte Dissing

Fairbanks, Alaska  
December 2003

UMI Number: 3119681

### INFORMATION TO USERS

The quality of this reproduction is dependent upon the quality of the copy submitted. Broken or indistinct print, colored or poor quality illustrations and photographs, print bleed-through, substandard margins, and improper alignment can adversely affect reproduction.

In the unlikely event that the author did not send a complete manuscript and there are missing pages, these will be noted. Also, if unauthorized copyright material had to be removed, a note will indicate the deletion.

**UMI**<sup>®</sup>

---

UMI Microform 3119681

Copyright 2004 by ProQuest Information and Learning Company.

All rights reserved. This microform edition is protected against unauthorized copying under Title 17, United States Code.

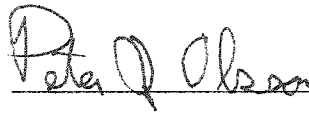
ProQuest Information and Learning Company  
300 North Zeeb Road  
P.O. Box 1346  
Ann Arbor, MI 48106-1346


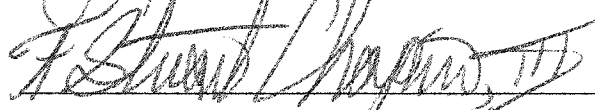
Landscape Control of Thunderstorm Development  
in Interior Alaska.

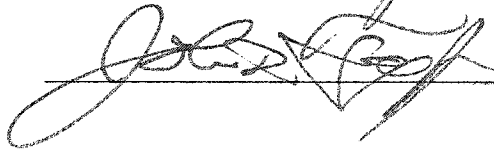
By

Dorte Dissing

RECOMMENDED:

  
\_\_\_\_\_

  
  
\_\_\_\_\_

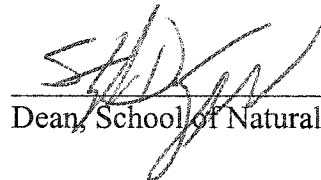
  
\_\_\_\_\_

David Vubola  
Advisory Committee Chair

  
\_\_\_\_\_

Department Head

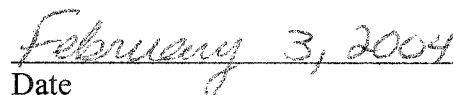
APPROVED:

  
\_\_\_\_\_

Dean, School of Natural Resources and Agricultural Sciences

  
\_\_\_\_\_

Dean, Graduate School

  
\_\_\_\_\_

Date

## Abstract

General Circulation Models suggest a future climate of warmer and possibly drier summers in the boreal forest region, which could change fire regimes in high latitudes. Thunderstorm development is a dominant factor in the continental boreal forest fire regime, through its influence as a fire starting mechanism. Global Climate Change research has identified the land-atmosphere interface as a vital area of needed research in order to improve our predictions of climate change.

This dissertation has focused on the development of thunderstorms and lightning strike activity in a boreal forest region in Interior Alaska and on how the underlying surface can influence their development. I have examined the distributions and correlations between lightning strikes, thunderclouds, thunderstorm indices (CAPE and LI), elevation, and vegetation variables in Alaska. The relationships were examined at scales ranging from the Interior region of the state to individual wildfire burn scars, and at temporal scales ranging from annual to daily. The objective is to understand the influential factors and processes responsible for thunderstorm development in Alaska, such that we may produce well-founded predictions on future thunderstorm regimes caused by a changing climate.

The scale-related studies of this dissertation show that both processes and important variables for development of thunderstorms and lightning activity vary within and between the scales. It appears that on the larger scales, the combined effects of boreal forest and elevation on increased lightning strike activity were more prevalent than at the smallest scale (local). When the scale gets too small for the boundary layer to be affected (<10km), land surface effects on lightning cannot be. My results suggest that the underlying surface (in the form of areal forest coverage and vegetation) has more of an influence on convective development on days with airmass storms than on days with synoptic storms.

## Table of Contents

Signature Page .....	i
Title Page .....	ii
Abstract .....	iii
Table of Contents .....	iv
List of Figures .....	ix
List of Tables .....	xi
Acknowledgments .....	xv
Chapter 1. General Introduction .....	1
1.1. Literature Cited .....	3
Chapter 2. Spatial Patterns of Lightning Strikes in Interior Alaska and their Relations to Elevation and Vegetation. ....	7
Abstract .....	7
2.1. Introduction .....	7
2.1.1 Objectives .....	12
2.2. Study Area .....	12
2.2.1 Alaska Thunderstorm Characteristics .....	13
2.3. Data .....	14
2.3.1 Lightning Detection and Protection Network Data .....	14
2.3.2 GIS Data .....	16
2.4. Methods .....	16
2.4.1 Regional Scale (Interior Alaska) .....	17

2.4.2 Mesoscale (Longitudinal Transects) . . . . .	17
2.4.3 Local Scale (Physiographic Regions) . . . . .	18
2.4.4 Statistical Analysis . . . . .	18
2.4.5 Proximity Study . . . . .	19
2.5. Results . . . . .	19
2.5.1 Interior Region . . . . .	19
2.5.2 Longitudinal Transects . . . . .	20
2.5.3 Physiographic Regions . . . . .	21
2.6. Discussion . . . . .	21
2.7. Conclusions . . . . .	26
2.7.1 Regional Scale (Interior Alaska) . . . . .	26
2.7.2 Mesoscale (Longitudinal Transects) . . . . .	26
2.7.3 Local Scale (Physiographic Sub-regions) . . . . .	26
2.7.4 Overall Interpretation and Suggestions for Future Work . . . . .	27
2.8. Acknowledgments . . . . .	27
2.9. Literature Cited . . . . .	28
Chapter 3. A potential mechanism for wildfire-feedback in Alaskan boreal forest: do burn scars increase lightning activity ? . . . . .	42
Abstract . . . . .	42
3.1. Introduction . . . . .	43
3.2 Objective and research approach . . . . .	46
3.3. Study area . . . . .	47
3.4. Data . . . . .	48

3.4.1. Satellite data	48
3.4.2. Burn scar data	49
3.4.3. Lightning data	49
3.4.4. Synoptic weather maps and atmospheric soundings	50
3.5. Methods	51
3.5.1. Changes in lightning activity	51
3.5.2. Radiant temperature (AVHRR and Landsat ETM)	52
3.5.3. Multiple Regressions	54
3.5.4. Cloud Imaging	54
3.6. Results	55
3.6.1. Lightning strike data (1986-99) - changes in activity over time.	55
3.6.2. Radiant temperature: AVHRR and Landsat ETM	56
3.6.3. Multiple regression	56
3.6.3.1. Scar Lightning	56
3.6.3.2. Buffer Lightning	57
3.6.4. Cloud Imaging	58
3.6.4.1. Case Study 1 (24 June 2000, 10:00AM AST).	58
3.6.4.2. Case Study 2 (29 June 1991 10:00AM AST).	59
3.7. Discussion	60
3.7.1. Study Constraints	64
3.8. Conclusions	65
3.9. Literature cited:	66
Chapter 4. Thunderstorm Activity in Interior Alaska for the Summer of 2001	93
Abstract	93

4.1. Introduction .....	94
4.1.a. Background .....	96
4.2. Study area .....	98
4.3. Methods .....	99
4.3.a. Lightning data .....	99
4.3.b. Satellite data .....	100
4.3.c. Elevation and vegetation data .....	100
4.3.d. Meteorological data .....	101
1) CAPE .....	102
2) LI .....	102
4.3.e. CAPE and LI climatology .....	102
4.3.f. Thundercloud analysis .....	103
4.3.g. Lightning strike climatology .....	104
4.3.h. Statistical analysis .....	104
4.4. Results .....	105
4.4.a. Seasonal variations in CAPE and LI .....	105
4.4.b. Seasonal variation in thundercloud occurrence .....	107
4.4.c. Seasonal variation in lightning strike distribution .....	107
4.4.d. Regression analysis .....	108
4.5. Discussion .....	110
4.6. Summary .....	114
4.7. Acknowledgments .....	116
4.8. References .....	116



Chapter 5. General Conclusions .....	143
5.1. A hierarchy of spatial scales .....	143
5.2. Assumptions .....	146
5.3. Alaska lightning strike climatology .....	148
5.4. Future under a changing climate .....	149
5.4.1. CAPE .....	150
5.4.2. Treeline expansion .....	151
5.4.3. Fire severity .....	152
5.4.4. Length of fire season .....	152
5.5. Suggestions for future work .....	153
5.6. Literature cited .....	153

## List of Figures

Figure 2.1. Interior Alaska, the area south of the Brooks Range and North of Alaska Range. . . . .	34
Figure 2.2. Vegetation distribution in Interior Alaska. . . . .	34
Figure 2.3. Physiographic regions within Interior Alaska. . . . .	35
Figure 2.4. Mean (1986-99) lightning strike density per km <sup>2</sup> divided into elevation interval (100m) for Interior Alaska (dark triangles). . . . .	35
Figure 2.5. Mean (1986-99) tundra lightning strike density (per km <sup>2</sup> ).. . . .	36
Figure 2.6. Mean (1986-99) forest lightning strike density (per km <sup>2</sup> ). . . . .	36
Figure 2.7. Mean (1986-99) lightning strike density (per km <sup>2</sup> ) as a function of the longitudinal transects.. . . .	37
Figure 3.1. The location of the Yukon Flats study region in the Eastern part of Interior Alaska. . . . .	74
Figure 3.2. Acreage of historic burns in the Yukon Flats.. . . .	74
Figure 3.3. Time series of Cloud to Ground-lightning strikes in the Yukon Flats from 1986-1999. . . . .	75
Figure 3.4. Yukon Flats study area and the 13 selected wildfire burn scars.. . . .	75
Figure 3.5. Normalized lightning strike density at the burn scars, buffers, and control areas. . . . .	76
Figure 3.6. Time series of radiant temperature derived from AVHRR (1989-99 data) and Landsat ETM (1991-2001) satellite images. . . . .	76
Figure 3.7. Cloud “chasing” image number 1. Image is from June 24 2000. . . . .	77
Figure 3.8. Terrain features and rivers within the area represented in figure 3.7 and surroundings. . . . .	77
Figure 3.9. Cloud “chasing” image number 2. Image is from June 29 1991. . . . .	78
Figure 3.10. Terrain features and rivers within the area represented in figure 3.9 and surrounding area. . . . .	78
Figure 3.11. Conceptual model of the initiation of a NCMC across a burn scar boundary in the early post- fire succession stages . . . . .	79
Figure 3.12. The wildfire burn scar mosaic of the Yukon Flats, showing our selected 13 scars along with historic scars from 1950-1999. . . . .	79

Figure 4.1. Annual lightning variation in Interior Alaska. ....	124
Figure 4.2. Atmospheric sounding shown on a skew-T diagram .....	124
Figure 4.3. The Alaska study area, including the physiographic regions used for geographical reference purposes. ....	125
Figure 4.4. The analysis was conducted for six longitudinal sectors, which follow a climatological gradient from continental to maritime .....	125
Figure 4.5. The hour of maximum lightning activity for the 2001 season in Alaska and north of the Arctic Circle (66°N) .....	126
Figure 4.6. Construction of data sets used for linear regression .....	126
Figure 4.7a and 4.7b. Seasonal spatial distribution of CAPE for the summer of 2001 .....	127
Figure 4.8a and 4.8b. Seasonal spatial distribution of LI for the summer of 2001 .....	128
Figure 4.9a and 4.9b. Seasonal spatial distribution of thundercloud occurrences for the summer of 2001 .....	129
Figure 4.10a and 4.10b. Seasonal spatial distribution of lightning strikes for the summer of 2001 .....	130
Figure 4.11a-f. Coefficient of determination ( $r^2$ ) results from the multiple regression analysis .....	131
Figure 4.12a-f. Lightning strike distribution by 6-hourly periods for the 2001 lightning season .....	132
Figure 4.13. Precipitation (a) and temperature (b) data from 8 Interior Alaska stations in 2001 .....	132
Figure 4.14a-f. Seasonal lightning strike distribution by two-week period for the six longitudinal transects. .....	133
Figure 4.15. Seasonal distribution of lightning strikes in Interior Alaska for two-week periods .....	133
Figure 5.1 Seasonal distribution of lightning strikes in Interior Alaska, two-week periods. ....	149

## List of Tables

Table 2.1. Results from forwards stepwise multiple regression, Interior region. In the dependent variable column, the letters refer to the model tested, and the numbers after the variables refer to the beta value numbers. ....	38
Table 2.2. Results from the forwards stepwise multiple regression analysis of the longitudinal transects. In the dependent variable column, the letters refer to the model tested, and the numbers after the variables refer to the beta value numbers. ....	39
Table 2.3. Main physiographic property, lightning strike density(lsd) (strikes per km <sup>2</sup> ), total for the sub-region, and separately for the three vegetation types, and mean elevation (meters) for the 17 physiographic sub-regions. ....	40
Table 2.4. Results from the forwards stepwise multiple regression analysis of the physiographic regions. In the dependent variable column, the letters refer to the model tested, and the numbers after the variables refer to the beta value numbers. ....	41
Table 3.1. Spatial and temporal resolution of AVHRR, Landsat 4, 5 TM, Landsat & ETM, and GOES 10. ....	80
Table 3.2. Independent variables, their representation and predicted correlation for multiple linear regression model runs. ....	81
Table 3.3. Typical range of values for albedo, emmisivity, and bowen ratio for deciduous, black spruce, and burn scars. It also shows that emmisivities of burned and unburned areas are similar. Sources for numbers: 1) Eugster et al. 2000; 2) Pielke and Avissar 1990; 3) Chambers and Chapin 2003; 4) Oke 1987; 5) Betts and Ball 1997; 6) Pattey et al. 1997. ....	82
Table 3.4. Normalized lightning for the period before versus the period after the fires. The numbers are shown for a) burn scars, b) buffers, and c) control areas (1-3). For the control areas we produced mean values for the four fire years of the selected scars (1988, 1990, 1991, and 1993) and showed	

similar scenarios. Note that the time periods for the averages vary based on when the fires occurred and the time series of lightning strikes (1986-99). . . . .	83
Table 3.5. Lightning strike data for any area were normalized with respect to the total lightning in the Yukon Flats region to account for inter-annual variability. A mean normalized lightning strike value from the 2-year period pre-fire (1-2before) is used as a baseline, and the changes for any 2-year-period post-fire (for example 5-6after) are reported as the difference from this baseline [in %]. The tables show the changes in normalized lightning [%] in 2-year intervals following fires and $\chi^2$ -analysis of significance of differences for (a) burn scar areas and (b) unburned (buffer) areas. As with table 3.4, we produced mean values for the control areas for the four fire years of the selected scars (1988, 1990, 1991, and 1993) and showed similar scenarios (c). We did not run $\chi^2$ -analysis of significance of differences for the control areas as this would be the same area and numbers compiled four times. . . . .	86
Table 3.6. Extracted data of lightning strike densities (lightning per unit area) within the burn scars, buffers, and control areas from Fig. 3.5. . . . .	89
Table 3.7. The AVHRR post-fire temperature differences were significantly different from the pre-fire temperatures ( $p < 0.0001$ ). The Landsat post-fire temperature differences were also significantly different from the pre-fire temperatures ( $p = 0.0016$ ) . . . . .	90
Table 3.8. Multiple linear regression results for lightning changes in burn scars. Only the variables that entered the model are included in the table. The variables “in” or “out” refers to the overlap with older burn scars in the scar and buffers, respectively. . . . .	91
Table 3.9. Multiple linear regression results for lightning changes in buffers. Only the variables that entered the model are included in the table. The variables “in” or “out” refers to the overlap with older burn scars in the scar and buffer, respectively. . . . .	92
Table 4.1 Typical values of LI (from Sturtevant, 1995 ). . . . .	134

Table 4.2. Typical CAPE values (from Sturtevant, 1995). . . . .	134
Table 4.3 Temporal coverage of meteorological data for summer 2001. . . . .	134
Table 4.4 Statistics for the two-week segment clustering algorithm of CAPE. Values of mean, standard deviation, maximum and minimum values for each clustered group. See figure 4.7a-b for spatial representation of the clustered groups. . . . .	135
Table 4.5 Statistics for the two-week segment clustering algorithm of LI. Values of mean, standard deviation, maximum and minimum values for each clustered group. See figure 4.8 for spatial representation of the clustered groups. . . . .	136
Table 4.6. Comparison of 5 intense lightning days (synoptic storms, lightning strikes > 700day-1) with 4 non-intense lightning days (air-mass storms, lightning strikes 100-200day-1). . . . .	137
Table 4.7. Predicted values of LI for set numbers of lightning strikes per 45km by 45km cell, using the results of the multiple regression analysis for two of the longitudinal zones (140 and 160), showing extreme continental and extreme maritime conditions. . . . .	137
Table 4.8. Predicted values of CAPE for set numbers of lightning strikes per 45km by 45km cell, using the results of the multiple regression analysis for two of the longitudinal zones (140 and 160), showing extreme continental and extreme maritime conditions. . . . .	138
Table 4.9. Temporal lightning strike distribution over the 2-week periods of summer season 2001. The last column represents an average temporal lightning strike distribution for Interior Alaska, based on lightning data from the 1986-99 period. . . . .	139
Table 4.10. Results of the regression analysis modeling lightning strike frequency as a function of vegetation and elevation. The table shows significant $r^2$ -values for the regression for each longitudinal zone. . . . .	140
Table 4.11. Correlations between CAPE and LI, similar to Blanchard (1998). . . . .	141
Table 4.12. Comparison ( $r^2$ -values) between the 45km by 45km cells of modeled Eta CAPE and LI and	

CAPE and LI calculated from the raw sounding data from Fairbanks and McGrath. ....	142
Table 5.1. Distribution of lightning strikes for days classified as airmass days based on two different distinction methods. ....	148

## Acknowledgments

Many people played a role in the production of this dissertation. Thanks to all of you, even if you are not specifically mentioned here.

First, thanks to my committee, Dave Verbyla, Terry Chapin, John Fox, Peter Olsson, and John Yarie. You have all been very supportive and always ready to listen and help. I greatly appreciate that.

Funding for this study was generously provided by Bonanza Creek Long Term Ecological Research site (LTER), UAF Graduate School Thesis Completion Fellowship, and a Student Competition Grant from the Center for Global Change and Arctic System Research.

To the great folks at the Fairbanks National Weather Service Forecast Office (Jim Brader, John Gallagher, Eric Stevens, Pete Adamovicz, and Ed Plumb), thank you for all the time you took to discuss concepts and data with me.

Thanks to Thor Weatherby at Alaska Fire Service, who provided information and lightning strike data, to Kevin Engle for processing of satellite imagery, to Nazila Merati at PMEL for emailing me the program to convert from NetCDF to ArcInfo format, and to Jonathan Henkelman and Bob Bolton for actually making the conversions happen.

And last, but not least, thanks to my wonderful husband, Bjarke Bennedsen for supporting me through this. Thank also to my family in Denmark, without your support this would never have happened, and to all the great people of Fairbanks.



## Chapter 1. General Introduction

General Circulation Models suggest a future climate of warmer and possibly drier summers in the boreal forest region (Ryan, 1991; IPCC, 1996) and some recent observations support these predictions (Serreze *et al.*, 2000). The predicted climatic changes would change fire regimes in high latitudes (Smith, 1992; Kasischke *et al.*, 1995; Li *et al.*, 2000). Accurate future predictions will require identification of the relationships between regional scale climate and fires (Skinner *et al.*, 1999). Thunderstorm development is a dominant factor in the continental boreal forest fire regime, through its influence as a fire starting mechanism. Global Climate Change research has identified the land-atmosphere interface as a vital area of needed research in order to improve our predictions of climate change (Harding *et al.*, 2001).

Mesoscale modeling has suggested that landscape heterogeneity and the presence of fire scars are part of a feedback mechanism that promotes convective activity (Weis and Purdom, 1974; Knowles, 1991; Weaver *et al.*, 2002). This could cause a strong, enforced fire regime as a possible result of the predicted warm, dry climate. Understanding the forcing factors that control thunderstorm development is a vital part of understanding the atmosphere / ecosystems interactions that control the boreal forest dynamics. This study has tested issues that were originally developed in modeling studies by the use of regional remote sensing and geographical information system techniques to validate the ideas.

Most books on lightning and thunderstorms in the U.S. do not even mention Alaska or include the state on their distribution maps (Court and Griffiths, 1992; Price and Rind, 1994; Schneider, 1996). However, lightning is responsible for more area burned in Alaska annually than in any other state in the U.S. (Court and Griffiths, 1992), because many lightning fires occur in remote areas, which are difficult to access, have a low priority for fire suppression and are expensive to control (Chapin *et al.*, 2003).

In Alaska, thunderstorms can be grouped into two general categories; localized air-mass and widespread synoptic (Biswas and Jayaweera, 1976). I use this classification throughout this dissertation. Air-mass thunderstorms form as isolated storms in confined areas, and result from air-mass interactions with the underlying surface. Synoptic thunderstorms are typically formed by frontal activity (Biswas and

Jayaweera, 1976). Air-mass thunderstorms are either convective or orographic, although these lifting processes often work in combination with each other (Schroeder and Buck, 1970). In Interior Alaska, low-level advection provides the moisture that fuels air-mass thunderstorms (Sullivan, 1963; Biswas, 1976), since the atmosphere is relatively dry.

Most days with recorded lightning in Alaska are due to air-mass storms formed in the absence of significant large-scale circulation (Biswas and Jayaweera, 1976; Henry, 1978). Air-mass thunderstorms start most of the lightning-caused fires in Interior Alaska (Henry, 1978).

This project focused on airmass thunderstorms in a boreal forest region and how the underlying surface might influence their development. I examined the distributions and correlations between lightning strikes, thunderclouds, thunderstorm indices, elevation, and vegetation in Alaska. I examined the relationships between these variables at spatial scales ranging from the entire Interior region of the state to individual historic wildfire burn scars and at temporal scales ranging from annual to daily. The objective was to understand the processes and factors responsible for thunderstorm development in Alaska, as a basis for well-founded predictions of future thunderstorm regimes caused by a changing climate.

Chapter two of this thesis examines the relationship between lightning strike density, vegetation and elevation at three different spatial scales: 1) Interior Alaska (~630,000km<sup>2</sup>), 2) six longitudinal transects (~100,000km<sup>2</sup>), and 3) 17 individual physiographic sub-regions (~50,000km<sup>2</sup>) within Alaska. Boreal forest and topography may influence the convective activity of Alaska's air-mass thunderstorms. I conclude this chapter with a discussion of potential processes leading to thunderstorm development based on the results, and the influence of scale on these results.

The third chapter examines for evidence of a wildfire feedback mechanism around 13 fire scars within the boreal forest of the Yukon Flats region, Interior Alaska. Satellite imagery was used to find cases of convective cloud development that could be associated with burn scars. I used variables related to elevation, slope and fire severity to learn what factors influence the lightning strike activity in the vicinity of burn scars in the years / decade following the fire. Since the development of local circulation patterns

around burn scars is more likely on airmass thunderstorm days, this chapter concentrates exclusively on these.

Chapter four examined the links between the thunderstorm potential as represented by the Convective Available Potential Energy (CAPE) and the Lifted Index, surface characteristics, as represented by boreal forest coverage and elevation, and thunderclouds and lightning strike occurrence and frequency. Using these variables, the 2001 thunderstorm season in Alaska was investigated. The goal was to examine the links between convective activity and the underlying surface at scales representing the synoptic and the local end of the mesoscale range. For this chapter, the data gets split into days classified as airmass and days classified as synoptic thunderstorm days.

Chapters 2 through 4 are stand alone manuscripts that either have been or will be submitted and / or published in peer-reviewed journals. All three papers (chapter 2-4) were coauthored with Dave Verbyla. Chapter 3 additionally had Scott Chambers and John Yarie as coauthors. John Yarie provided the initial idea for chapter 3, and Scott Chambers provided field data for and helped develop the hypotheses in that chapter, in addition to editorial guidance. All coauthors, especially Dave Verbyla, provided help and guidance, as well as assisted in editing the papers. As a first author I contributed the major part of research and writing.

### **1.1. Literature Cited**

Biswas, A.K. and Jayaweera, K.O.L.F. 1976: NOAA-3 Satellite Observations of Thunderstorms in Alaska. *Monthly Weather Review*, **104**, 292-297.

Chapin, F.S., Rupp, T.S., Starfield, A.M., DeWilde, L., Zavaleta, E.S., Fresco, N., Henkelman, J. and McGuire, A.D., 2003: Planning for resilience: modeling change in human-fire interactions in the Alaska boreal forest. *Frontiers in Ecology and the Environment*, **1** (5), 255-261.

Court, A. and Griffiths, J.F., 1992: Thunderstorm climatology. *Thunderstorm Morphology and Dynamics*, Vol.2, E. Kessler, Ed., University of Oklahoma Press, 9-40.

Harding, R.J., Gryning, S.-E., Halldin, S. and Lloyd, C.R., 2001: Progress in understanding of land surface-atmosphere exchanges at high latitudes. *Theoretical and Applied Climatology*, **50**, 5-18.

Henry, D.M., 1978: Fire occurrence using 500 mb map correlation. NOAA Technical Memorandum, NWS AR-21, 31 pp.

Intergovernmental Panel on Climate Change (IPCC), 1996: Climate Change 1995: The Science of Climate Change. Contribution of Working Group I to the Second Assessment Report of the Intergovernmental Panel on Climate Change. Houghton, J.J., Meiro Filho, L.G., Callander, B.A., Harris, N., Kattenberg, A. and Maskell, K. (Eds.). Cambridge University Press: Cambridge and New York, 572 pp.

Kasischke, E.S. Christiansen, N.L., and Stocks, 1995: Fire, Global Warming, and Carbon Balance of Boreal Forests. *Ecological Applications*, **5** (2), 437-451.

Knowles, J.B., 1993; M.S. Thesis: The influence of forest fire induced albedo differences on the generation of mesoscale circulations. Department of Atmospheric Science, Colorado State University, 86 pp.

Li, C., Flannigan, M.D. and Corns, I.G.W., 2000: Influence of potential climate change on forest landscape dynamics on West-Central Alberta. *Canadian Journal of Forest Research*, **30**, 1905-1912.

Price, C. and Rind, 1994: Modeling global lightning distributions in a general circulation model. *Monthly*

*Weather Review*, **22**, 1930-1939.

Ryan, K.C., 1991: Vegetation and Wildfire Fire: Implications of Global Climate Change. *Environmental International*, **17**, 169-178.

Schneider, S.H. (Ed.), 1996: *Encyclopedia of Climate and Weather*. Oxford University Press, 929 pp.

Schroeder, M.J. and Buch, C.C., 1970: Fire Weather. Agriculture Handbook 360, U.S.Department of Agriculture, Forest Service, May 1970.

Serreze, M.C., Walsh, J.E., Chapin, F.S., Osterkamp, T., Dyurgerov, M., Romanovsky, V., Oechel, W.C. , Morison, J, Zhang, T. and Barry, R.G., 2000: Observational evidence of recent change in the northern high-latitude environment. *Climatic Change*, **46**, 159-207.

Skinner, W.R., Stocks, B.J., Martell, D.L., Bonsal, B., and Shabbar, A., 1999: The Association Between Circulation Anomalies in the Mid-Troposphere and Area Burned by Wildland Fire in Canada. *Theoretical and Applied Climatology*, **63**, 89-105.

Smith, T.M., Leemans, R., and Shugart, H.H., 1992: Sensitivity of terrestrial carbon storage to CO<sub>2</sub>-induced climate change: comparison of four scenarios based on general circulation models. *Climatic Change*, **21**, 367-384.

Sullivan, W.G., 1963: Low-level convergence and thunderstorms in Alaska. *Monthly Weather Review*, **91**, 89-92.

Weaver, C.P., Baidya Roy, S., and Avissar, R., 2002: Sensitivity of simulated mesoscale atmospheric circulations resulting from landscape heterogeneity to aspects of model configuration. *Journal of Geophysical Research*, **107** (D20), 10.1029/2001JD000376.

Weiss, C.E. and Purdom, J.F.W., 1974: The effect on early morning cloudiness on squall line activity. *Monthly Weather Review*, **102**, 400-402.

## **Chapter 2<sup>1</sup>. Spatial Patterns of Lightning Strikes in Interior Alaska and their Relations to Elevation and Vegetation.**

### **Abstract**

The relationship between lightning strike density, vegetation and elevation was investigated at three different spatial scales: 1) Interior Alaska (~630,000km<sup>2</sup>), 2) six longitudinal transects(~100,000km<sup>2</sup>), and 3) 17 individual physiographic sub-regions (~50,000km<sup>2</sup>) within Alaska. The data consisted of 14 years (1986-1999) of observations from the Alaska Fire Service lightning strike detection network. The best explanations for the variation in lightning strike density was provided by a combination of the areal coverage of boreal forest and elevation. Each of these factors have the potential to influence the convective activity. Our study suggests that in a region that is climatically favorable for air-mass thunderstorms surface properties may enhance local lightning storm development in the boreal forest. Lightning strikes were found to occur frequently both in mountainous areas as at river flats, which is contrary to results from previous Alaskan studies.

### **2.1. Introduction**

Thunderstorms and lightning at high latitudes are typically rare compared to areas like the Midwestern U.S. Great Plains, Florida, Alberta or Saskatchewan (Orville and Silver, 1997; Nash and Johnson, 1996). Throughout Interior Alaska however, lightning is not only relatively common, but plays a large role in the structure and diversity of the dominant ecosystem, boreal forest (Kasischke and Stocks 1999). For example, in the period 1990-1996, over 2.7 million hectares burned in Interior Alaska, 93% of which burned as a result of lightning-initiated wildfires (Boles and Verbyla 2000). Lightning, combined

---

1

This paper was published under the same title exactly as presented in this chapter by Dorte Dissing and Dave Verbyla in *The Canadian Journal of Forest Research*, Vol.33, pp.770-782, 2003.

with remote, sparsely populated regions (thus less need for fire suppression) and particularly flammable fuels, cause lightning-initiated wildfires to burn 9-10 times more area annually in Alaska than in any state of the contiguous US (Court and Griffiths 1992).

There is insufficient evidence to indicate whether the predisposition to lightning activity is due to (a) the dry continental climate of Interior Alaska being particularly conducive to thunderstorms, (b) the surface-atmosphere exchange characteristics of boreal forests providing effective triggering mechanisms for thunderstorm development, or (c) a combination of the two. In Alberta and Saskatchewan, lightning-initiated fires were found to occur most frequently during periods of local and meso-scale convection (Nash and Johnson, 1996). Land-surface-atmosphere interface has been identified as a key area to reducing the uncertainties in contemporary regional and global climate models (Harding et al., 2001) and major research has been done on the topic (Pielke and Vidale, 1995; Serreze et al., 2001; Foley et al., 1994; Bonan et al., 1995).

Climate is a dominant factor controlling the distribution of vegetation. Since controls over climatic factors are exerted at many spatial scales (globally, regionally and locally), a similar scale dependence on vegetation distribution is observed (i.e. with latitude, continentality and topography) at multiple spatial scales. In Alaska for example, Viereck et al. (1992) noted the effect of continentality on the distribution of Sitka and White Spruce. Sitka spruce occur typically in maritime climates, whereas white spruce are largely restricted to continental climates (Viereck et al. 1992). At smaller scales, Van Cleve et al. (1991) relate the distribution of white and black spruce in Interior Alaska to topographically controlled microclimate.

Conversely, vegetation may also influence climate at various spatial scales. Surface albedo and roughness and the efficiency with which incident solar radiation is converted to net radiation are important factors influencing the mechanisms that vegetation can modify climate (Garrett, 1982; Bonan et al., 1995). Foley et al. (1994) modeled Holocene climate warming at the global scale and found that an expansion of the boreal forest region had a greater effect on regional climate warming than did variations in solar input associated with Milankovitch cycles. Chambers (1998) found that removal of native vegetation at the



mesoscale (10-200km; Oke 1987) was sufficient to sustain circulations at this scale. At the local scale (0.01-50km; Oke, 1987), the “oasis effect” happens when warm dry air is blown over a cool, moist oasis and gets latently cooled due to evaporation, thus modifying the local climate (Stull, 1997).

There are two possible mechanisms in which edge effects can influence convective triggering, depending upon the synoptic wind conditions. One possibility is through mesoscale circulations, another due to surface roughness effects (Vidale et al., 1997).

Elements of surface patchiness can create horizontal gradients in surface and boundary layer heat fluxes, due to differential solar radiation absorption, evaporation, transpiration, and aerodynamic transfer, which may in turn generate mesoscale circulations (Vidale et al., 1997). During periods of low synoptic wind conditions, mesoscale circulations can result in heating of the convective boundary layer and cooling aloft. When the synoptic flow becomes stronger, differential surface roughness effects are the predominant factor in convective triggering (Vidale et al., 1997). Both mesoscale circulations and surface roughness effects depend on the scales on the surface inhomogeneity. For the BOREAS study, Vidale et al. (1997) found that patches between 4 and 280km had the potential to influence the convective boundary layer development. They also found that the mesoscale circulations may have significance even on days with sustained synoptic winds.

The issue of causal relationships between vegetation and climate is still under debate. Bryson (1966) analyzed summer air-mass distributions in relation to the boreal forest extent, and found that the northern edge of the boreal forest is related to the mean summer position of the Arctic front. Pielke and Vidale (1995), using data from the BOREAS experiment, suggested that the northern boreal forest boundary influences the summer location of the Arctic front across the North American continent. Conversely, other studies argue that the position of the northern treeline represents a response to, rather than a forcing on, the summer position of the Arctic front (Serreze et al., 2001, Beringer et al., 2001). However, the authors conclude that the differences in energy partitioning between tundra and boreal forest could be significant enough to drive local-scale circulations of ecological importance (Beringer et al., 2001).

Surfaces can act to trigger convection. The triggering mechanisms are usually lifting, and could be due to orographic effects, frontal uplift, low-level convergence, or heating from below (Schroeder and Buck, 1970). Smaller convective storms generally result from an unstable atmosphere which, when triggered, results in the movement of boundary layer air to the level of free convection (Nash and Johnson, 1996).

Two factors strongly influence surface properties and thus controls over triggering potential; vegetation and physiography. Convection can be affected by albedo, sensible heat flux, surface roughness and landscape heterogeneity (Knowles 1993, Rabin et al. 1990), properties that differ among vegetation types. This is related to the differences between the surface types and the resulting partitioning of energy. In general, sensible heat fluxes are larger over boreal forest than over tundra (Chapin et al., 2000; Lafleur and Rouse 1995; Pielke and Vidale 1995; Eugster et al., 2000).

At the mesoscale, O'Neal (1996) found that deciduous forest in mountainous areas promoted more convective fluxes and associated cloud cover than the surrounding flat, non-forested areas in midwestern North America. In Southern California, local scale studies found that conifer forest and chaparral brush had higher lightning strike densities than broadleaf woodland, coastal sage shrub and herbaceous vegetation types (Wells and McKinsey 1993). However, the authors concluded that elevation (rather than vegetation) was the dominant factor influencing lightning distribution.

In mountainous areas, differential heating of mountain slopes results in upslope winds and thus low-level convergence, which is the major factor contributing to the sustained instabilities necessary for thunderstorm development (Biswas, 1976). Slope winds are produced by the local pressure gradient caused by the difference in temperature between air near the slope and air at the same elevation away from the slope (Schroeder and Buch, 1970).

The physiographic features can influence convective triggering through three factors with separate effects and mechanisms that is included in the physiographic factor: (1) elevation, (2) aspect and (3) topography. The most influential of the three factors are topography and aspect. Topography influences

convective activity through the mechanism of differential heating described above. Likewise, aspect, especially in high latitudes, can cause significant differences in surface heating, leading to possible triggering. However, both topography and aspect with scale, and has less importance at the 1km<sup>2</sup> or 100km<sup>2</sup> scale level, thus simple elevation values are often used as a proxy for topography, assuming that higher elevation represents ridges and escarpments.

At the regional scale, topography has been found to have a dominant role in influencing lightning strike activity in the conterminous United States (Wells and McKinsey 1993; Lopez and Holle 1986). Court and Griffiths (1992) showed a positive correlation between the elevation of weather stations and mean days per year of registered thunderstorms in the western United States. In Alaska, Reap (1991) found a generally positive relationship between lightning strike density and elevation below 800 meters above sea level and a negative correlation above 800 meters. At the local scale, Wells and McKinsey (1993) found a positive correlation between elevation and the density of lightning strikes for San Diego county, California.

Based upon the demonstrated links between lightning and fire in the Alaskan boreal forest (Court and Griffiths, 1992; Boles and Verbyla, 2000), and the dominant role that fire plays in the spatial and temporal heterogeneity of the species that constitute this ecosystem (Bourgeau-Chavez et al., 2000), feedback systems between climate, vegetation and wildfire may exist in this region. However, whether these observations should be mostly attributed to an atmosphere that is regionally favorable for convection, of direct effects of the landscape remains undetermined. Numerical modeling studies suggest a positive feedback system between wildfire burn scars and meso-scale circulation patterns (Knowles 1993). Through changes in surface properties and differences in heat fluxes between the burned area and the unburned areas (Chambers and Chapin in press), large burned areas may be capable of setting up "land-breeze" circulations patterns similar to land/"sea-breeze" systems. Knowles (1993) concluded that such positive feedback was potentially strong enough to result in increased convection that in turn produces lightning.

### 2.1.1 Objectives

As an independent means to verify the hypothesis that landscape effects are responsible for the prevalent convective development within Interior Alaska, the objective of this study was to analyze the relationship between lightning strike density and both vegetation and elevation, at three spatial scales: 1) Interior Alaska (630,000km<sup>2</sup>), 2) longitudinal transects (50,000-150,000km<sup>2</sup>), and 3) physiographic regions (6,000-110,000km<sup>2</sup>).

## 2.2. Study Area

Interior Alaska is bound in the north by the Brooks Range (1000-2500M ASL) and in the south by the Alaska Range (1000-6000M ASL) (figure 2.1). The topographic corridor provided by the bounding mountain ranges, and extensive Canadian continent to the east, mostly restricts the Interior to a single water source for atmospheric moisture, the Bering Sea. Maritime moisture is transported from west to east across the region by large-scale advection (Reap 1991; Sullivan 1963). As a consequence of the west-east moisture and temperature gradients, and progression from a maritime to a continental climate across the Interior, the dominant vegetation cover changes from tundra, to boreal forest with distance from the coast (figure 2). Boreal forest is the dominant vegetation type in the study region, covering 63% of the total area.

The coastal areas experience a relatively mild climate, buffered by the stable maritime influence. The central and eastern regions of the Interior experience large annual temperature extremes, with relatively hot summers (Hammond and Yarie 1996). In spite of the moisture gradient, there is generally sufficient moisture available throughout the Interior to fuel thunderstorms, either as a result of recent transport, or released from large stores in permafrost or deep organic soils that trap snow-melt. In the western Interior, where tundra is the dominant vegetation type, high surface albedo and near saturated soils result in minimal atmospheric heating and relatively stable air masses. These conditions inhibit extensive convective activity.

The coastal areas have a milder climate with more stable air masses, less surface heating, and warmer air aloft, inhibiting extensive convective activity.

There were two primary considerations that led to the choice of Interior Alaska as a study region. Firstly, it is a confined region where most thunderstorms develop without the influence of synoptic-scale weather systems (Biswas and Jayaweera 1976; Henry 1978). The infrequent intrusion of synoptic-scale weather systems is a crucial factor because large-scale forcing can confound the effects of vegetation and topography on convective activity. Secondly, almost 90% of the annual Alaskan lightning strikes are recorded in this area.

In this study, the data was examined at three different spatial scales. The Interior Alaska region represented the regional scale, the longitudinal transects the mesoscale, and the physiographic sub-regions, which some times corresponded to individual watersheds, represented the local scale (upper end). The east-west orientation of the topographic bounds to the Interior result in a good correlation of longitude with climate (from maritime to continental) across the study region. Since there was no physiographic classification of Interior Alaska at the time of this study, we divided Interior Alaska into 17 physiographic regions (figure 2.3), based primarily on physical landscape features such as relief and proximity to major rivers. The delineations were constructed for this study, and do not necessarily match existing management units. The physiographic regions are delineated after large-scale landscape forms, representing local large-scale topographical landscape changes (Yukon Flats to White Mountains, for example), to examine local semi-homogeneous sub-regions.

### **2.2.1 Alaska Thunderstorm Characteristics**

Biswas and Jayaweera (1976) used NOAA Very High Resolution Radiometer data to study the predominant patterns of thunderstorm meteorology in Alaska and found two different types; air-mass and synoptic thunderstorms. An air-mass is defined as any widespread body of air that is approximately homogeneous in its horizontal and vertical extent, particularly with reference to temperature and moisture

(Huschke 1959). Air-mass thunderstorms consisted of isolated storms in confined areas and were mainly associated with sloping topography. Synoptic thunderstorms featured widespread and intense activity over large areas, triggered by large-scale weather systems that were often tied to effects of the jet stream (Biswas and Jayaweera, 1976).

A large fraction of the annual number of lightning strikes recorded in Alaska are due to a few days of intense synoptic storms. However, most days with recorded lightning are due to air-mass storms, formed in the absence of significant large-scale circulation (Biswas and Jayaweera 1976; Henry 1978). These low lightning strike frequency air-mass thunderstorms are the starters of most of the lightning-caused fires in Interior Alaska (Henry, 1978). Under conditions conducive to air-mass thunderstorms, properties associated with topography and vegetation such as sensible heat flux and albedo, surface roughness and heterogeneity are more likely to influence convection and subsequently lightning patterns. Vidale et al., (1997) looked at development of mesoscale circulation of the BOREAS region and found the circulation to be strongest during periods of weak synoptic flow. However, the circulations were still present under stronger synoptic flow pattern (Vidale et al., 1997).

## **2.3. Data**

### **2.3.1 Lightning Detection and Protection Network Data**

The Bureau of Land Management Alaska Fire Service (AFS) operates an automated network of cloud-to-ground lightning sensors (Reap, 1991). This lightning detection network was constructed as an aid for fire suppression, since Interior Alaska has the highest potential for thunderstorms and the highest number of lightning-ignited fires in the state. The network has been in operation since 1976 and consists of 9 stations in Alaska and 3 in the Yukon Territory (figure 2.1).

The position of a lightning strike is estimated by triangulation. Consequently, a strike is only recorded only if it is detected by more than one of the sensors. Positional accuracy of estimated lightning

strike locations varies with the number of detectors sensing the strike, and with detector location geometry. For more details on how the lightning strike detection network functions, we refer to Hiscox et al. (1984). The data recorded for each detected strike includes an estimates of time, location, and the positional accuracy of the strike. Before the start of the 1995 fire season, the network underwent corrections for systematic site errors. In the U.S. National Lightning Detection Network, data are reprocessed within a few days of real-time acquisition. These reprocessed data are not subject to site errors (Cummins et al., 1998). Lightning strike data within the Interior Alaska region processed after May 1995 are assumed to have a positional accuracy of 2-4 km, at best (Global Atmospheric, Inc, written communication). The detection efficiency is assumed to be 60-80% in Interior Alaska, decreasing rapidly towards the coastal regions (Global Atmospheric, Inc, written communication). Reap (1991) using a sub-set of the same data (1987-1989) assumes the location efficiency to be on the order of 5-10km, and the detection efficiency to be 70% or better.

Studies concerning detection efficiency and location accuracy have not been done in Alaska. However, for the U.S. National Lightning Detection Network in eastern New York, Idone et al. (1998a and 1998b) did a performance evaluation comparing the network lightning data with video-derived locations of cloud-to-ground lightning and found a median location accuracy of 2-4km. The detection efficiency was found to be 67-86%. A study of detection efficiency of the British Columbia network yielded results around 50-70% (Gilbert et al., 1987).

Unless otherwise stated, all analyses conducted as part of this study have been based on a 14-year data set, which cover the 1986-99 period and can be accessed at the Bonanza Creek Long Term Ecological Research Site website (<http://www.lter.uaf.edu>). The entire 1986-99 lightning strike data set consists of 272,079 lightning strikes. The Alaska lightning detection network was during the 2000 fire season upgraded to IMPACT sensors (AFS, pers.comm.). We have chosen not to include these data in this study, due to the changed detection efficiencies and location accuracies.

The data set shown in this study uses 14 year averages or sums of individual 1km grid cells, which we have applied a smoothing scheme to in the areas around the stations, where the site error corrections otherwise would have influenced our results.

Throughout this paper, a “lightning strike” refers to a recorded cloud-to-ground lightning discharge. Nothing is inferred about whether a particular strike causes ignition.

### 2.3.2 GIS Data

Elevation at 1-km resolution was resampled from United States Geological Survey (USGS) 1:250,000 series digital elevation models (figure 2.1, USGS, 1990). We used a vegetation grid produced by Markon et al. (1995) at 1km resolution. The vegetation classes were produced using an unsupervised classification of 1991 multi-temporal AVHRR Normalized Difference Vegetation Index data (Markon et al. 1995) and can be obtained from the Alaska Field Office of the EROS Data Center. We then aggregated the vegetation classes to four major categories: boreal forest (63% of total area), tundra (21%), shrubs (12%), and other (4%) (figure 2.2). The “other” category consisted of snow, ice, water, and the 1990 and 1991 wildfire burn scars.

The data detected by the AFS lightning strike detection network was converted to a GIS point coverage, based on the location coordinates (latitude, longitude) assigned at the time of detection. For each lightning strike in the 1986-99 time period, an elevation and a vegetation class were assigned.

## 2.4. Methods

Based on previous studies (i.e. Reap, 1991; Wells and McKinsey, 1993; Lopez and Holle 1986) on the topic, we expected elevation to be the most influential factor, thus explaining the greatest variation in the lightning strike data. The hypothesis tested at all three scales was: How does elevation and %areal coverage of boreal forest influence the lightning strike density?



At the three scales the data were summarized by elevation zone in order to obtain information like %cover of boreal forest and lightning strike density and to reduce the data set from more than 630,000 cells.

#### **2.4.1 Regional Scale (Interior Alaska)**

At the regional scale, the data set contained four variables for each data point (elevation zone, %boreal forest, lightning strike density, elevation zone\*%boreal forest).

The data set was summarized by 100m elevation zone (i.e. 0-100m, 100-200m etc.) and the lightning strike density and percentage of the area covered by boreal forest were calculated for each elevation zone. The lightning strike density data were based on the sum of all lightning strikes per 1km<sup>2</sup> for the entire 14-year data set (1986-99). The data set was based on the 1km<sup>2</sup> grid cells to capture as much of the variation as possible, and the data set consisted, after summarization, of 19 data points.

For all statistical analyses, boreal forest was entered as the only vegetation factor. This was done because boreal forest is the dominant vegetation type in Interior Alaska. Combined, tundra and boreal forest cover 81 to 100% of the area at all elevations, and the relationship between the two variables is inversely proportional. Thus similar analysis with several vegetation types would have produced redundant results.

A 10km by 10km grid of tundra and forest data was used for the study of potential edge effects. This was done to minimize edge effects that a 1km by 1km patch could have produced. The mean lightning strike density for all (tundra and forest) 100km<sup>2</sup> cells was calculated and stratified into lightning density classes of 0.1 strikes/km<sup>2</sup>.

#### **2.4.2 Mesoscale (Longitudinal Transects)**

For the longitudinal transects a combined data set was made, containing 6 sets of data, one for each transect. Each data set (1 for each of the 6 transects) was summarized by 100m elevation zones (i.e. 0-100m, 100-200m etc.) and the lightning strike density was calculated for every elevation zone.

The data set was based on the 1km<sup>2</sup> grid cells to capture as much of the variation as possible, and the data set consisted, after summarization, of 86 data points.

#### 2.4.3 Local Scale (Physiographic Regions)

The physiographic regions were treated similarly to the longitudinal transects data set, and were similarly based the 1km<sup>2</sup> grid cells. The data set consisted of 161 data points.

#### 2.4.4 Statistical Analysis

The data were tested for normality, using a Chi-Square normality curve fit. The variables were found to not be significantly different from normal with p-values < 0.05.

To explore the effects of elevation and %boreal forest areal coverage on lightning strike density we developed a multiple linear regression model. To select the model with the best fit we first tested the relation between each variable and lightning strike density separately, and then applied models that included both variables as well as an interaction term. The multiple regression was done as a forwards stepwise regression, with a probability of 0.05 to enter the model and 0.1 to remove. The regressions were run 4 times at each scale, examining the following models:

- a) Lightning strike density =  $a_1 + b_1$  (elevation zone)
- b) Lightning strike density =  $a_2 + b_2$  (%boreal forest)
- c) Lightning strike density =  $a_3 + b_3$ (%boreal forest) +  $c_3$  (elevation zone)
- d) Lightning strike density =  $a_4 + b_4$  (%boreal forest) +  $c_4$  (elevation zone) +  $d_4$  (%boreal forest\*elevation zone)

The model chosen as the best fit had the highest adjusted r<sup>2</sup>-value.

### 2.4.5 Proximity Study

Previous work has focused on the difference in surface heat fluxes between boreal forest and tundra (Pielke and Vidale, 1995). We have chosen to focus the study of edge effects similarly, because the difference in the lightning strike density was greater between boreal forest and tundra than between boreal forest and shrubs. Additionally, these two vegetation types are the two most abundant within the study area, providing for a larger sample size than any other vegetation transitions. For each class the mean distance from a tundra patch to the closest boreal forest patch, regardless of size, was computed. Similarly, mean distances from boreal forest patches to tundra patches were computed.

## 2.5. Results

### 2.5.1 Interior Region

The relationship between lightning strike density and elevation was generally positive up to a maximum elevation of 1100-1200 m (figure 2.4). Above this elevation, the relationship was negative. The boreal forest covers 70-90% of the area between 200-1100m elevation. Above and below these elevations, the forest areal coverage is much less (figure 2.4). Most of the area below 200m fell within the coastal tundra / shrubs, and most of the area above 1100m was above the altitudinal limit for forest.

Tundra lightning density was greater in tundra cells close to boreal forest (figure 2.5). However, the distribution was such that only 1% of the grid cells fell in the 0-20km distance, 29% in the 20-30km distance and 70% in the greater than 30km distance to the nearest forest edge. Within the cells that are 20-30km from the forest edge, the lightning strike density varied from 0.02-0.08 strikes / km<sup>2</sup>. The similar plot for the forest pixels, testing the proximity to tundra pixels, showed similar trends with the curve shape being almost a mirror image of the curve in figure 2.5 (figure 2.6). Here the distribution showed that 53% of the pixels are in the 0-10km span, 47% in the 10-25km span, and only one pixel in the greater than 25km span.

The lightning strike density within the 10-25km distance to tundra edges varies from 0.02 to 0.17 strikes / km<sup>2</sup>.

The multiple regression at the Regional scale showed that the best model, explaining the largest percent of the variance ( $r^2 = 0.66$ ) in the lightning strike density data was model (d), which was based on the interactive effect of elevation and %boreal forest (table 2.1). The second best model ( $r^2 = 0.57$ ) was model (c), involving the effects of both elevation and %boreal forest, with boreal forest entering the model first. Elevation did not enter the model at all as a sole influence, whereas %boreal forest explains 19% of the variability in the lightning data.

### 2.5.2 Longitudinal Transects

The boreal forest had the highest lightning strike density across the climate gradient of continentality from the eastern Interior to the first of western zones (figure 2.7). In the furthest western zone, shrub and tundra vegetation had lightning strike densities that were similar to those of the forested areas. However, the forest lightning strike densities in this transect were smaller than it was in the other 5 zones. The lightning strike densities of tundra were relatively consistent across the climate gradient (figure 2.7). In the shrub vegetation the density remained at low in all but the two climatic transition zones.

Multiple regression analysis indicated that the best model was model (d), where %forest enters the model first and explains 21% of the variability in the data of the overall 57%, the inclusion of elevation-zone and elevation\*%boreal forest improve the model significantly. Both variables are positively related to lightning strike density, whereas their combined product is negatively related (table 2.2). The second best model was model (c), which explains 45% of the variation in the data. Like at the regional scale level, elevation did not enter the model at all as a sole influence.

### 2.5.3 Physiographic Regions

For each of the 17 physiographic sub-regions the mean lightning strike density for the 1986-99 time period was computed (table 2.3). The three physiographic sub-regions with the highest lightning strike densities were mountain regions, followed by 5 regions of river flats. The lowest lightning density occurred at Nulato Hills. In 65% of the sub-regions, the highest average lightning strike density was recorded in the boreal forest. In general, the highest lightning strike densities occurred in the sub-regions with the higher (mean) elevation. A definitely east-west trend can also be traced, identifying the high lightning density sub-regions as the eastern regions.

The multiple regression analysis indicated that again, the best model was model (c), where %forest enters the model first and explains 18% of the variability in the data of the overall 27%, the inclusion of elevation-zone is improving the model significantly. Again, both variables are positively related to lightning strike density (table 2.4). The second best model was model (b), using %boreal forest as the sole influential factor, explaining 18% of the lightning data variability. At this scale, elevation did enter the model as a sole influential factor, but could only account for 1.2 percent of the lightning variation.

## 2.6. Discussion

The highest lightning strike density occurred in the boreal forest vegetation at all three scales. The trend was consistent for all of Interior Alaska, and persisted along the climatological gradient of continental (eastern Interior) to maritime (western Interior) climate (figure 2.7). More than half of the physiographic regions had the highest lightning strike densities within boreal forest (table 2.3). The two regions with the lowest lightning strike density in boreal forest were Yukon Delta and Innoko Flats. Both of these regions are in the western part of the Interior, and their low strike densities may likely reflect the maritime climatic influence.

For all the examined scales, boreal forest and elevation combined were found to be positively related to lightning strike density (tables 2.1, 2.2, and 2.4). The statistical results strongly indicate that it is the interaction or combination between elevation and boreal forest which accounts for a large fraction of the variability seen in the lightning strike data.

The interactive influence of elevation and boreal forest coverage at the regional level accounted for approximately 66% of the variability in the lightning strike data. At the two smaller scales, the combined effects of elevation and boreal forest coverage explained the greater part of the variation (meso-scale:  $r^2 = 0.57$ ; local scale  $r^2 = 0.27$ ). This suggests that longitude (i.e. the degree of continentality) is a more important factor explaining the lightning strike distribution in Interior Alaska than the physiographic sub-regions, and that the longitudinal transects provide a built in climatic (continentality) control factor.

However, this also presents a surprising result in showing that for the scales shown and the data used in this study, it is the interaction or combined effects of boreal forest coverage and elevation that influences the lightning strike densities, not elevation as a factor by itself. On the contrary, this factor seems to have the least influence. An important thing to consider here are potential biases in the lightning detection network, as mentioned by Gilbert et al. (1987) from their study in BC, where the detection efficiencies were below average in mountainous regions. Also, this lightning detection network is focused on Cloud-to-ground lightning, leaving the possibility open that thunderstorms can still develop over higher terrain, but our lightning strike data will not portray this adequately. However, our main focus are the Cloud-to-ground lightning strikes, due to their role as potential fire starters.

The persistent trend of a positive relationship between lightning strike density, boreal forest and elevation represents a difference from most previous results in the field, which have concentrated on the positive relationship between elevation and lightning strike density (Wells and McKinsey 1993; Lopez and Holle 1986; Reap, 1991). For all of Interior Alaska (figure 2.4), the decrease in boreal forest areal coverage at upper elevation treeline of 1000-1200m corresponded to a decrease in lightning strike density. This could reflect the differences in energy partitioning between the boreal forest below, and the tundra above the

treeline, similar to the arguments from Pielke and Vidale (1995). A second small lightning strike density peak occurs at 1600-1700m elevation. These high lightning strike densities at the 1600-1700m elevation occurred only in the eastern Interior, and have huge standard deviations associated with them, making it hard to draw any conclusions about it.

Some discrepancies exist between the data from our analysis and the study of Reap (1991). The positive relationship between elevation and lightning strike density up to 1100-1200m that we found for all of Interior Alaska followed the general trend observed by Reap (1991), although Reap found the maximum lightning strike density to occur at 800m. This difference in the elevation at which the maximum lightning strike density occur is likely attributable to the differences in grid-cell sizes between our studies (our study: 1km grid, Reap's study: 48 km). The larger grid sizes compute mean elevation over a larger area, which would produce lower values.

Furthermore, our study focused on the Interior of the state while Reap's study area included the whole state of Alaska, thus incorporating the low elevation, low lightning strike density areas along the north and west coast and southeastern Alaska. Additionally, the lightning data on which Reap's study was based (1987-89, also AFS data) included two of the three lowest lightning-strike years in the 14 year (1986-99) data series that were used for this study.

The highest lightning strike physiographic regions were found to be in mountainous areas of eastern Alaska (table 2.3). However, the Kantishna River, Tetlin, Koyukuk, Yukon, and Tanana Flats have relatively high lightning strike densities, higher than several mountainous regions (Kuskokwim and Purcell Mountains, Nulato Hills, table 2.3). This somewhat contradicts the conclusions of Reap (1991) and Biswas and Jayaweera (1976), who found that no river flats, with the exception of the Tanana Flats, showed any significant thunderstorm development or lightning strike frequencies. Both of these studies were based on relatively few years of data (3, and 1, respectively), and at least 2 of these years were very low lightning-strike years. Possibly this discrepancy is explainable if low-lightning years also can be assumed to have

fewer air-mass storms and thus the influence of elevation could be of greater importance than that of boreal forest, therefore resulting in a higher lightning strike density over higher terrain.

One question that arises from our results is: can the boreal forest itself enhance thunderstorm development or does it simply occur in a climatic region that sustains convective activity? The most likely explanation is a combination of both: in a region already favorable for convective activity, the differential heating due to landscape heterogeneity and therefore variation in surface energy partitioning over the boreal forest provide the triggering mechanism to enhance thunderstorm development. Lynch et al. (2001) suggest from their studies of correlations between vegetation, topography and the Arctic frontal zone, that although vegetation contrasts were found to be insufficient for inducing frontal activity, it could and would contribute to topographically generated preferred frontal zones. These findings supports the idea of convective triggering being provided by a combined effect of the vegetation and topography, although our statistical results suggests that the relative importance of the two factors are that of vegetation (boreal forest) being the most important.

Our proximity study showed that most of the higher lightning strike densities, both within pixels classified as tundra and as boreal forest, fall within the 10-15km range of the edges of the vegetation patches. However, a large variation in lightning strike density exists within this zone (figures 2.5 and 2.6). It is beyond the scope of this paper to examine the meteorological conditions associated with these results, although this information would provide some important understanding of the processes taking place. Speculations based on the studies of Vidale et al. (1997), Knowles (1993), Chambers (1998) would suggest that the orientation of a mesoscale circulation across a boreal forest / tundra boundary as the one examined here would be from the cool surface air towards the warmer surface air. The effects of theses circulations would be strongest around the edges of a developed circulation cell, which is dependent on the size of the forest patches, but likely within 10 times the convective boundary layer depth (~ 2km), so 5-20km, approximately. This coincides with the distance within which we see the higher lightning strike densities on figures 2.5 and 2.6. However, this phenomenon is observed on both sides of the vegetation boundaries,



whereas, according to above reasoning, the effects would be expectable on the forest side of the edge. Wind patterns could influence the location of these effects.

Knowles (1993) modeling study suggested that under favorable meteorological conditions wildfire burn scars were capable of enhancing convective activity of sufficient strength to produce lightning. Combining the conclusions of Knowles (1993) and Pielke and Vidale (1995), perhaps the boreal forest, through relatively high sensible heat fluxes, can enhance convective activity if an already unstable atmospheric environment is present. Beringer *et al.* (2001) suggest that although surface heating differences due to energy partitioning between the boreal forest and tundra are unlikely determinants of the summer position of the Arctic front, they still may be sufficient to support local-scale circulations.

If boreal forest is capable of enhancing thunderstorm development then a feedback loop which creates more fires might exist. An increased frequency of wildfires, despite a cooler, moister climate in the boreal forest ecosystem following the appearance of black spruce (Hu *et al.* 1993; Lynch *et al.* in press) could reflect an increased availability of flammable fuels. The increased fire frequency could also be due to the energy partitioning in a black spruce forest, resulting in higher sensible heat fluxes than over other vegetation types, thus providing triggering mechanisms for thunderstorm development (Chambers and Chapin in press).

Such a feedback is less likely to develop in the atmospherically more stable (for example maritime) environment, because stable conditions would suppress the circulation centers induced by the heating differences between the wildfire burn scars and the surrounding unburned surface, thus resulting in fewer thunderstorms than the unstable environment (Knowles 1993). This explains our finding of a weaker correlation between boreal forest and lightning strike density in the maritime western longitudinal transects. The maritime climate is also cooler, providing much less heating differences to induce circulations.

## 2.7. Conclusions

We examined the interrelationships between vegetation, elevation and lightning strike density for a 14 year time series at three spatial scales.

### 2.7.1 Regional Scale (Interior Alaska)

- \* Lightning strike density was consistently higher in boreal forest than in tundra or shrub vegetation.
- \* The interaction between increasing boreal forest area and elevation is correlated with increasing lightning strike density, providing explanation for 66% of the variation in the lightning strike densities at this scale.
- \* Most of the 10km by 10km pixels with the highest lightning strike densities falls within 10-25km on either side of the boundary between boreal forest and tundra.

### 2.7.2 Mesoscale (Longitudinal Transects)

- \* Consistent with the observed trend for the regional scale the mesoscale showed higher lightning strike densities within the boreal forest, followed by shrubs and tundra. The effect is more pronounced in the continental than in the maritime climate.
- \* The combination of boreal forest areal coverage, elevation, and a build-in continentality factor provides explanation for ~57% of the variation in the lightning strike density. The boreal forest areal coverage carries the highest weight in the model.

### 2.7.3 Local Scale (Physiographic Sub-regions)

- \* More than half of the sub-regions showed the highest lightning strike densities within boreal forest.
- \* Elevation and %boreal forest do not provide as good an explanation for the variability in lightning strike data as at the mesoscale (~27%). However, the best model was still the combined model of elevation and boreal forest areal coverage.

#### 2.7.4 Overall Interpretation and Suggestions for Future Work

Boreal forest, due to its high sensible heat fluxes, may enhance convective activity of *air-mass* thunderstorms. Another explanation is that the boreal forest biome exists in a climatic region that sustains the convective activity. Our data suggest that both explanations are important. Our statistical analysis indicates that it is the interaction or combination between elevation, boreal forest and a climatic (continental) factor, which influences the variation in lightning strike density. This has strong implications for future climate change scenarios, where lots of speculations about extension of the boreal forest and treeline have been made.

The combined effects of boreal forest and elevation on increased lightning strike activity was found in the larger scales (regional and mesoscale), but was less prevalent at the smallest scale (local). The zones at the local scale that were examined were delineated based on physiographic features such as proximity to major rivers, or mountainous areas. Possibly not all of these delineations were appropriate for showing the above effects, thus we only saw trends similar to the larger scales at some zones, whereas the statistical analysis, incorporating all the zones, did not show as strong a pattern. Likewise, the proximity study did not portray a consistent pattern at the patch scale (regardless of size).

Several factors have not been included in this study: patch sizes (and shapes), effects of wildfire burn scars, topography, and aspect and meteorology. All of these could be likely candidates for explaining some of the results from this study.

### 2.8. Acknowledgments

This research was funded by the National Science Foundation Bonanza Creek Long Term Ecological Research Project. We thank Scott Chambers, Terry Chapin, Merav Ben-David, John Fox, Carolyn Kremers, Peter Olsson, T. Scott Rupp, David Valentine, and the anonymous reviewers for helping us improve the manuscript. We also wish to thank Thor Weatherby, Alaska Fire Service for providing information and data from the lightning strike detection network.

## 2.9. Literature Cited

Biswas, A.K. 1976. Climatology of Thunderstorms in Alaska. M.S. thesis, University of Alaska Fairbanks. 75 p.

Biswas, A.K., and Jayaweera, K.O.L.F. 1976 .NOAA-3 Satellite Observations of Thunderstorms in Alaska. *Monthly Weather Review* **104**: 292-297.

Beringer, J., Tapper, N.J., McHugh, I., Chapin III, F.S., Lynch, A.H., Serreze, M.C., and Slater, A. 2001. Impact of Arctic treeline on synoptic climate. *Geophysical Research Letters*, **28**: 4247-4250.

Boles, S.H., and Verbyla, D.L. 2000. Comparison of Three AVHRR-Based Fire Detection Algorithms for Interior Alaska. *Remote Sensing of Environment* **72**: 1-16.

Bonan, G.B., Chapin, F.S. and Thompson, S.L. 1995. Boreal Forest and Tundra Ecosystems as Components of the Climate System. *Climatic Change*, **29**: 145-167.

Bryson, R.A.1966. Air masses, streamlines, and the boreal forest. *Geographical Bulletin* **8**: 228-269.

Bourgeau-Chavez, L.L., Alexander, M.E., Stocks, B.J., Kasischke, E.S. 2000. Distribution of forest ecosystems and the role of fire in the North American boreal region. *In Fire, Climate Change, and Carbon Cycling in the Boreal Forest. Edited by E.S. Kasischke, and B.J. Stocks, pp. 111-131, Ecological Studies* 138, Springer Verlag

Chambers, S.D. 1998. Short- and Long-Term Effects of Clearing Native Vegetation for Agricultural Purposes. Ph.D. Thesis. Flinders Institute for Atmospheric and Marine Sciences, The Flinders University of South Australia, GPO Box 2100, Adelaide 5001, Australia. 166 p.

Chambers SD and Chapin FS III. Fire effects on surface-atmosphere energy exchange in Alaskan black spruce ecosystems: implications for feedbacks to regional climate. Accepted for special FROSTFIRE edition of the Journal of Geophysical Research.

Chapin III, F.S., Eugster, W., McFadden, J.P., Lynch, A.H., and Walker, D.A. 2000. Summer Differences among Arctic Ecosystems in Regional Climate Forcing. *Journal of Climate* **13**: 2002–2010.

Court, A. and Griffiths, J.F. 1992. Thunderstorm climatology. *In* Thunderstorm Morphology and Dynamics. Edited by E. Kessler. University of Oklahoma Press. pp. 9-40.

Cummins, K.L., Murphy, M.J., Bardo, E.A., Hiscox, W.L., Pyle, R.B., and Pifer, A.E. 1998. A Combined TOA/MDF Technology Upgrade of the U.S. National Lightning Detection Network. *Journal of Geophysical Research*, **103D**: 9035-9044.

Eugster W., Rouse W.R., Pielke R.A., McFadden J.P., Baldocchi D.D., Kittel T.G.F., Chapin F.S. III, Liston G.L., Vidale P.L., Vaganov E., and Chambers S.D. 2000. Land-atmosphere energy exchange in Arctic tundra and boreal forest: available data and feedbacks to climate. *Global Change Biology*, **6** (suppl.1): 84-115.

Foley, J.A., Kutzbach, J.E., Coe, M.T., and Levis, S. 1994. Feedbacks between climate and boreal forests during the Holocene epoch. *Nature*, **371**: 52-54.

Gilbert, D.E., Johnson, B.R., and Zala, C. 1987. A reliability study of the lightning locating network in British Columbia. *Canadian Journal of Forest Research*, 17: 1060-1065.

Global Atmospheric, Inc. Written comm. from Global Atmospheric to AFS containing estimated lightning strike detection efficiency and location accuracy of the ALDF and IMPACT sensors. Letters dated May 18, and September 7, 1995.

Hammond, T. and Yarie, J. 1996. Spatial prediction of climatic state factor regions in Alaska. *Ecoscience* 3: 490-501.

Henry, D.M. 1978. Fire occurrence using 500mb map correlation. NOAA Technical Memorandum, NWS AR-21, 31 pp.

Hiscox, W.L., Krider E.P., Pifer, A.E., and Uman, M.A. 1984. A systematic method for identifying and correcting "site errors" in a network of magnetic directions finders. International Aerospace and Ground Conference on Lightning and Static Electricity, Orlando, Florida, June 26-18.

Hu, F.S., Brubaker, L.B., and Anderson, P.E. 1993. A 12000 year record of vegetation change and soil development from Wien Lake, central Alaska. *Canadian Journal of Botany*. 71: 1133-1142.

Huschke, R.E. 1959. Glossary of Meteorology. American Meteorological Society, Boston. 638 p.

Idone, V.P., Davis, D.A., Moore, P.K., Wang, Y., Henderson, R.W., Ries, M., and Jamason, P.F. 1998a. Performance evaluation of the U.S. National Lightning Detection Network in eastern New York. 1. Detection efficiency. *Journal of Geophysical Research*, 103D: 9045-9055.

Idone, V.P., Davis, D.A., Moore, P.K., Wang, Y., Henderson, R.W., Ries, M., and Jamason, P.F. 1998b. Performance evaluation of the U.S. National Lightning Detection Network in eastern New York. 2. Location accuracy. *Journal of Geophysical Research*, **103D**: 9057-9069.

Kasischke, F.S. and Stocks, B.J.(editors) 1999. *Fire, Climate Change, and Carbon Cycling in the Boreal Forest*. Springer Verlag. 464 p.

Kessler, E. (editor)1992. *Thunderstorm Morphology and Dynamics*, Vol. 2. 2<sup>nd</sup> Edition. University of Oklahoma Press, Norman, Oklahoma. 411 p.

Knowles, Captain J.B. 1993. M.S. Thesis. The influence of forest fire induced albedo differences on the generation of mesoscale circulations. Department of Atmospheric Science, Colorado State University, 86 p.

Lafleur, P.M. and Rouse, W.R 1995. Energy partitioning at treeline forest and tundra sites and its sensitivity to climate change. *Atmosphere-Ocean*. **33**: 121-133.

Lopez, R.E. and Holle, R.L. 1986. Diurnal and spatial variability of lightning activity in Northeastern Colorado and Central Florida during the summer. *Monthly Weather Review*. **114**: 1288-1312.

Lynch, J.A., Clark, J.S., Bigelow, N.H., Edwards, M.E. and Finney, B.P. In press. Geographic and temporal variation in fire history in boreal ecosystems of Alaska. *Journal of Geophysical Research*.

Lynch, A.H., Slater, A.G., and Serreze, M. 2001. The Alaskan frontal zone: forcing by orography, coastal contrast and the boreal forest. *Journal of Climate*, **14**: 4351-4362

- Markon, C.J., Fleming, M.D., and Binnian, E.F. 1995. Characteristics of vegetation phenology over the Alaskan landscape using AVHRR time series data. *Polar Record*. **31**: 179-191.
- Nash, C.H. and Johnson, E.A. 1996. Synoptic climatology of lightning-caused forest fires in subalpine and boreal forests. *Canadian Journal of Forest Research*. **26**: 1859-1874.
- Oke, T.R. 1987. *Boundary Layer Climates*, second edition. Routledge, 435 p.
- O'Neal, M. 1996. Interactions between land cover and convective cloud cover over Midwestern North America detected from GOES satellite data. *International Journal of Remote Sensing*. **17**: 1149-1181.
- Orville, R.E. and Silver, A.C. 1997. Lightning Ground Flash Density in the Contiguous United States: 1992-95. *Monthly Weather Review*. **125**: 631-638.
- Pielke, R.A. and Vidale, P.L. 1995. The Boreal Forest and the Polar Front. *Journal of Geophysical Research*. **100D**: 25,755-25,758.
- Rabin, R.M., Stadler, S., Wetzel, P.J., Stensrud, D.J., and Gregory, M. 1990. Observed effects of landscape variability on convective clouds. *Bulletin of American Meteorological Association*. **71**: 272-280.
- Reap, R.M. 1991. Climatological Characteristics and Objective Prediction of Thunderstorms in Alaska. *Weather and Forecasting*. **6**: 309-319.
- Serreze, M.C., Lynch, A.H., and Clark, M.P. 2001. The Arctic Frontal Zone as seen in the NCEP-NCAR Reanalysis. *Journal of Climate* **14**: 1550-1567.



Stull, R.B. 1997. *An Introduction to Boundary Layer Meteorology*. Kluwer Academic Publishers, Dordrecht, The Netherlands. 670 p.

Sullivan, W.G. 1963. Low-level convergence and thunderstorms in Alaska. *Monthly Weather Review*. **91**: 89-92.

Van Cleve, K., Chapin, F.S.III, Dyrness, C.T. and Vierick, L.A. 1991. Element cycling in taiga forests: State-factor control. *Bioscience*. **41**: 78-88.

Vidale, P.L., Pielke, Sr., R.A., Steyaert, L.T., and Barr, A. 1997: Case study modeling of turbulence and mesoscale fluxes over the BOREAS region. *Journal of geophysical Research*, **102D**: 29,167-29,188.

Viereck, L. A., C. T. Dyrness, A. R. Batten, and K. J. Wenzlick. 1992. *The Alaskan Vegetation Classification*. USDA Forest Service General Technical Report PNW-GTR-286. 278 p.

Wells, M.L. and McKinsey, D.E. 1993. The Spatial and Temporal Distribution of Lightning Strikes in San Diego County, California. *GIS / LIS Proceedings*, 2-4 Nov., Minneapolis Convention Center. **2**: 1993.

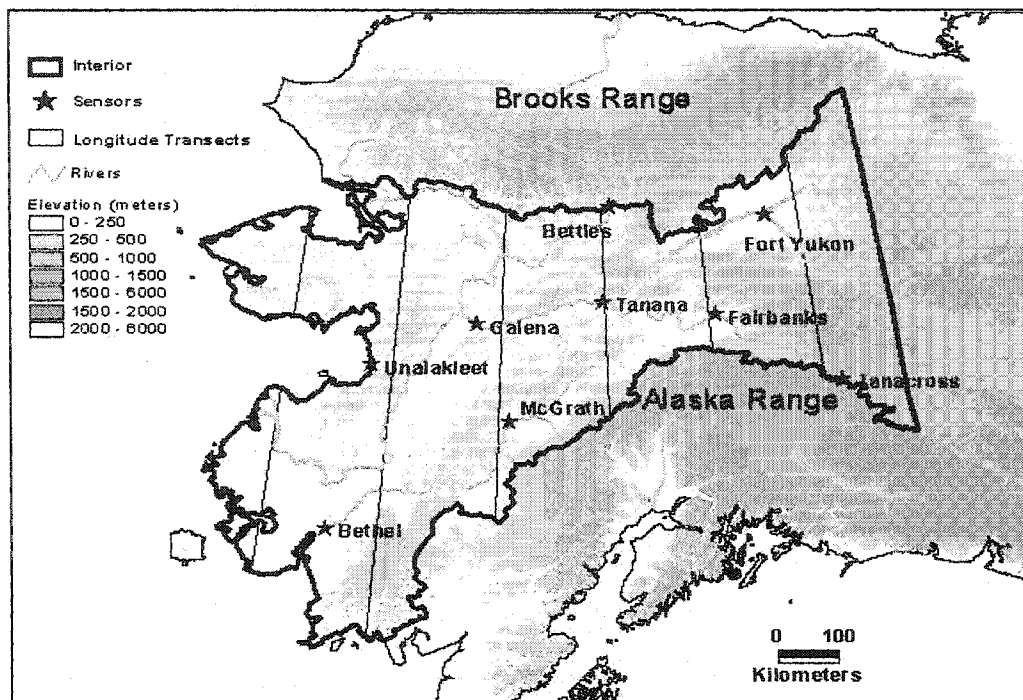


Figure 2.1. Interior Alaska (-), the area south of the Brooks Range and North of Alaska Range. Bound by the Alaska-Canada border in the East ( $141^{\circ}\text{W}$ ), and the Bering Sea in the west. 9 Lightning detection network sensors are shown ( $\star$ ). The meridians (-) mark the boundaries for the longitudinal transects.

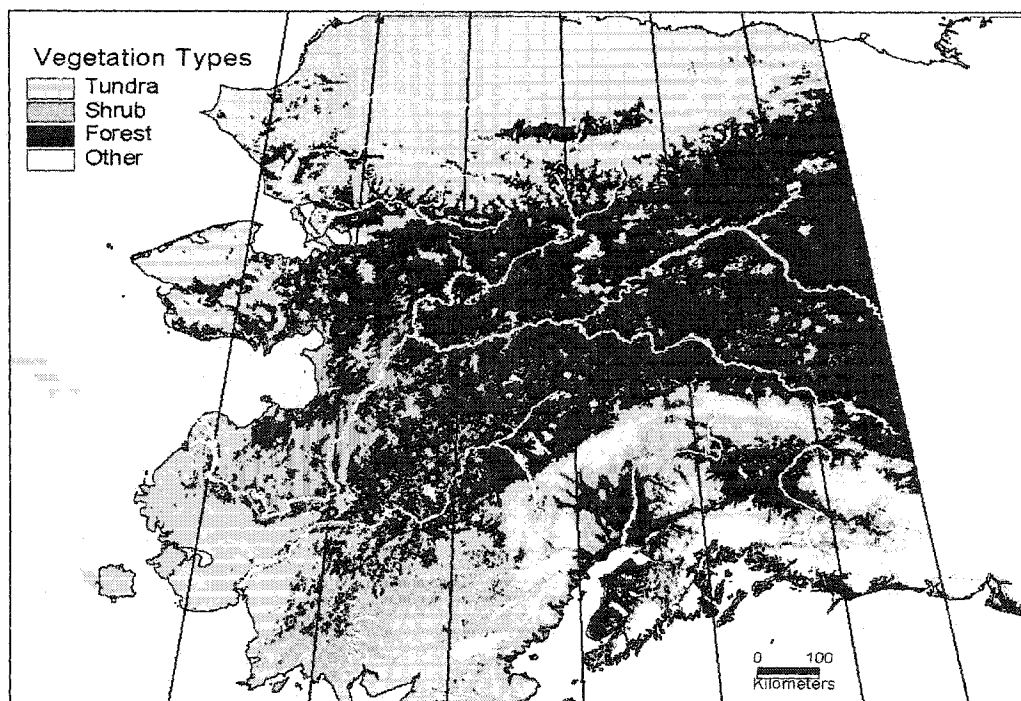


Figure 2.2. Vegetation distribution in Interior Alaska, based on vegetation classes produced by unsupervised classification of 1991 multi-temporal AVHRR Normalized Difference Vegetation Index data (Markon *et al.* 1995). Vegetation classes are here simplified into 4 broad categories.

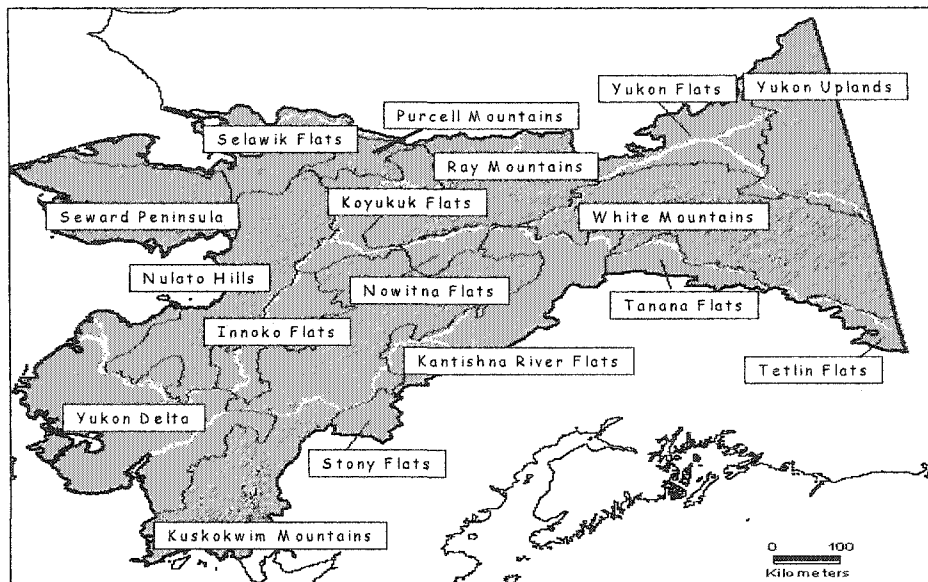


Figure 2.3. Physiographic regions within Interior Alaska.

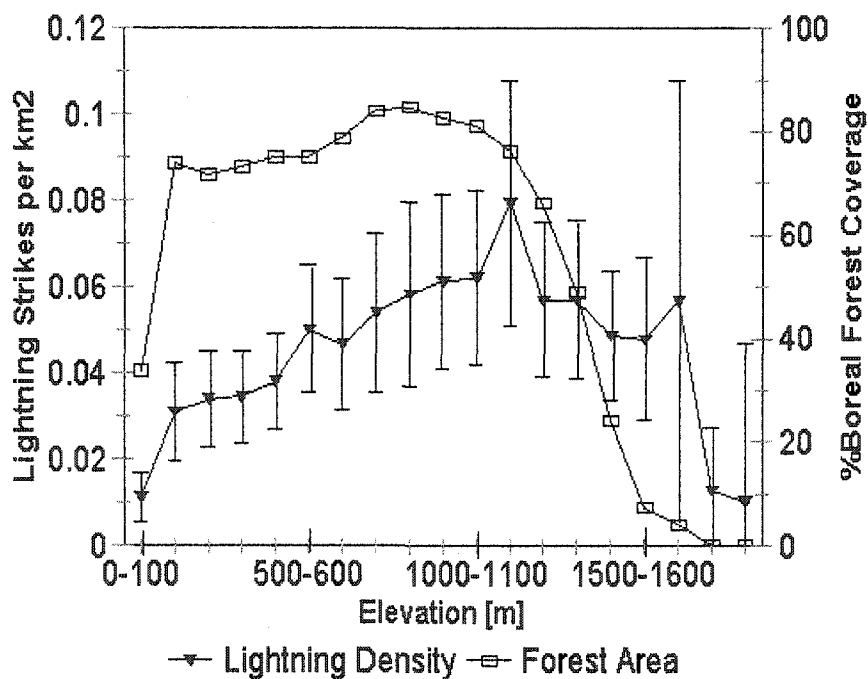


Figure 2.4. Mean (1986-99) lightning strike density per km<sup>2</sup> divided into elevation interval (100m) for Interior Alaska (dark triangles). Horizontal lines represent  $\pm$ one standard deviation. The open squares represent the percent of the total area within each elevation zone covered by boreal forest.

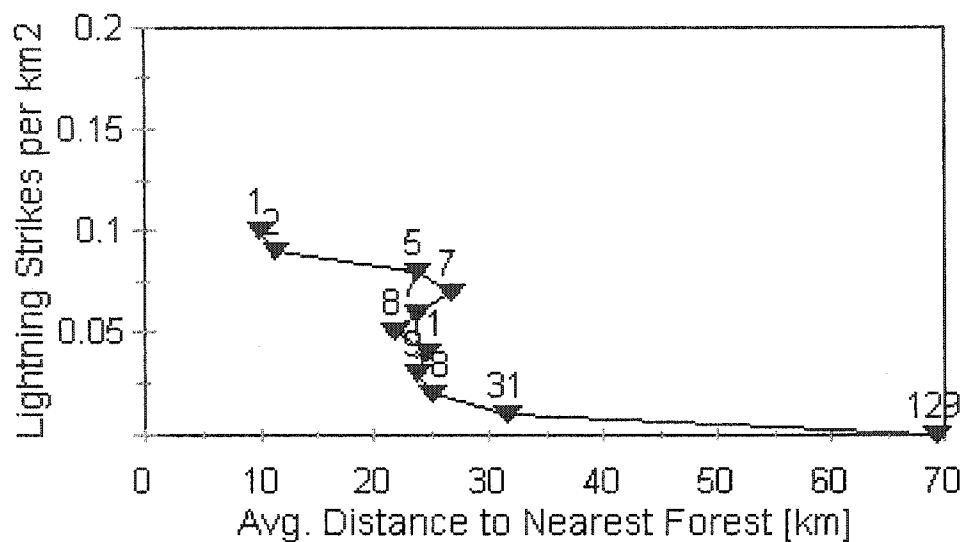


Figure 2.5. Mean (1986-99) tundra lightning strike density (per km<sup>2</sup>) as a function of the mean distance from the tundra 10km by 10km patches to the nearest forest patch of 10km by 10km or greater size. Numbers of grid blocks per lightning strike density class are included next to the markers.

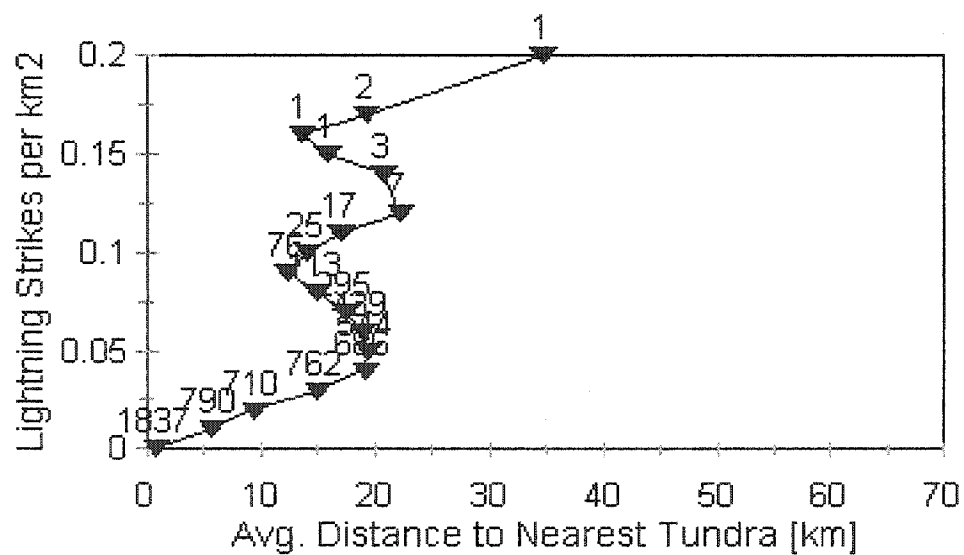


Figure 2.6. Mean (1986-99) forest lightning strike density (per km<sup>2</sup>) as a function of the mean distance from the forest 10km by 10km patches to the nearest tundra patch of 10km by 10km or greater size. Numbers of grid blocks per lightning strike density class are included next to the markers.

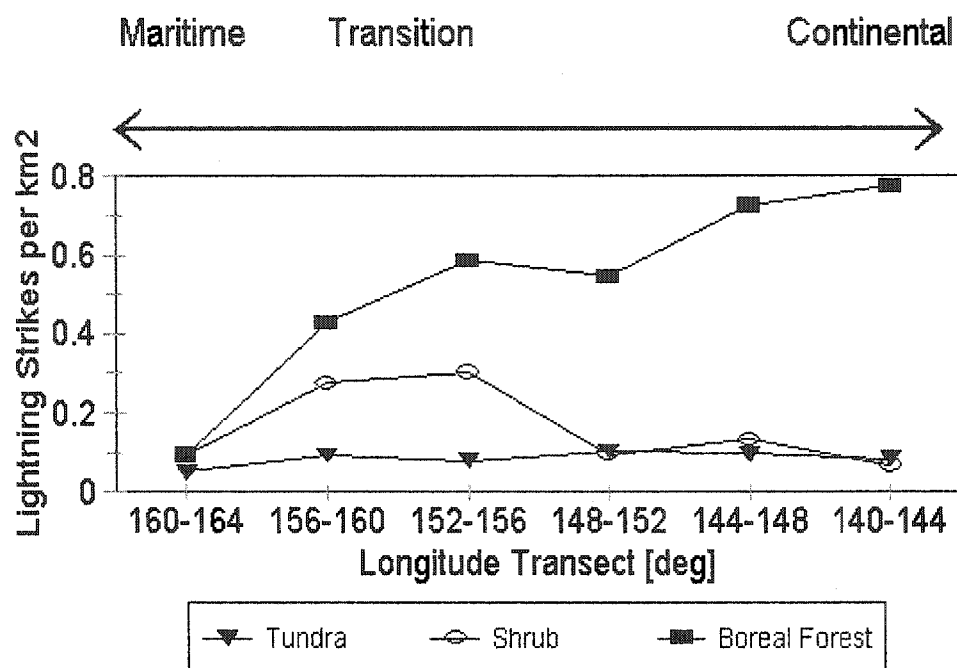


Figure 2.7. Mean (1986-99) lightning strike density (per km<sup>2</sup>) as a function of the longitudinal transects, divided into the three vegetation classes tundra, shrub and boreal forest. The right side of the figure is the eastern part of the Interior Alaska, the left side the western. The climatic zone is marked above the chart panel.

Table 2.1. Results from forwards stepwise multiple regression, Interior region. In the dependent variable column, the letters refer to the model tested, and the numbers after the variables refer to the beta value numbers.

dependent variable	p-value	r <sup>2</sup> (adj)	beta (1)	beta (2)	beta (3)	intercept	std.err. estimate	std.err. intercept	n	F
(a) elevation	The variable did not enter the model at all									
(b)%boreal forest	0.002	0.19	0.485			40.84	23.62	10.97	19	5.23
(c) elev. (1) & %bf (2)	0.0021	0.57	0.839	1.05		-411.17	17.19	112.38	19	13.09
(d) elev. (1) & %bf (2) elev*%bf(3)	< 0.0001	0.66			0.824	35	15.29	5.79	19	30.07

Table 2.2. Results from the forwards stepwise multiple regression analysis of the longitudinal transects. In the dependent variable column, the letters refer to the model tested, and the numbers after the variables refer to the beta value numbers.

dependent variable	p-value	r <sup>2</sup> (adj)	beta (1)	beta (2)	beta (3)	inter-cept	std.err. estimate	std.err. inter-cept	n	F
(a) elevation	The variable did not enter the model at all									
(b) %boreal forest	< 0.0001	0.21	0.466			31.20	31.59	6.50	86	23.27
(c) elev. (1) & %bf(2)	< 0.0113	0.45	0.639	0.856		-28.74	26.29	11.10	86	35.94
(d) elev. (1) & %bf (2) elev*%bf (3)	< 0.0001	0.57	0.669	0.971	-0.16	-51.46	21.20	0.11	2879853	1287967

Table 2.3. Main physiographic property, lightning strike density (lsd) (strikes per km<sup>2</sup>), total for the sub-region, and separately for the three vegetation types, and mean elevation (meters) for the 17 physiographic sub-regions.

Region	Physiography	Mean Elev.	Total Lsd.	Tundra	Shrub	Forest
White Mountains	mountains	647	8.0	8.8	8.6	8.8
Ray Mountains	mountains	365	5.0	5.5	4.4	5.6
Yukon Uplands	mountains	443	5.0	3.9	7.3	5.4
Kantishna River Flats	flats	277	4.4	6.0	3.3	4.8
Tetlin Flats	flats	666	3.8	0.6	0.3	4.6
Koyukuk Flats	flats	105	3.5	2.8	5.2	3.7
Yukon Flats	flats	155	3.1	0.3	0.1	8.0
Tanana Flats	flats	325	2.9	0.1	3.4	4.8
Kuskokwim Mountains	mountains	293	2.8	1.3	2.1	5.1
Nowitna Flats	flats	155	2.7	0.5	4.0	5.5
Selawik Flats	flats	123	1.6	0.8	0.0	1.4
Yukon Delta	flats	48	1.1	1.2	1.2	0.9
Stony Flats	flats	136	1.0	1.3	1.0	1.5
Purcell Mountains	mountains	298	0.9	1.3	0.0	2.0
Innoko Flats	flats	100	0.6	0.6	0.6	0.5
Seward Peninsula	mountains / flats	208	0.5	0.4	0.6	0.7
Nulato Hills	mountains	277	0.3	0.1	0.5	0.4



Table 2.4. Results from the forwards stepwise multiple regression analysis of the physiographic regions. In the dependent variable column, the letters refer to the model tested, and the numbers after the variables refer to the beta value numbers.

dependent variable	p-value	r2 (adj)	beta (1)	beta (2)	beta (3)	inter-cept	std.err. estimate	std.err. inter-cept	n	F
(a) elevation	< 0.0001	0.012	0.135			38.00	30.60	4.29	161	2.94
(b) %boreal forest	< 0.0001	0.18	0.428			22.00	27.91	4.30	161	35.63
(c) elev. (1) & %bf(2)	1E-06	0.27	0.334	0.549		0.67	26.91	6.15	161	30.7
(d) elev. (1) & %bf (2) elev*%bf (3)	< 0.0001	0.12	0.846	0.799	-0.84	-34.69	28.62	0.11	4893601	230840

## **Chapter 3<sup>2</sup>. A potential mechanism for wildfire-feedback in Alaskan boreal forest: do burn scars increase lightning activity ?**

### **Abstract**

Lightning-induced wildfires are responsible for 80-90% of the area burned annually in Alaskan boreal forests. How random is this important modification of the Alaskan landscape? We looked for evidence of a wildfire feedback mechanism around 13 fire scars within the boreal forest of the Yukon Flats region, Interior Alaska. We found that in general, relative lightning activity decreased in the burned areas as well as the control areas following a fire. In some areas, however, lightning activity increased in the surrounding unburned areas. These changes in lightning strike activity were tied more closely to vegetation parameters describing fire severity than to environmental variables such as slope and elevation. We found two satellite images where convective cloud development could be associated with burn scars. In one of these cases, thunderstorm and lightning activity developed in the immediate area, suggesting a possible burn-scar-induced circulation. In general, the Yukon Flats is a vegetation mosaic heavily influenced by areas with an history of active wildfire, making it difficult to demonstrate a feedback mechanism conclusively.

---

2

This paper was prepared as a manuscript under the same title by Dorte Dissing, Scott Chambers, Dave Verbyla and John Yarie.

### 3.1. Introduction

Wildfires are a dominant disturbance mechanism in boreal forests (Vierick 1973; Yarie 1981; Kasischke et al. 1995). Fire frequency and severity influence the speed and trajectory of vegetative succession and fuel accumulation (Bourgeau-Chavez et al. 2000), and thus directly impact the regional carbon budget (Campbell and Flannigan 2000). Since the boreal forest is the second largest terrestrial biome (Whitaker 1975), containing approximately 40% of the global reactive soil carbon (McGuire et al. 1995), changes in the fire regime of boreal forests could have global significance.

Over the past decade an average of  $3.02 \times 10^6$  ha / year of North American boreal forests have burned (Kasischke et al. 1995). In Alaska, 43% of fires that occurred during the period 1966-75 were started by lightning, with these fires accounting for 82% of the total area burned (Court and Griffiths 1992). Between 1990 and 1996, lightning-caused fires were responsible for 93% of the total area burned (Boles and Verbyla 2000).

Global Climate Models predict that the largest climatic changes will occur at high latitudes (IPCC 1996), and some observations support these predictions (Serreze et al. 2000). This has led to speculation of increased fire frequency (Kasischke et al. 1995; Li et al. 2000). An increased frequency of wildfires in the boreal forest during the Holocene followed the appearance of black spruce on the landscape (Hu *et al.* 1993; Lynch *et al.* 2003) reflecting increased availability of flammable fuels. This vegetation change might also have enhanced the development of thunderstorms at the local scales (Chapter 2). However, changes in the wildfire ignition process - the thunderstorm have never been suggested as a component of vegetation-induced changes in the fire regime during the Holocene<sup>3</sup>.

In Alaska, thunderstorms can be grouped into two general categories; localized and widespread. Localized (*air-mass*) thunderstorms result from interactions between an air-mass<sup>3</sup> and surface

---

<sup>3</sup> An air-mass is defined as any widespread body of air that is approximately homogeneous in its horizontal extent, particularly with reference to temperature and moisture distribution; in addition, the vertical temperature and moisture variations are approximately the same over its horizontal extent (Huschke, 1959).

characteristics, producing isolated storms in confined areas. The more widespread (*synoptic*) thunderstorms are typically formed by frontal activity (Biswas and Jayaweera 1976).

In general, thunderstorm formation requires a conditionally unstable airmass, sufficient moisture<sup>4</sup> in the atmospheric boundary layer (<3km), and a triggering mechanism to set off the convective activity (Henderson-Sellers and Robinson 1986; Schneider 1996; Huntrieser et al. 1997). Moisture provides energy to the thunderstorm through the release of latent heat as convection brings the air to its lifting condensation level (Grice and Comisky 1976; Schneider 1996). A triggering mechanism acts to release the instability and is usually associated with either (i) surface heterogeneities (in unstable or convective conditions), (ii) lifting (orographic or frontal), (iii) low-level convergence (Schroeder and Buck 1970), or (iv) upper-level short waves..

Air-mass thunderstorms can be broadly categorized as either convective or orographic, although these lifting processes often work in combination with each other (Schroeder and Buck 1970). Dry thunderstorms, a particular kind of air-mass thunderstorm, are important as wildfire starters since their high cloud-base often results in very little accompanying precipitation (less than 0.25cm or 0.1 inches) precipitation, and less than 45% humidity; NOAA, NWS Storm Prediction Center; <http://www.spc.noaa.gov>), which increases the probability of ignition following a lightning strike. Under conditions conducive to the formation of air-mass thunderstorms (low wind speed and the absence of frontal activity), triggering mechanisms associated with the surface characteristics (changes in topography, differential heating or changes in surface roughness), are likely to have a strong influence on convection and subsequently lightning patterns.

Surface heterogeneity created after wildfire is important at, at least two spatial scales: locally, within individual fire scars; and regionally, at the scale of fire scars or the distance between scars. Local variations in topography, fuel moisture content, vegetation type and other factors contribute to

---

<sup>4</sup> The amount of moisture (to be "sufficient") will depend upon the strength of convection (whether it is deep enough to reach the lifting condensation level) and the vertical profile of virtual potential temperature (which dictates how much latent heating is required before free convection starts, and what the vertical extent will be). (Stull 1988)

heterogeneity within each fire scar. Each of these heterogeneities is a potential triggering mechanism for buoyant surface layer plumes, which either individually or by coalescence, may lead to mixed layer thermals (Williams 1991) sufficiently strong to initiate convective development.

At the regional scale, effects can be even larger. Many lightning induced fires within Interior Alaska occur in remote (difficult to access), sparsely populated (low suppression priority) regions. Consequently, individual scars can be quite large (400-2,300 km<sup>2</sup>), such that relatively few scars make up the bulk of the total area burned annually. These large burn scars are thus usually of a scale sufficient to sustain mesoscale circulations (Shuttleworth 1988; Pielke and Vidale 1995; Chambers 1998).

In the absence of frontal activity, there are two important mechanisms responsible for enhancing the necessary vertical motion for thunderstorm development: (i) non-classical mesoscale circulations (NCMCs), which include "land-breezes", and (ii) low level convergence associated with an increase in surface roughness (Vidale et al. 1997). The strength of the prevailing near-surface winds can control these mechanisms (Vidale et al. 1997).

NCMCs are driven by pressure gradient forces set up by horizontal differences in near-surface air temperatures (Vidale et al. 1997; Weaver et al. 2002). Since the pressure gradients are usually small, NCMCs are most commonly observed under conditions of low synoptic winds. These circulations are oriented such that the flow is from cool air to warm air at the surface (ie. high to low pressure, where the low pressure results from the rising of buoyant air) (Segal and Arritt 1992). Contrasts in surface characteristics (e.g. terrain aspect, surface roughness, albedo and moisture availability), that affect radiation absorption, evapotranspiration and aerodynamic transfer, are usually responsible for the horizontal gradients in atmospheric heating. Such contrasts are evident across burn scar boundaries (Vidale et al. 1997; Chambers and Chapin 2003). NCMCs are conceptually similar to sea-breeze cells (Segal and Arritt 1992; Cotton and Pielke 1995), and they can transport large quantities of heat and moisture within the boundary layer compared to turbulent transport mechanisms (André et al. 1989). They can reach similar strengths as their sea-breeze counterparts (Segal and Arritt 1992), and the associated convection is often strong enough

to trigger/enhance rainfall or induce thunderstorm formation (Weiss and Purdom 1974; Stull 1988; Blyth et al. 1994).

When prevailing lower-level winds increase, surface roughness conditions become the predominant factor in convective triggering (Vidale et al. 1997). While simulations have shown that mesoscale circulations can prevail even on days with strong lower-tropospheric winds (Weaver and Avissar 2001; Baidya Roy and Avissar 2002), the point of deepest convection was advected downwind of the location from which the initial convection was triggered (Baidya Roy and Avissar 2002). The effect of a change in surface roughness is such that a transition from rough to smooth results in increased wind speed, low-level divergence and subsidence, whereas a flow from smooth to rough results in decreased wind speed, low-level convergence and uplift (Claussen 1987; Samuelsson and Tjernström 2001). In general, surface roughness effects can be more important in generating mesoscale motions than differences in surface temperatures (Samuelsson and Tjernström 2001).

### 3.2 Objective and research approach

The main objective of this study was to determine changes in convective activity in the vicinity of wildfire burn scars in the years following the fire. We were interested in whether we could find evidence of feedback between wildfire burn scars and convective activity in the Alaskan Interior boreal forest, and if so, explain the driving mechanisms. In this study, change in lightning strike frequency was used as a proxy for change in convective activity to supplement available satellite imagery.

To examine the convective activity in the area we initially compared lightning strike frequencies within a region defined by the burn scar and within an unburned forest surrounding the burn scar both pre- and post-fire. To investigate the most important driving mechanisms we regressed lightning strike activity against environmental variables (slope, elevation) and variables associated with the wildfire burn scars (overlap with older scars, vegetation composition in scar and buffer, scar size etc.).

### 3.3. Study area

The Yukon Flats (figure 3.1) are located towards the northern end of the discontinuous permafrost region of Interior Alaska (Gallant et al. 1996). They represent a level region dominated by open spruce and closed mixed forest mosaics with large areas of spruce forest, interspersed with patches of moist shrubby tundra and bog.

The Yukon Flats covers almost 25000km<sup>2</sup> and have an active history of wildfire. Over the past 30 years, the decadal area burned increased from 2500km<sup>2</sup> to 4400km<sup>2</sup> (figure 3.2). Between 1950 and 2000, a total of 134 fires have burned within the Yukon Flats, with an average size of > 400 km<sup>2</sup>. This has resulted in a heterogeneous vegetation mosaic across the region. With the large burn areas, as well as the relative and absolute (figure 3.3) amounts of lightning strikes in the area increasing, it is an ideal region for studying feedbacks between burn scars and thunderstorms.

The region has a continental climate, and since it is bounded between the White Mountains and Brooks Range (Fig. 3.1) it is largely sheltered from strong synoptic / frontal activity. These factors, along with the relatively simple topography, make the region particularly favorable for air-mass thunderstorm development. About half of the total annual precipitation in the Yukon Flats falls during the thunderstorm season (May- August).

By Alaskan standards, the Yukon Flats receive a relatively large number of lightning strikes. Although the region constitutes only 4% of Interior Alaska, it receives on average 6% of the lightning strikes within Interior Alaska. In fact, the fraction of Interior Alaska's lightning strikes that occur within the Yukon Flats has been increasing (from 4% in 1986 to 8% in 1999; Fig. 3.3).

In spite of the sheltered nature of Interior Alaska, a large fraction of its annual total of recorded lightning strikes are received during the few periods of relatively intense synoptic storms. However, since each of these synoptic events occurs over just a few days, the majority of days in the year on which lightning strikes are recorded can be attributed to air-mass thunderstorms (Biswas and Jayaweera 1976; Henry 1978). It is these localized, low lightning-frequency air-mass thunderstorms, with little (if any)

associated rainfall, that ignite most of the lightning-caused fires in Interior Alaska (Henry 1978). The localized nature of the storms also increases the likelihood that if rainfall is associated with the storm that the associated lightning may strike in a dry region.

### 3.4. Data

#### 3.4.1. Satellite data

AVHRR satellite image data were used because they covered as much of the time span of 1986-99 as possible (1989-99). The data were obtained from the NOAA Satellite Active Archive (SAA) website (<http://www.saa.noaa.gov>). The images are from the time period 15 June - 5 July (which corresponds to the highest thunderstorm activity in the area), and it was a requirement of the study that the images were cloud-free.

Radiant temperatures were derived from the thermal channel 4 data (bandwidth 10.30-11.30  $\mu\text{m}$ ) which have a spatial resolution at nadir of 1km (table 3.1). The images are from passes over the study area between 9:30AM and 7:30PM Alaska Standard Time. It was impossible to obtain cloud-free images from exactly the same time of day during the thunderstorm season.

Landsat 7 Enhanced Thematic Mapper (ETM) images were used to delineate the burn scars due to the 30-60m pixel size (table 3.1). These images were from June and August 2000 and 2001, and were chosen based on availability and low cloud cover. For each of the five images we calculated a digital Normalized Difference Vegetation Index (NDVI), based on bands 3 and 4. Radiant temperatures were also extracted from the Landsat 7 ETM+ images and a few additional Landsat 5 TM images for the time period of 1986-2000. The radiant temperatures were based on band 6, and conversions were performed as described in Chapter 11 of the Landsat 7 Science Data User's Handbook ([http://ftpwww.gsfc.nasa.gov/IAS/handbook/handbook\\_toc.html](http://ftpwww.gsfc.nasa.gov/IAS/handbook/handbook_toc.html)).

For the cloud imaging, the Landsat images chosen for analysis were selected on the basis of location, cloud cover, time of year and time of day. We visually determined the onset of convective activity



in the vicinity of the burn scars by the presence / absence of convective clouds. For this part of the study, we examined images from Landsat 4,5 and 7 for the 1990-2002 thunderstorm seasons (May-September). This yielded only 78 images due to the sparseness of passes (1 in 16 days) and few relatively cloudfree (<40% cover) summer days.

A paradox complicated our study. If the positive feedback mechanism between wildfire burn scars and increased convective activity exists, then increased convective clouds might obscure views and make radiant temperature derivation difficult, thus disabling studying the very effect which brought the clouds in place. Thus our study is likely to under-represent any relationship between fire scars and convective activity.

#### **3.4.2. Burn scar data**

The Alaska Fire Service (AFS) maintains a database of Alaskan wildfire burn scars. The burn scars are digitized and the area, year of burn and identification numbers are recorded for each burn scar (Murphy *et al.*, 2000). Burn scars were selected from the AFS data set if they were located in or close to the Yukon Flats area, were greater than 20,000 ha (200 km<sup>2</sup>), and occurred between 1988 and 1993 (figure 3.4). The time frame was based on the availability of lightning data (1986-99), which we wanted to compare to the burn scar data before and after the fires.

The burn scar boundaries were more accurately delineated using a Landsat ETM color composite of bands 4-7-2, which was the delineation methods of Koutsias and Karteris (2000).

#### **3.4.3. Lightning data**

The Alaska Fire Service operates an automated network of cloud-to-ground lightning sensors. If a lightning strike is detected by more than one sensor, the position of the strike is then estimated by triangulation. Positional accuracy of estimated lightning locations varies with the number of detectors sensing a strike and with detector location geometry. Each detection includes estimates of time, location,

and the positional accuracy of the strike. In Alaska, the network has been in operation since 1976 and consists of 9 stations within the state and 3 in the Yukon Territory. The best positional accuracy of lightning strike data processed after May 1995 is estimated to be 2-4 km (Global Atmospheric, Inc.). Data included in this study cover the 1986-99 period and are available from the Bonanza Creek Long Term Ecological Research Site website at <http://www.lter.uaf.edu>.

Since the focus of this study is air-mass thunderstorms, we attempted to exclude days where the lightning was due to large-scale (synoptic) thunderstorms. An artificial threshold value of 1000 lightning strikes per day represents a reasonable division between the influence of large-scale (synoptic) thunderstorms and that of air-mass thunderstorms for Alaska. Thus days when the total statewide lightning strikes exceeded 1000 strikes were excluded from the data set.

#### **3.4.4. Synoptic weather maps and atmospheric soundings**

Very few synoptic weather maps and soundings are archived in Alaska. We have included all available information useful for analyzing the weather situation for the two case studies of convective clouds around the burn scars. This mainly includes surface maps, 500, 750 and 850hPa. There was only one Alaskan relevant afternoon sounding available, and the applicability of this sounding, which was from Fairbanks (225km southwest of Fort Yukon, on the opposite side of the White Mountains), is dependent on the weather pattern and therefore arguable. The two closest Canadian soundings are from Norman Wells and Inuvik, Northwest Territories, which, respectively, are situated 855km east and 535km northeast of Fort Yukon. These soundings were judged to be too far away and additionally under too strong a maritime influence to be relevant for the Yukon Flats study area. All times below are given as Z (GMT) and Alaska Daylight Savings Time (ADT).

Case 1: 18Z (10:00AM ADT) 06-29-91 surface map, 00Z (4:00PM ADT) 06-30-91 surface map, 00Z (4:00PM ADT) 06-30-91 500hPa map, soundings from Fairbanks, Alaska 00Z (4:00PM ADT).

Case 2: 00Z (4:00PM ADT) 06-25-00 500hPa map, 00Z (4:00PM ADT) 06-25-00 700hPa map, 00Z (4:00PM ADT) 06-25-00 850hPa map, soundings from Fairbanks, Alaska, 00Z (4:00PM ADT).

### 3.5. Methods

We selected a total of 13 burn scars within the Yukon Flats for analysis. We defined a 25km buffer zone around each of the burn scars to represent the surrounding unburned areas (figure 3.4). A buffer zone of this size was thought to be sufficient to account for uncertainty in the position of lightning strikes and burn scar boundaries, as well as the advection of developing thunderstorms by local winds. Three areas were selected as control areas (figure 3.4) in the general vicinity of the burn scars and buffers, but sufficiently isolated to receive as little influence as possible from the burns or surroundings. As a first step we investigated pre- to post-fire changes in lightning strike activity over each combined region (scar + buffer and controls). We subsequently considered changes in lightning activity within the scar, buffer and control regions independently.

The study used proxies for burn severity classification and net radiation, which were extracted from remotely sensed data. These proxies help in understanding the observed changes in lightning strike activity.

#### 3.5.1. Changes in lightning activity

To minimize effects of the large inter-annual variation in lightning strike data, we normalized the data by relating it to the total lightning in Yukon Flats region. The lightning data are therefore expressed as a percentage of the lightning strikes in Yukon Flats. The normalized lightning strike data were computed for the following group averages; 1-2 years pre-fire, and 1-2, 3-4, 5-6, 7-8 years post-fire. For each of the three control areas, we calculated the same statistics as for the burn scars and buffers, using all four possible fire year scenarios (1988, 1990, 1991, 1993).

For each of the five possible before-versus-after-fire scenarios, we used a  $\chi^2$ -test and a threshold p-value of 0.01 to determine significant differences. The period with the largest  $\chi^2$ -values was defined as the period of the largest changes, regardless of the direction (positive or negative) of these changes. The difference in normalized data for the time periods of largest changes for scar and buffer were used for multiple regression analysis. All mention of changes in lightning activity throughout this paper refers to changes in normalized lightning.

Lightning strike activity was used a proxy for convective activity. This was done because lightning strike data are detected fairly reliably throughout the thunderstorm season, as opposed to convective cloud data, which would have to be retrieved from satellite imagery with problems such as temporal and spatial resolution of the images (table 3.1).

### **3.5.2. Radiant temperature (AVHRR and Landsat ETM)**

The change in radiant temperature was used as a proxy for a change in net radiation. With high relative post-fire surface temperature, the outgoing longwave radiation is larger, resulting in reduced net radiation (Chambers et al. Submitted). Furthermore, permafrost retreat and the typically high stomatal conductance of successional vegetation results in a reduced partitioning of net radiation into atmospheric heating. An increased partitioning of net radiation into sensible heat flux immediately following fire usually results in a gradient in heating from the unburned to the burned region (Amiro et al. 1999), which may initiate a NCMC.

Radiant temperature statistics for the burn scars and buffer zones were extracted. For each year, and each scar-buffer pair, the mean radiant temperature difference between the two areas was calculated. Since it was the relative difference in temperature between the burned and unburned regions that was of interest in this study, no effort was made to converting the extracted radiant temperatures to absolute surface temperatures. This procedure was applied to both the AVHRR and the ETM data.

For each scar-buffer pair, the mean radiant temperature difference was related to the time after the fire, and was used to examine the duration of elevated temperatures within the scars. NDVI (digital numbers) for each scar-buffer pair was calculated from the high resolution ETM data. As with the radiant temperature data, statistics on the NDVI data were calculated for each scar and buffer.

The standard deviation of NDVI ( $\sigma_v$ ) within a burn scar was used as one proxy for fire severity and the post-fire successional stage of the burn scar. Whilst there may not be a straightforward relationship between fire severity and  $\sigma_v$ , it is likely that  $\sigma_v$  within a severe burn scar would be low relative to that of moderate burn scar, since the nature of the fire would be more homogeneous.

A simplified vegetation cover classification within the burn scars and buffer zones was determined using the high resolution ETM data. Color composites of bands 4-3-2 and threshold values were utilized to delineate non-vegetated from vegetated areas and to separate coniferous vegetation from deciduous.

The percent cover of coniferous vegetation and deciduous vegetation was used as another proxy for fire severity and the post-fire successional age of the burn scar. Based on established post-fire succession trajectories (Van Cleve and Vierick 1981), we assumed that, if a burn scar contains a large percentage of coniferous vegetation, it is likely to have been a light to moderate burn. Similarly, a large relative cover of deciduous vegetation would suggest a severe fire. Whilst broadly true, these assumptions are not without caveats, for example, a light burn within a hardwood forest leaving many pockets of unburned deciduous trees would be classified as a severe burn under this scheme.

It is likely that if the vegetation in the buffer zone surrounding the scar was homogeneous, that it would exhibit a low  $\sigma_v$ . A homogeneous cover of conifers (high percent cover) within a buffer area would offer the strongest contrast to the burn scar vegetation, and provide the strongest potential for the development of a NCMC. As a result of typically high albedo (table 3.3) and low Bowen ratios, a burn scar surrounded by deciduous vegetation would not create as strong a gradient in near surface air temperature as a burn scar surrounded by conifers. Combining the assumptions and information that we have regarding the vegetation composition of the scar and buffer, we made an assessment of fire severity for each scar (high,

medium, or low). This information, in conjunction with matching information for the buffer regions, is used to assess the potential for, and direction of, NCMCs.

It should be mentioned that a given burn scar would rarely represent a single severity class, rather a patchwork of severity. This is likely to result in some mixed signals of factors important for lightning activity within the burn scars.

### **3.5.3. Multiple Regressions**

We used a stepwise multiple regression analysis to examine the factors (table 3.2) potentially related to the changes in lightning strike activity in the burn scars and buffer zones. Slope and elevation variables were included to account for the influence of sloping topography, which is related to the need to account for a lifting mechanism (trigger). The scar and buffer size represent the scale of the examined surface heterogeneity introduced by the wildfires, an important factor for the possible initiation of NCMCs. Year of fire was used as a variable to control for effects due to inter-annual lightning variation. The differences in radiant temperature (mean and extreme) were used as indicators of net radiation differences.

The analysis was run twice (once for each of the dependent variables: “%change in buffer lightning” and “%change in scar lightning”) for the two periods of largest changes. The analysis was run as a forward stepwise multiple regression with  $F = 1.00$  to enter and  $F = 0.00$  to remove. The linear regression between each of the independent variables and the dependent variable was tested first, as well as together in a final run where all variables were included. This was done for both of the dependent variables.

### **3.5.4. Cloud Imaging**

We examined each of the 78 Landsat images for apparently non-random convective clouds associated with all the wildfire burn scars in the general Yukon Flats area, not just limited to the 13 scars shown in figure 3.4. Days with a relatively low overall cloud cover were selected, because a high cloud coverage would obscure the view and decrease the likelihood of it being a day with localized convective

activity. The images were examined for isolated convective clouds, which did not appear to be part of a street or any larger-scale cloud systems, and we would determine if this cloud (or clouds) could be linked to any terrain features.

We found only two such cases, and for each of these cases synoptic weather maps and atmospheric soundings were examined to determine the general flow pattern and potential for local thunderstorms. The potentials were then related to the convective cloud occurrence at the two burn scars and the lightning that actually occurred on each of the two days. This way we determined if the convective clouds occurring at the two burn scars could be caused by local circulations induced by the burn scars.

## 3.6. Results

### 3.6.1. Lightning strike data (1986-99) - changes in activity over time.

All the fire scars show decreased or no change in lightning activity (0-81%) or no change in activity (table 3.4a). Most buffers (table 3.4b) show a similar decrease or no change, except for four (895, 998, 1002, and 1099) which show 10-30% increases. The control areas followed the trend in the burned areas with decreasing or no change in the lightning strike activity (table 3.4c).

While more than two thirds of the scars show a decrease in normalized lightning when measured as mean 2-year-period comparisons (table 3.5a), some scars (895 and 905) show a strong increase in relative lightning for some or all of the two-year comparisons. The largest changes (positive and negative) for any of the 2-year-period comparisons (before vs. after fires) occur in the 1-2 years post-fire time span (table 3.5a, b). Some changes were highly significant ( $p < 0.001$ ) however, as mentioned above, they were not consistently positive or negative.

The buffer areas surrounding the burn scars show mixed trends (table 3.5b). Four buffer areas show strong increases in overall relative lightning. The biggest changes (positive and negative) occur in the 5-6 years post-fire time span. However, two of the three biggest burns (891, 1099) show their highest (and in one case, only) fractional increases 7-8 years post-fire.

Only one of our 12 control cases (lightning data from the 3 control areas compiled for 4 different fire years) show consistent positive changes (table 3.5c). Most of the control cases show negative or mixed positive and negative changes in lightning strike activity.

These results present a mixed picture. The effect of area in the normalized lightning data was removed and enabled a comparison between lightning strike density between the burn scars and surrounding buffers, and the control areas (figure 3.5). Generally, the control areas receive a significantly smaller fraction of the Yukon Flats lightning per unit area than does the scars and buffers. Table 3.6 shows how different these distributions really are. Control areas 2 and 3 fall clearly at lower values than the burns and buffers, whereas control area 1 have a distribution closer to that of the burn scars. However, this control area (1) is situated only 25 miles from the closest fire scars included in this study, whereas the two other control areas (2 and 3) are almost twice as far away from the closest burn scars (figure 3.4).

### **3.6.2. Radiant temperature: AVHRR and Landsat ETM**

The AVHRR radiant temperature data indicate that temperature remains elevated within the burn scars for more than 10 years post-fire (figure 3.6). The Landsat temperature differences were in general higher than the AVHRR temperatures (figure 3.6, table 3.7). However, the spectral and temporal resolution differ between the AVHRR and Landsat data (table 3.1, figure 3.6).

### **3.6.3. Multiple regression**

#### *3.6.3.1. Scar Lightning*

The normalized lightning in the burn scars ((1-2 years post-fire) - (1-2 years pre-fire)) final run with all the variables produced the following equation ( $p < 0.0087$ ,  $r^2$  (adj.)=0.61,  $n = 13$ ). All the variables included in the following expression are significant (table 3.8):

$$X_s = -322.60 + 0.752 \cdot \Delta T_R + 0.465 \cdot D_{vs}$$



where  $X_s$  = difference in normalized lightning in scar[%]

$\Delta T_R$  = difference in radiant temperature for the time period

$D_{vs}$  = the percentage of deciduous vegetation within the burn scar

The positive relationship with the radiant temperature difference within the first 2 years post-fire and to the amount of deciduous vegetation within the burn scar (table 3.8) were in agreement with our initial hypothesis (table 3.2).

### 3.6.3.2. Buffer Lightning

The normalized lightning in the buffers ((5-6 years post-fire) - (1-2 years pre-fire)) final run with all the variables produced the following equation ( $p < 0.0056$ ,  $r^2$  (adj.)=0.60,  $n = 13$ ). All the variables included in the following expression are significant (table 3.9):

$$X_b = -165663.34 - 0.80*A + 0.987*Y$$

where  $X_b$  = difference in normalized lightning in buffer[%]

A = The percentage overlap of the burn scars with burn scars from the 1970-79 period

Y = year of fire

Contrary to our initial expectations (table 3.2), buffer lightning activity was negatively related to the overlap with older (1970-79) burn scars within the burned area.

The year of fire was included in the multiple regression analysis to account for inter-annual variation in climatic conditions (meteorological conditions favoring thunderstorm development). This factor contributed significantly as a positive factor in the model of lightning changes in the buffer areas (table 3.9). The historical development of lightning strike frequency in the Yukon Flats showed an increasing trend (figure 3.6). It would therefore be tempting to relate the increase in lightning strikes in the area to the year of the fire as we saw in the analysis. The important thing to emphasize here is that the fact that two variables have similar trends is not sufficient evidence to imply causality.

The Yukon Flats is a vegetation mosaic that, although it contains black spruce, is not limited to this tree type. According to our vegetation classification, two thirds of the vegetated areas on the ETM images used were coniferous. Most other vegetation types would yield a smaller difference in albedo and net radiation between the burned and unburned areas. It is therefore not surprising that deciduous vegetation coverage for the burn scar contributed to the multi-variable regression as a positively related factors.

#### **3.6.4. Cloud Imaging**

Only two of the 78 Landsat images were found that showed likely connections between wildfire burn scars and the onset of convective activity (figures 3.7 and 3.9). They are shown as color composite images of bands 4-7-2, which is a band combination that exposes burn scars very clearly (Koutsias and Karteris 2000). We will use these two images as two case studies.

##### *3.6.4.1. Case Study 1 (24 June 2000, 10:00AM AST).*

The image shows a portion of the Yukon River near Circle, Alaska (Fig. 3.7). Convective clouds occur in the image in the southeastern corner, and north of the Yukon River in the northeastern corner. The clouds in the southeastern corner appear to be associated with elevated terrain (Fig. 3.8). However, the cumulus clouds north of the river show no obvious relationship to topography and are located right off the northwestern flank of burn scar #1585, which burned 1 year before this image was taken (1999, 154km<sup>2</sup> burned).

Examination of the synoptic weather maps show a weak synoptic flow day for Interior Alaska. A deep low pressure system over the Gulf of Alaska, and similarly over the Arctic Ocean, resulted in a weak upper level high pressure ridge over Interior Alaska, a situation conducive to thunderstorm development. The flow in the Interior was directed from east to west bringing moisture into the region. The air aloft is cool, and the 850hPa map indicates fairly warm air at the surface. Overall it is a day with weak synoptic scale activity, ideal for the development of convective activity by local heating differences. The

atmospheric sounding from Fairbanks, which was taken at 4PM ADT shows a fairly unstable profile with a good thunderstorm potential.

There were 989 lightning strikes scattered throughout central Alaska on this day, close to our synoptic condition threshold of 1000 strikes. Some local activity was detected around burn scar #1585, although the majority of strikes occurred in a concentrated region northwest of this scar (Fig. 3.8). The lightning activity showed a temporal progression from east to west.

In spite that the number of lightning strikes on this day are near our arbitrary threshold of 1000 strikes for synoptically influenced convection, this day appears to be a good candidate for the development of strong NCMCs. A series of AVHRR images, combined with the Landsat ETM morning image (Fig. 3.7), support the hypothesis that the local lightning strikes could be due to a burn scar-related temperature-induced NCMC system. The AVHRR images suggested that the lightning activity seemed to end when more organized cloud cover moved into the area.

#### *3.6.4.2. Case Study 2 (29 June 1991 10:00AM AST).*

The image (Fig. 3.9) shows a portion of the Yukon River about 500-600km downstream of the region shown in Fig. 3.7. Two active fires are identifiable in the image, the western fire resulting in burn scar #1002 (Fig. 3.4). Convective clouds occur in the western third of the image. Some seem to be associated with the 1002-burn, and those furthest to the south could be associated with elevated terrain (Fig. 3.10). However, some cumulus clouds (circled), appear off the northwestern edge of burn scar #979, which burned 1 year before the image was taken (1990; 1.1km<sup>2</sup>).

On this day, winds were weak and conditions generally those of a dry pattern throughout Interior Alaska. A surface-level front (The Arctic Front) was moving south towards the Arctic coast, bringing in a lifting mechanism which is likely the cause of the convective (lightning activity) along the central Brooks Range (Fig. 3.10). There was the potential for some convective activity in the Upper Yukon Valley due to the presence of the "thermal trough". The general pattern was not very unstable, but had potential for the development of small-scale local circulations. The atmospheric sounding from Fairbanks support

the diagnosis of a not particularly unstable pattern with a 4PM profile with little to no thunderstorm potential.

Two stray lightning strikes were recorded northeast of the Yukon River within 100km of burn scar #1099. The weak synoptic flow was favorable for local convective activity as the general pattern in the Interior. The morning image (Fig. 3.9) showed the onset of convective activity concentrated around higher terrain, as was likely the case with the clouds in the southwest corner of the image. The convective clouds east of the fires are due to the heat of those fires. No lightning was detected in the immediate vicinity of the burn scar. However, the clouds associated with scar #979 seem un-associated with higher terrain and could thus be due to heating effects of burn scar #979.

The closest lightning strike was located about 84km to the north of #979. However, since this strike was within 30km of the large burn scar #1099 it is possible that the scar influenced the convective development that caused the strike.

### 3.7. Discussion

The largest temperature difference between the burned and unburned areas occurred in the first 1-3 years post-fire (Fig. 3.6). Surprisingly, the radiant temperature time series had less variation a decade after than before the fires, although a smaller sample size has to be taken into account. The large standard deviations in the 1-8 year period post-fire may be due to differences in fire severity and therefore variation in the resultant speed and trajectory of succession within the burn scars.

The examples of convective clouds near burn scars (Figs. 3.7, 3.9) are both from one year after the wildfire that created the scar suspected of triggering those clouds. In both cases, the convective clouds occurred on days when synoptic conditions favored air-mass thunderstorms and do not seem to be explainable by other factors (topography etc.). Thus, both case studies support our hypothesis, and suggest the existence of a feedback mechanism between fire scars and convective development. Only one of the

clouds in the two cases conceivably developed into a thunderstorm that produced lightning (case 1, figure 3.8).

Not all cumulus clouds that occur over a hot surface develop into active thunderstorms, and the fact that cumulus clouds are observed over a burn scar does not guarantee that a NCMC is present. However, such signs do indicate a potential for the development of a thunderstorm enhanced by a NCMC. NCMCs and changes in surface roughness can both trigger and enhance convective development, but many other potential triggers for convection exist within a burn scar (caused by the heterogeneity) that may lead to convective development. Without further enhancement (and sufficient moisture and instability), the plumes and thermals that result from these triggers are more likely to result only in fair-weather cumulus over the burn scar.

The formation of NCMCs depends on the spatial scale of the surface inhomogeneities which trigger them (Shuttleworth 1988; Segal and Arritt 1992; Avissar and Schmidt 1998; Pielke et al. 1998). At smaller spatial scales (<5 km), the effect of the turbulent fluxes is limited to the lower part of the boundary layer (Pielke et al. 1998). At such small scales the atmospheric boundary layer is unable to respond in an organized way to changes in surface fluxes caused by the vegetation, and instead, acts as an averaging mechanism (Shuttleworth 1988). However, when the scale is larger (>10km) horizontal differential heating can lead to NCMC formation, which can affect the whole boundary layer. Several studies have found ~10km to be the smallest scale of surface heterogeneity to influence cloud formation (Klaassen 1992; Blyth et al. 1994; Mahrt et al. 1994).

Knowles (1993) simulated convective activity and found that while a burn scar of 400km<sup>2</sup> triggered cloud development, a 150km<sup>2</sup>-sized scar did not. He used Alaska lightning data and the Colorado State University Regional Atmospheric Modeling System (RAMS) for the simulations. The burn scars chosen for this study were all larger than 200km<sup>2</sup>, but only 62% of the scars were larger than 400km<sup>2</sup>. However, satellite images of burn scars and cumulus clouds suggest that even smaller (110-154km<sup>2</sup>) burn scars produce clouds (Figs. 3.7, 3.9), which is consistent with theory, as explained above.

The number of recorded lightning strikes increased in the buffer zone around a third of the burn scars (table 3.5b). As a general trend, there was a notable reduction in lightning strike activity within most of the burn scars, control areas, and a number of the buffers (table 3.5a, b, c). However, since this trend was not consistent for all scars and buffer regions, perhaps other factors influence the potential for these local circulation patterns.

Primary effects of fire are reduced albedo and reduced transpiration. Usually, this causes increased radiation absorption, and greater partitioning of net radiation into sensible heat flux, leading to a substantial gradient in atmospheric heating from the unburned to the burned region (Amiro et al. 1999). Fire severity is likely to have a large influence on both the strength and direction of any local circulation, because it enhances the differences in surface properties that would drive one of the hypothesized circulations. It is therefore reasonable that the half of the explaining factors, such as radiant temperature differences between burn and buffer and deciduous vegetation in the burn scar, were associated with fire severity.

To explain the cases where lightning activity increased in both the scar and buffer regions, it is worth restating our lack of wind data. It is possible that either local winds, or stronger lower-tropospheric winds could have obscured the results by advecting the circulations away from their source regions as coherent units, as suggested by Baidya Roy and Avissar (2002).

However, at some of the selected burn scars (998, 1002, 1099), lightning increased in the unburned buffer areas, suggesting that a potential circulation would be directed from the burned area towards the unburned buffers. A possible explanation for this could relate to the changes in surface roughness and atmospheric coupling that occurs after fire. A severe fire in a typical Alaskan black spruce stand consumes most of the canopy, resulting in a large reduction in surface roughness. The smoother surface following a severe fire is less efficient at conducting heat to the overlying atmosphere, as surface temperature and radiative heat losses increase, leading to a reduction in net radiation (Chambers et al., submitted). This would happen throughout early to mid post-fire succession, where Chambers and Chapin (2003) have shown that a combination surface roughness, stomatal conductance and a non-linear albedo change can

rapidly reverse the gradient in sensible heat flux ( $H$ ) across a burn scar boundary (that is initially from the unburned to the burned region). Figure 3.11 illustrates the hypothesized scenario in early post-fire succession following a severe fire of a circulation system directed towards the unburned region. With high relative post-fire surface temperature, the outgoing longwave radiation is larger, resulting in a reduced net radiation.

Based on the above assumptions, the greatest difference in net radiation between the burned area and the surrounding boreal forest should appear in the 3-7 year post-fire time span (figure 3.2). At this point, the cover of predominantly herbaceous vegetation and tree seedlings has developed sufficiently to increase the albedo of the burn scar above that of the unburned forest, but not by enough to substantially increase the surface roughness and coupling with the atmosphere.

Burn scars maintained an elevated surface temperature for at least 10 years post-fire (Fig. 3.6), indicating that factors that warm the surface (e.g. less efficient coupling to the atmosphere due to the smoother canopy) have greater impact than factors tending to cool the surface (e.g. increased albedo, increased stomatal conductance and evapotranspiration). The difference in surface temperature creates the potential for a local circulation system. Although the role of increased surface temperature in this process may be limited to the first decade post-fire, the other effects may continue for much longer.

Future climate scenarios from contemporary GCMs indicate a pronounced warming in northern high latitudes with correspondingly higher fire frequency (Clark, 1988) and expansion of the boreal forest (Smith *et al.*, 1992). Climate and fire data show that the length of fire season and fire severity are linked to temperature (Lynch *et al.*, 2003) Since the speed and trajectory of vegetative succession is a function of fire severity, changes in the size and severity of fires could feedback to the strength and frequency of convective development at and around the burn scars, and thus to regional fire return frequency.

### 3.7.1. Study Constraints

We have found that for the Yukon Flats study area, it is almost impossible to find scar and buffer areas that do not overlap other scars (figure 3.12), which each contain vegetation at other stages of post-fire vegetation succession. Thus our analysis is often performed on a vegetation patchwork area, making it difficult to obtain an isolated signal of fire effects on vegetation contrasts and potential circulations. Instead, we may be seeing the result of an averaging mechanism produced by the atmospheric boundary layer in response to smaller scale changes in the surface vegetation, as described by Shuttleworth (1988).

The potential for interaction between NCMCs is also a factor that could be important. For example, convective activity can be very strong in the case of a peninsula or island, where sea-breeze cells can form from both sides, and converge in the middle. During the Maritime Continental Tropical Thunderstorm Experiment (MCTEX) it was found that a dominant flow pattern would oppose the sea-breeze development and result in enhanced frontal development and likely thunderstorm initiation (Beringer et al. 2001). Reap (1994) found organized coastal maxima in lightning activity related to land-sea-breeze convergence zones that form as a direct response to the low-level wind flow on the Florida Peninsula. A patch of unburned spruce between two severely burned regions could produce a similar effect.

Because many factors influence the production of a land-breeze NCMC, it is often very difficult to isolate a single cause, and one rarely has a straightforward scenario. Fires rarely burn uniformly across the landscape and therefore introduce heterogeneity with respect to vegetation, as represented by the standard deviations of NDVI. Interestingly, these standard deviations are larger for the buffers than for the burn scars in all cases. This must be attributed to the fact that these data were obtained from images taken 7-13 years after the fires occurred, thus allowing time for the vegetation in the burn scars to become reasonably homogeneous, whereas the buffers contain old burn scars, new scars, water etc.

The overall accuracy of a study depends on the individual accuracies of the data involved. Thus this study is probably limited in accuracy by the ~ 2km locational and 90%+ detection accuracy of the lightning data. We maximized the size of the study regions to minimize this problem. Fair-weather-cumulus



clouds develop rapidly and have a relatively short life span (hours) and a limited spatial expanse (few km's) (Stull 1988). The use of satellite imagery to study cumulus clouds at high latitudes and their link to specific surface properties is therefore challenging, since good spatial and temporal resolution does not occur simultaneously (table 3.1).

### 3.8. Conclusions

We looked for evidence of a wildfire feedback mechanism around 13 fire scars within the boreal forest of the Yukon Flats region, Interior Alaska. We found two satellite images where convective cloud development could be associated with burn scars. In one of these cases, thunderstorm and lightning activity developed in the immediate area, suggesting a possible burn scar-induced circulation.

We found that in general, relative lightning activity decrease in the burned areas as well as the control areas following a fire. In some areas, however, lightning activity increased in the surrounding unburned areas. In the four cases of positive lightning activity changes in buffers and some scars the positive lightning activity changes seemed to be concentrated in 2-3 geographical areas.

Primary effects of fire are reduced albedo and reduced transpiration. Initially, this causes increased radiation absorption, and greater partitioning of net radiation into sensible heat flux, leading to a substantial gradient in atmospheric heating from the unburned to the burned region (Amiro et al. 1999). Fire severity is likely to have a large influence on both the strength and direction of any local circulation, because it enhances the differences in surface properties that would drive one of the hypothesized circulations. It is therefore sensible that the half of the explaining factors, such as radiant temperature differences between burn and buffer and deciduous vegetation in the burn scar, were associated with fire severity.

### 3.9. Literature cited:

André JC, Bougeault P, Mahfouf J-F, Mascart P, Noilhan J, Pinty J-P (1989) Impact of forests on mesoscale meteorology. *Philosophical Transactions of the Royal Society of London, Series B*, **324**, 407-422.

Amiro BD, MacPherson JI, Desjardins RL (1999) BOREAS flight measurements of forest-fire effects on carbon dioxide and energy fluxes. *Agriculture and Forest Meteorology*, **96**, 199-208.

Avissar R, Schmidt T (1998) An evaluation of the scale at which ground-surface heat flux patchiness affects the convective boundary layer using large-eddy simulations. *Journal of the Atmospheric Sciences*, **55**, 2666-2689.

Baidya Roy S, Avissar R (2002) Impact of land use/land cover change on regional hydrometeorology in Amazonia. *Journal of Geophysical Research* **107**, 10.1029/2000JD000266.

Beringer J, Tapper NJ, Keenan TD (2001) Evolution of maritime continent thunderstorms under varying meteorological conditions over the Tiwi Islands. *International Journal of Climatology* **21**, 1021-1036.

Biswas AK, Jayaweera KOLF (1976) NOAA-3 Satellite observations of thunderstorms in Alaska. *Monthly Weather Review* **104**, 292-297.

Blyth EM, Dolman AJ, Noilhan J (1994) The effect of forest on mesoscale rainfall: an example from HAPEX-MOBILHY. *Journal of Applied Meteorology*, **33**, 445-454.

Boles SH, Verbyla DL (2000) Comparison of three AVHRR-based fire detection algorithms for Interior Alaska. *Remote Sensing of Environment*, **72**, 1-16.

Bourgeau-Chavez, LL, Alexander, ME, Stocks, BJ, Kasischke, ES (2000) Distribution of forest ecosystems and the role of fire in the North American boreal region. In ' Fire, Climate Change, and Carbon Cycling in the Boreal Forest'. (Eds ES Kasischke and BJ Stocks), pp. 111-131. (Ecological Studies 138: Springer Verlag)

Campbell ID, Flannigan MD (2000) Long-term perspectives on fire-climate-vegetation relationships in the North American boreal forest. In ' Fire, Climate Change, and Carbon Cycling in the Boreal Forest'. (Eds ES Kasischke and BJ Stocks), pp. 151-172. (Ecological Studies 138: Springer Verlag)

Chambers SD (1998) Short- and long-term effects of clearing native vegetation for agricultural purposes. Ph.D Thesis, School of Earth Sciences, The Flinders University of South Australia, Bedford Park, South Australia 169pp.

Chambers SD, Chapin FS III (2003) Fire effects on surface-atmosphere energy exchange in Alaskan black spruce ecosystems: implications for feedbacks to regional climate. *Journal of Geophysical Research* **108** (D1), 8145, doi:10.1029/2001JD000530.

Chambers SD, Beringer J, Randerson J, Chapin FS III (Submitted) Canopy controls of net radiation and energy partitioning following fire in Alaskan black spruce and tundra ecosystems. *Agriculture and Forest Meteorology*.

Clark JS (1988) Effect of climate change on fire regimes in northwestern Minnesota. *Nature* **334**, 233-235.

Claussen M (1987) The flow in a turbulent boundary layer upstream of a change in surface roughness.

*Boundary Layer Meteorology* **40**, 31-86.

Cotton WR, Pielke RA (1995) Human impacts on weather and climate. Cambridge University Press, New York 288 pp.

Court A, Griffiths JF (1992) Thunderstorm climatology. In 'Thunderstorm Morphology and Dynamics'. (Eds E Kessler). pp. 9-40.(University of Oklahoma Press.)

Gallant AL, Binnian EF, Omernik JM, Shasby MB (1996) Ecoregions of Alaska: U.S. Geological Survey Professional Paper 1567, 73 p. 1 plate [map folded in pocket], scale 1:5,000,000.

Global Atmospheric, Inc. Written comm. from Global Atmospheric to AFS containing estimated lightning strike detection efficiency and location accuracy of the ALDF and IMPACT sensors. Letters dated May 18, and September 7 1995.

Grice GK, Comisky AL (1976) Thunderstorm climatology of Alaska. NOAA Technical Memorandum, NWS AR-14.

Henderson-Sellers A, Robinson PJ (1986) Contemporary Climatology. 439 pp. (Longman Scientific and Technical / Wiley and Sons, Inc.: New York)

Henry DM (1978) Fire occurrence using 500mb map correlation. NOAA Technical Memorandum, NWS AR-21, 31 pp.

Hu FS, Brubaker LB, Anderson PE (1993). A 12000 year record of vegetation change and soil development from Wien Lake, central Alaska. *Canadian Journal of Botany* **71**, 1133-1142.

Huntrieser H, Schiesser HH, Schmid W, Waldvogel A (1997) Comparison of traditional and newly developed thunderstorm indices for Switzerland. *Weather and Forecasting* **12**, 108-125.

Huschke RE (1959) Glossary of Meteorology. 638p. (American Meteorological Society: Boston)

Intergovernmental Panel on Climate Change (IPCC) (1996) Climate Change 1995: The Science of Climate Change. Contribution of Working Group I to the Second Assessment Report of the Intergovernmental Panel on Climate Change (Eds JJ Houghton, LG Meiro Filho, BA Callander, N Harris, A Kattenberg and K Maskell). 572 pp. (Cambridge University Press: Cambridge and New York)

Kasischke ES, Christensen NL Jr., Stocks BJ (1995) Fire, global warming, and the carbon balance of boreal forests. *Ecological Applications* **5**, 437-451.

Klaassen W (1992) Average fluxes from heterogeneous vegetated regions. *Boundary-Layer Meteorology*, **58**, 329-354.

Knowles, JB (1993) The influence of forest fire induced albedo differences on the generation of mesoscale circulations. M.S. Thesis. Department of Atmospheric Science, Colorado State University, 86 pp.

Koutsias N, Karteris M (2000) Burned area mapping using logistic regression modeling of a single post-fire Landsat-5 Thematic Mapper image. *International Journal of Remote Sensing* **21**, No.4, 673-687.

Labau VJ, Van Hess W (1990) An inventory of Alaska's boreal forests: their extent, condition, and potential use. In Proceedings of the International Symposium Boreal Forests: Condition, Dynamics, Anthropogenic Effects. 16-26 July 1990, Archangel, Russia. State Committee of USSR, part 6. Moscow. pp. 30-39.

Li C, Flannigan MD, Corns IGW (2000) Influence of potential climate change on forest landscape dynamics on West-Central Alberta. *Canadian Journal of Forest Research* **30**, 1905-1912.

Lynch JA, Clark JS, Bigelow NH, Edwards ME, Finney BP (2003). Geographic and temporal variation in fire history in boreal ecosystems of Alaska. *Journal of Geophysical Research* **108** (D1), 8152, doi:10.1029/2001JD000332.

Mahrt L, Sun J, Vickers D, MacPherson, JI, Pederson JR, Desjardins RL (1994) Observations of fluxes and inland breezes over a heterogeneous surface. *Journal of the Atmospheric Sciences* **51**, 2484-2499.

McGuire AD, Melillo JW, Kicklighter DW, Joyce LA (1995) Equilibrium responses of soil carbon to climate change: empirical and process-based estimates. *Journal of Biogeography* **22**, 785-796.

Murphy PJ, Mudd JP, Stocks BJ, Kasischke ES, Barry D, Alexander ME, French NHF (2000) Historical fire records in the North American boreal forest. In 'Fire, Climate Change, and Carbon Cycling in the North American Boreal Forest' (Eds ES Kasischke and BJ Stocks), pp. 274-288. (Springer-Verlag: New York)

Pielke RA, Avissar R, Raupach M, Dolman H, Zeng X, Denning S (1998) Interactions between the atmosphere and terrestrial ecosystems: Influence on weather and climate. *Global Change Biology* **4**, 461-475.

Pielke RA, Vidale PL (1995) The Boreal Forest and the Polar Front. *Journal of Geophysical Research* **100** (D12), 25,755-25,758.

Reap RM (1994) Analysis and prediction of lightning strike distributions associated with synoptic map types over Florida. *Monthly Weather Review* **122**, 1698-1715.

Samuelsson P, Tjernström M (2001) Mesoscale flow modification induced by land-lake surface temperature and roughness differences. *Journal of Geophysical Research* **106** (D12) 12,419-12,435.

Schneider SH (Ed.), (1996) *Encyclopedia of Climate and Weather*. 929pp. (Oxford University Press)

Schroeder MJ, Buck CC (1970) Fire weather. Agriculture Handbook 360, U.S. Department of Agriculture, Forest Service 229 pp.

Segal M, Arritt RW (1992) Nonclassical mesoscale circulations caused by surface sensible heat-flux gradients. *Bulletin of the American Meteorological Society* **73** (10), 1593-1604.

Serreze MC, Walsh JE, Chapin FS, Osterkamp T, Dyurgerov M, Romanovsky V, Oechel WC, Morison J, Zhang T, Barry RG (2000) Observational evidence of recent change in the northern high-latitude environment. *Climatic Change* **46**, 159-207.

Shuttleworth WJ (1988) Macrohydrology: the new challenge for process hydrology. *Journal of Hydrology* **100**, 31-56.

Smith TM, Leemans R, Shugart HH (1992) Sensitivity of terrestrial carbon storage to CO<sub>2</sub>-induced climate change: comparison of four scenarios based on general circulation models. *Climatic Change* **21**, 367-384.

Stull, RB (1988) *An Introduction to Boundary Layer Meteorology*, 670 pp. (Kluwer Academic Publishers: Dordrecht)

Van Cleve K, Vierick LA (1981) Forest succession in relation to nutrient cycling in the boreal forest of Alaska. In 'Forest Succession: Concepts and Application' (Eds D West, H Shugart, D Botkin) pp 185-211. (Springer-Verlag: New York)

Vidale PL, Pielke RA, Steyaert LT, Barr A (1997) Case study modeling of turbulent and mesoscale fluxes over the BOREAS region. *Journal of Geophysical Research* **102** (D24) 29,167-29,188.

Vierick LA (1973) Wildfire in the taiga of Alaska. *Quaternary Research* **3**, 465-495.

Weaver CP, Avissar R (2001) Atmospheric disturbances caused by human modification of the landscape. *Bulletin of the American Meteorological Society*, **82** 269-281.

Weaver CP, Baidya Roy S, Avissar R (2002) Sensitivity of simulated mesoscale atmospheric circulations resulting from landscape heterogeneity to aspects of model configuration. *Journal of Geophysical Research* **107** (D20), 10.1029/2001JD000376.

Weiss CE, Purdom JFW (1974) The effect on early morning cloudiness on squall line activity. *Monthly Weather Review* **102**, 400-402.



Whitaker RH (1975) *Communities and Ecosystems*. 2<sup>nd</sup> Edition, 385 pp. (Macmillan: New York)

Williams AG (1991) Internal structure and interactions of coherent eddies in the lower convective boundary layer. Ph.D Thesis, School of Earth Sciences, The Flinders University of South Australia, Bedford Park, South Australia 207pp.

Yarie J (1981) Forest fore cycles and life tables: a case study from Interior Alaska. *Canadian Journal of Forest Research* 11 (3), 554-562.

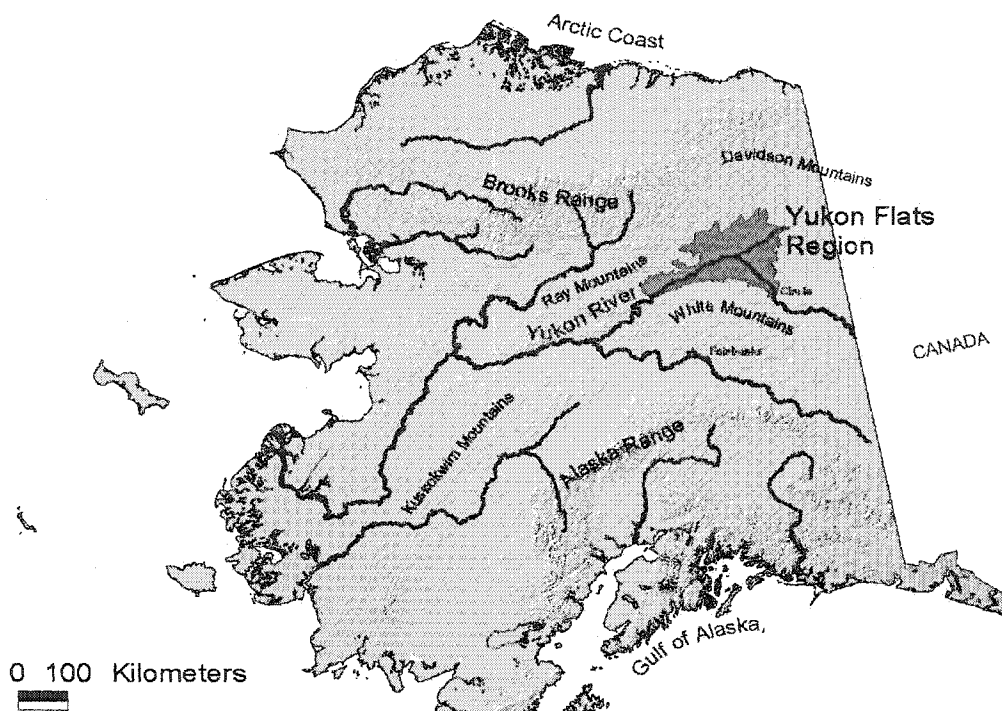


Figure 3.1. The location of the Yukon Flats study region in the Eastern part of Interior Alaska.

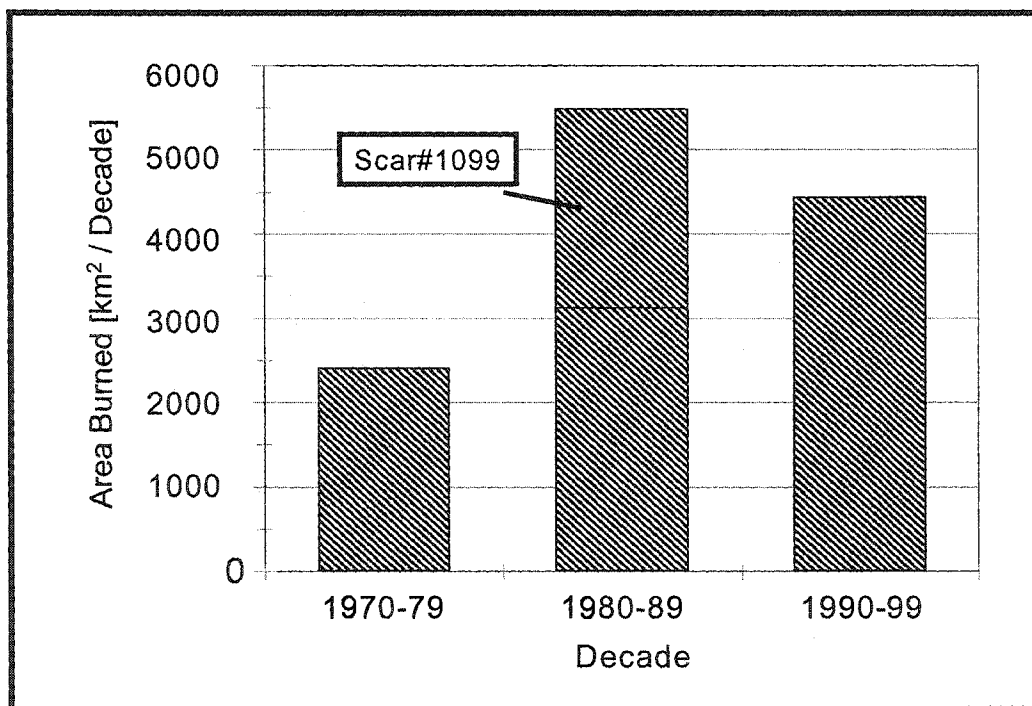


Figure 3.2. Acreage of historic burns in the Yukon Flats. The top portion of the 1980-89 bar is due to a single burn scar (#1099). This big burn scar is the only of the top 7 burns with respect to acreage that did not burn in the 1950's.

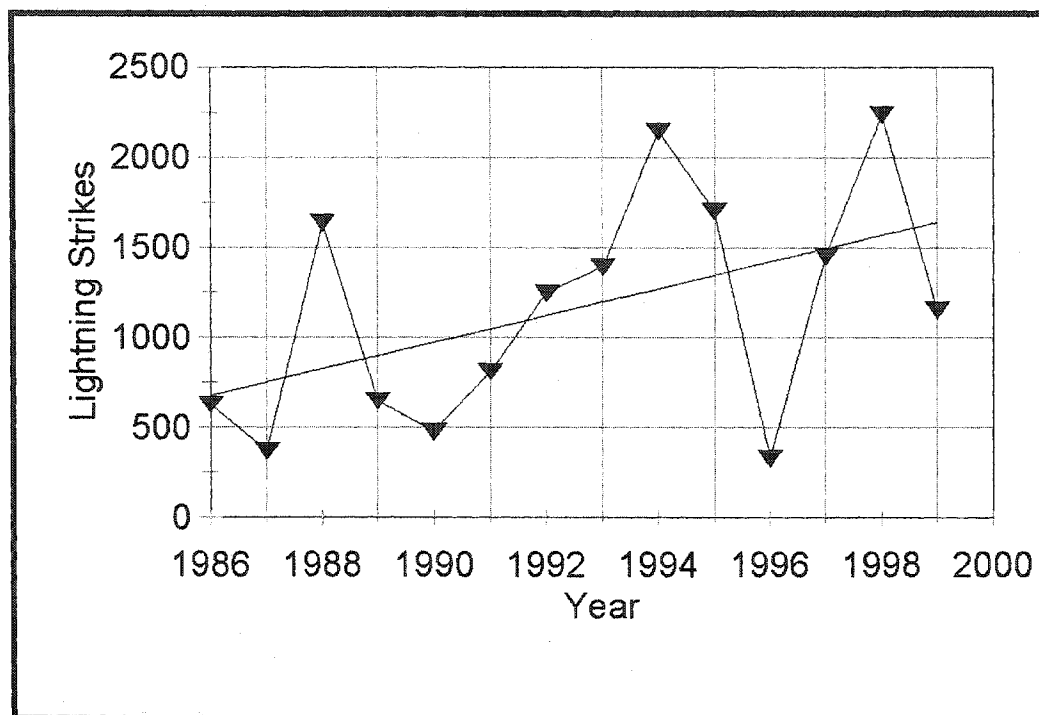


Figure 3.3. Time series of Cloud to Ground-lightning strikes in the Yukon Flats from 1986-1999. The straight line represents the trend (linear regression line).

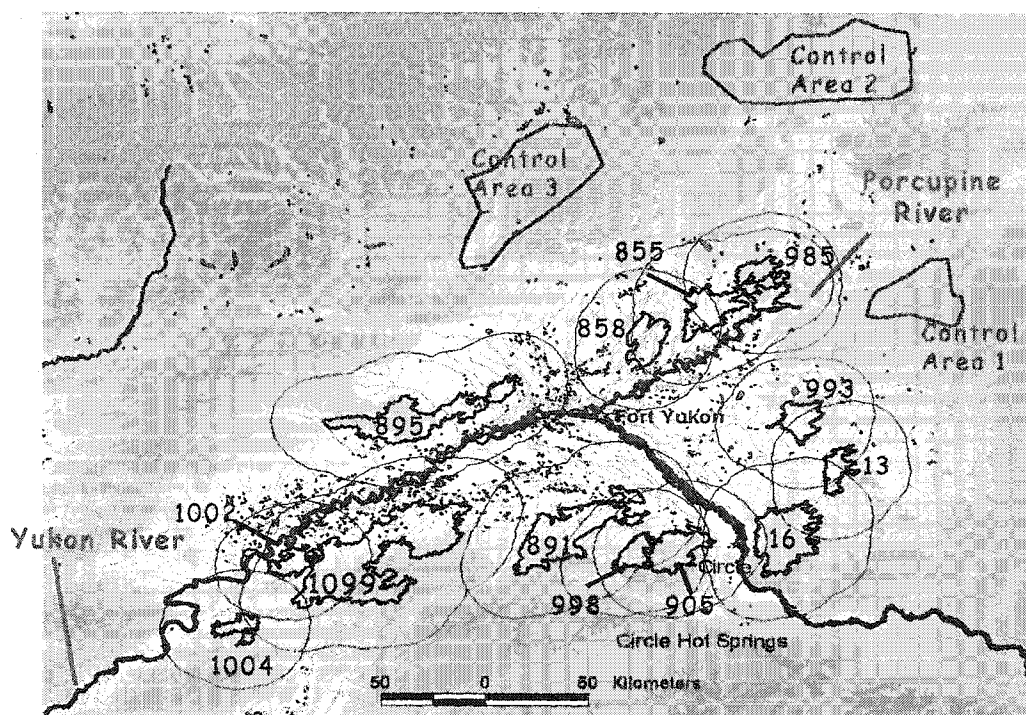


Figure 3.4. Yukon Flats study area and the 13 selected wildfire burn scars with identification numbers. 25km buffers around each burn scars denote the surrounding area used for the study.

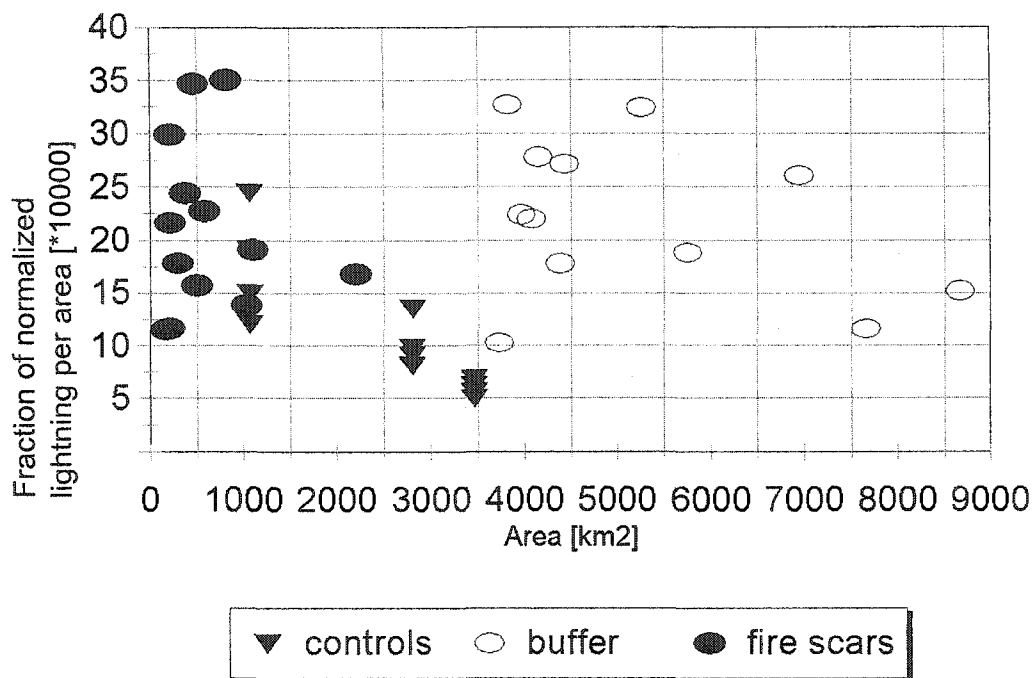


Figure 3.5. Normalized lightning strike density at the burn scars, buffers, and control areas.

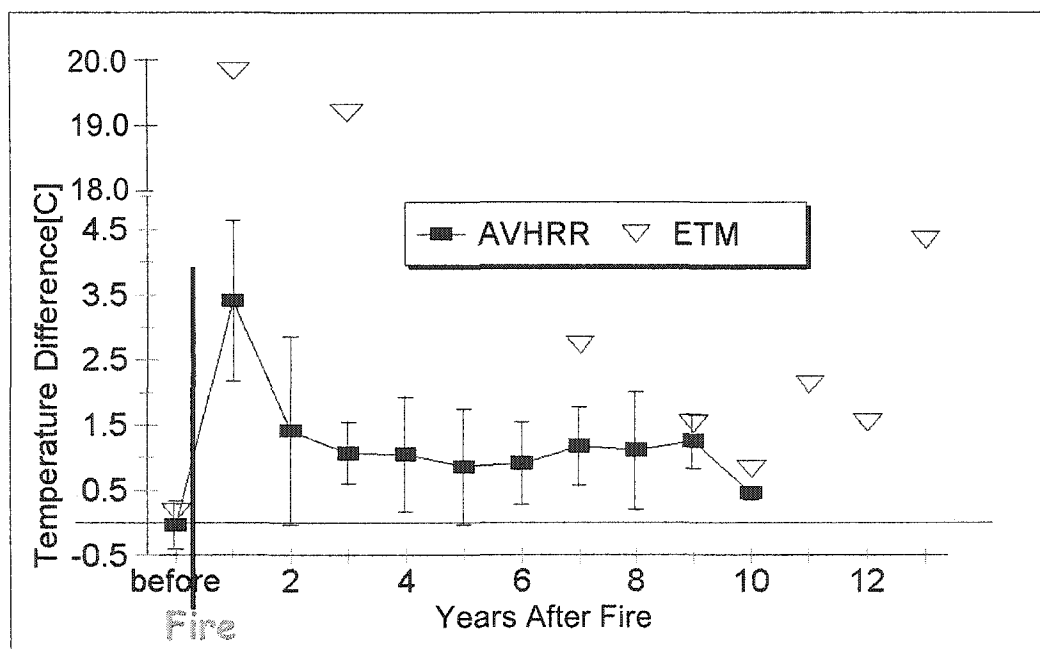


Figure 3.6. Time series of radiant temperature derived from AVHRR (1989-99 data) and Landsat ETM (1991-2001) satellite images. The values represent the mean difference between the burn scars and the surrounding unburned areas (buffers), and the error bars around the AVHRR data points are  $\pm 1$  standard deviation. The data are shown as a function of years before or post-fire. The numbers are sample sizes (number of scar-buffer pairs) represented by the individual data points.

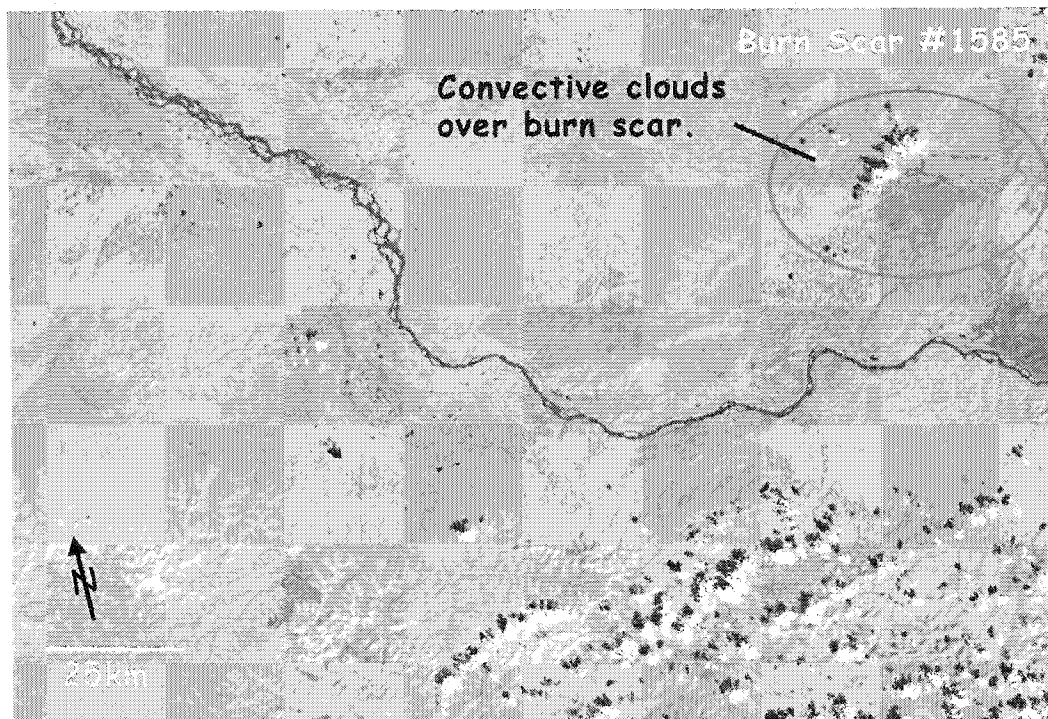


Figure 3.7. Cloud “chasing” image number 1. Image is from June 24 2000. The burn scar is 154km<sup>2</sup>, burn scar#1585. The fire burned the year before the image was taken, in 1999.

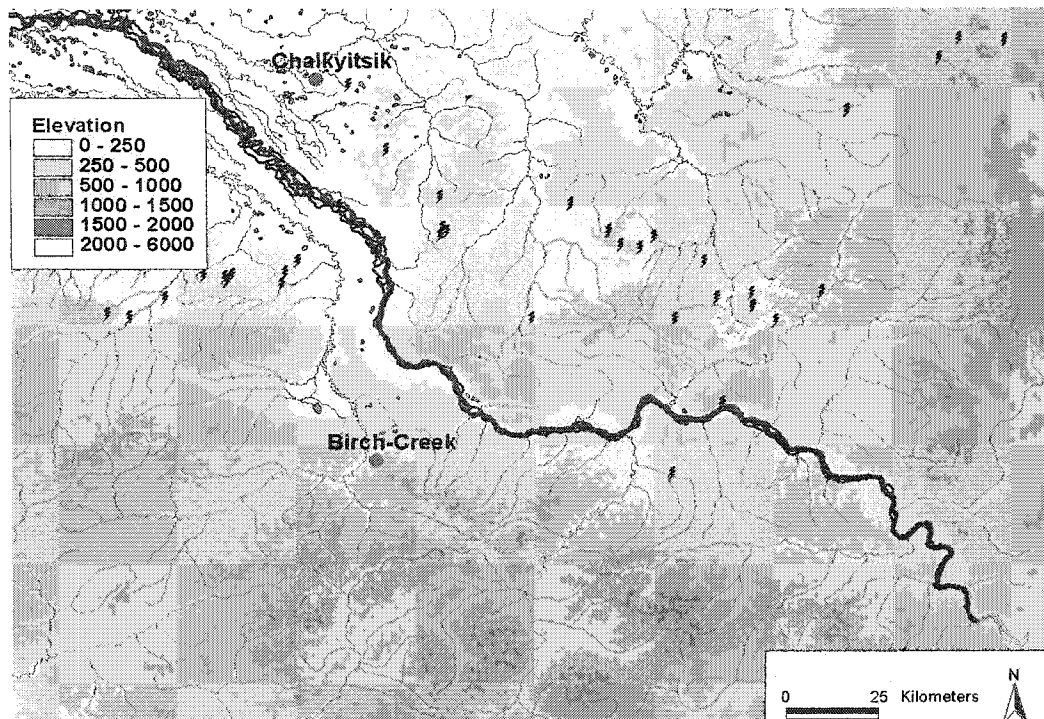


Figure 3.8. Terrain features and rivers within the area represented in figure 3.7 and surroundings. Burn scar#1585 is shown in outline as a point of reference.

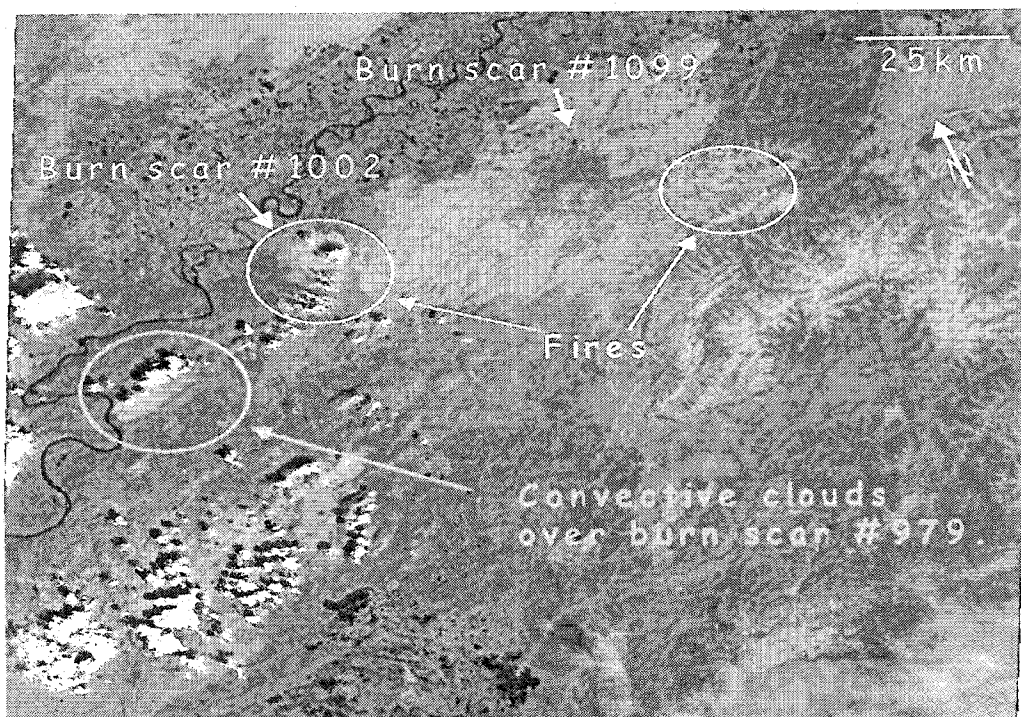


Figure 3.9. Cloud "chasing" image number 2. Image is from June 29 1991. The burn scar is 110km<sup>2</sup>, burn scar#979. The fire burned the year before the image was taken, in 1990.

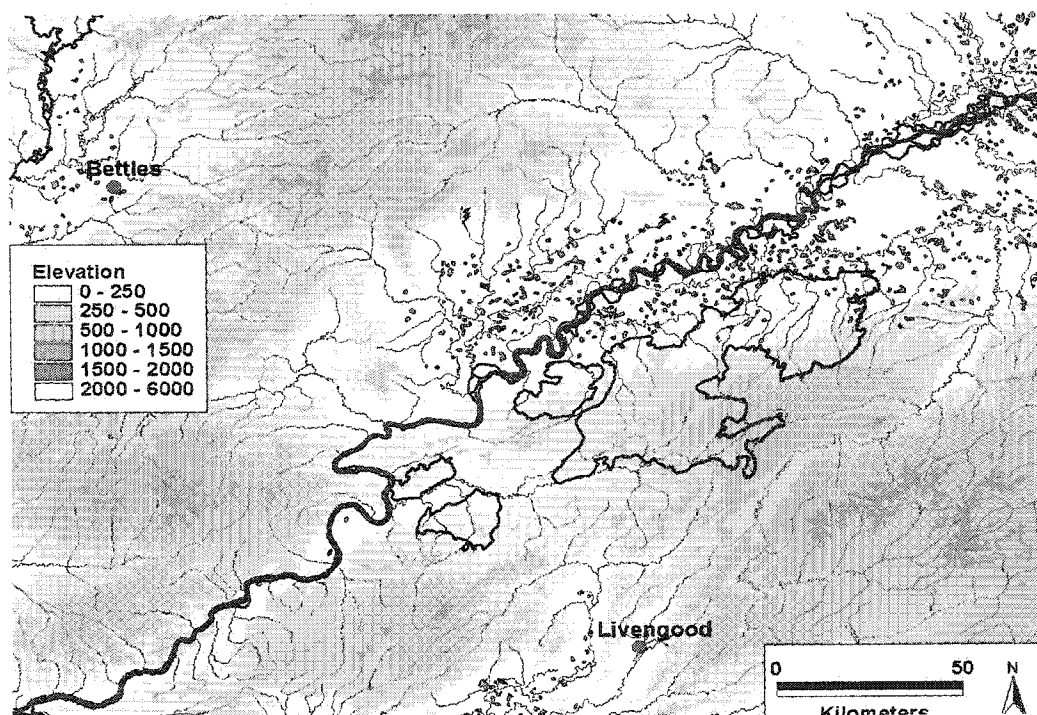


Figure 3.10. Terrain features and rivers within the area represented in figure 3.9 and surrounding area. Burn scar#979 1002 1004, and 1099 are shown in outline as points of reference.

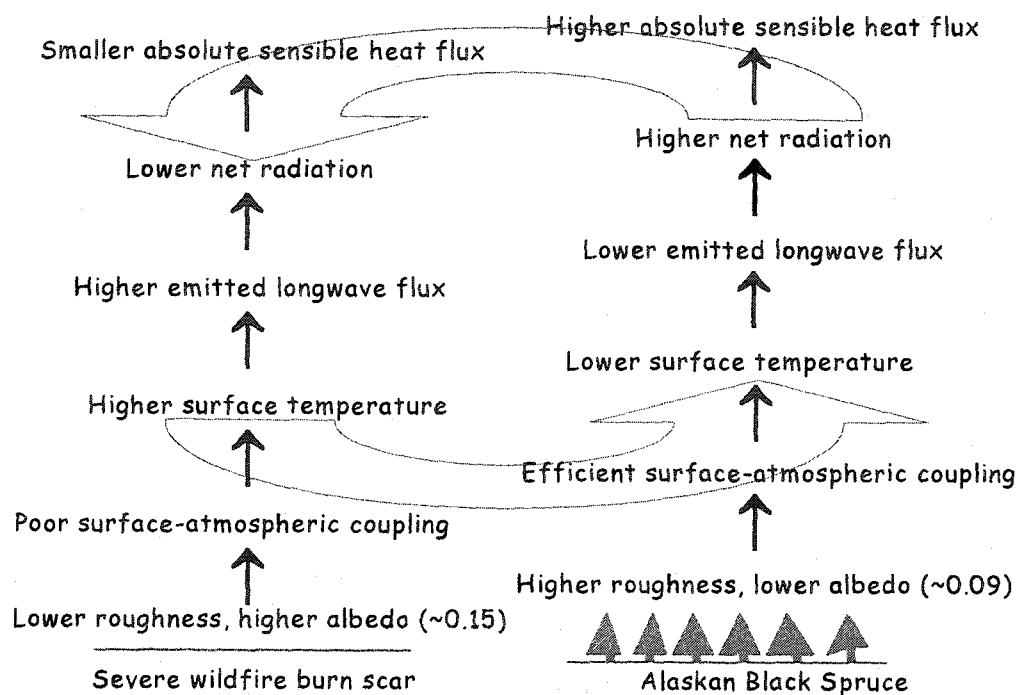


Figure 3.11. Conceptual model of the initiation of a NCMC across a burn scar boundary in the early post-fire succession stages. 3-15 years post-fire as surface roughness gradually increases in the burn scar there is a dramatic increase in albedo ( $\alpha = 0.15$ ) that perpetuates the reduced net radiation and sensible heat fluxes.

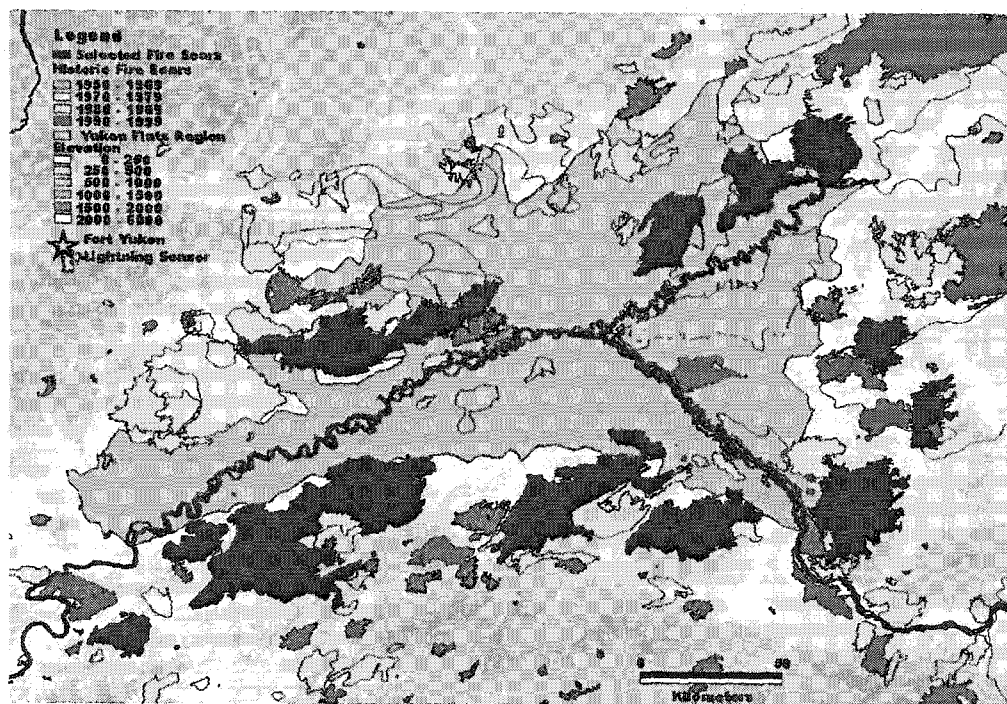


Figure 3.12. The wildfire burn scar mosaic of the Yukon Flats, showing our selected 13 scars along with historic scars from 1950-1999.

Table 3.1. Spatial and temporal resolution of AVHRR, Landsat 4, 5 TM, Landsat 7 ETM, and GOES 10.

Satellite	Spatial Resolution	Temporal Resolution
Landsat 4,5 TM	30m / 60m thermal	Every 16 days
Landsat 7 ETM	30m / 60m thermal	Every 16 days
AVHRR	1.09km	Twice a day
GOES	1-4km	Every half hour



Table 3.2. Independent variables, their representation and predicted correlation for multiple linear regression model runs.

Variable Name	Representation	Expected Correlation
Mean slope (buffer and scar)	Trigger	Positive
Max.slope (buffer and scar)	Trigger	Positive
Mean elev. (buffer and scar)	Trigger	Positive
Elev. range (buffer and scar)	Trigger	Positive
Max.Elev. (buffer and scar)	Trigger	Positive
Year of fire	Interannual variation in lightning	?
Scar size	Perturbed area (NMC)	Positive
Buffer size	Undisturbed area (NMC)	Negative
%of scar covered by old burn scars from 1970-79	Heterogeneity of perturbed area, burn severity, strength of potential circulation	Positive?
%of scar covered by old burn scars from 1980-89	Heterogeneity of perturbed area, burn severity, strength of potential circulation	Positive?
%of scar covered by old burn scars from 1990-99	Heterogeneity of perturbed area, burn severity, strength of potential circulation	Positive?
%of buffer covered by old burn scars from 1970-79	Heterogeneity of undisturbed area, strength of potential circulation	Negative
%of buffer covered by old burn scars from 1980-89	Heterogeneity of undisturbed area, strength of potential circulation	Negative
%of buffer covered by old burn scars from 1990-99	Heterogeneity of undisturbed area, strength of potential circulation	Negative
Diff. in mean radiant temperature between scar and buffer - AVHRR	Net radiation, strength of potential circulation	Positive
NDVI std.dev. (scar)	Heterogeneity of perturbed area, burn severity, strength of potential circulation	Negative
NDVI std.dev (buffer)	Heterogeneity of undisturbed area, burn severity, strength of potential circulation	Negative
%conifers in burn scar	Post-fire successional stage, strength of potential circulation	Negative
%deciduous in burn scar	Post-fire successional stage, strength of potential circulation	Positive
%conifers in buffer	Landscape successional stage, strength of potential circulation	Positive
%deciduous vegetation in buffer	Landscape successional stage, strength of potential circulation	Negative

Table 3.3. Typical range of values for albedo, emmissivity, and bowen ratio for deciduous, black spruce, and burn scars. It also shows that emmissivities of burned and unburned areas are similar. Sources for numbers: 1) Eugster et al. 2000; 2) Pielke and Avissar 1990; 3) Chambers and Chapin 2003; 4) Oke 1987; 5) Betts and Ball 1997; 6) Pattey et al. 1997.

	Deciduous	Conifer	Burn Scar
Albedo	0.15-0.20 <sup>2</sup>	0.08-0.09 <sup>5</sup> , 0.10-0.15 <sup>2</sup>	0.04-0.12 <sup>3</sup>
Bowen Ratio	0.2-0.7 <sup>1</sup>	1.18-1.53 <sup>6</sup> , 0.7-3.6 <sup>1</sup>	-----
Emmissivity	0.95 <sup>2</sup> , 0.97-0.98 <sup>4</sup>	0.95 <sup>2</sup> , 0.97-0.98 <sup>4</sup>	asphalt 0.95 <sup>4</sup>

Table 3.4a. Normalized lightning within burn scars

scar#	13	16	855	858	891	895	905	985	993	998	1002	1004	1099
before	1.37	2.61	2.14	1.47	2.64	1.60	2.75	1.18	1.07	2.10	0.27	0.25	4.24
after	0.66	2.66	0.96	0.69	2.27	1.61	1.76	0.68	0.47	0.38	0.19	0.24	3.77
difference	-0.71	0.05	-1.19	-0.78	-0.37	0.01	-0.99	-0.50	-0.61	-1.72	-0.08	-0.01	-0.47
%diff	-51.64	1.80	-55.43	-53.06	-13.99	0.73	-36.08	-42.46	-56.48	-81.72	-29.52	-4.49	-11.03

Table 3.4b. Normalized lightning within buffer areas

scar#	13	16	855	858	891	895	905	985	993	998	1002	1004	1099
before	15.50	20.87	17.59	13.07	26.77	8.65	14.15	9.50	18.63	11.42	3.72	6.38	12.49
after	8.27	15.94	9.04	7.24	16.49	9.77	13.32	6.40	8.55	12.58	4.63	6.04	16.17
difference	-7.23	-4.93	-8.55	-5.82	-10.28	1.11	-0.83	-3.11	-10.07	1.16	0.91	-0.34	3.67
%diff	-46.65	-23.63	-48.61	-44.56	-38.39	12.88	-5.90	-32.68	-54.09	10.19	24.48	-5.36	29.41

Table 3.4c. Normalized lightning within control areas

"Fire yr"/ control area	1988 1	1988 2	1988 3	1990 1	1990 2	1990 3	1991 1	1991 2	1991 3	1993 1	1993 2	1993 3
before	4.71	3.78	8.17	3.11	3.17	5.12	3.36	2.83	4.64	2.86	2.42	3.84
after	1.90	2.02	2.60	1.64	1.99	2.60	1.78	2.17	2.80	1.62	2.40	3.19
difference	-2.81	-1.75	-5.58	-1.47	-1.18	-2.52	-1.59	-0.66	-1.84	-1.24	-0.02	-0.65
%diff	-59.57	-46.41	-68.23	-47.39	-37.34	-49.22	-47.13	-23.16	-39.61	-43.48	-0.82	-16.84

Table 3.5a. scars

	13	16	855	858	891	895	905	985	993	998	1002	1004	1099	P2	P	sign?	n
12after-12before	11.57	-54.20	-13.90	-52.65	-24.20	114.87	111.23	22.35	228.49	-51.56	-52.15	13.20	-2.89	2728.07	<10 <sup>-6</sup>	yes	13
34after-12before	73.43	53.00	-70.09	-19.71	-1.91	137.70	70.55	-42.95	-43.63	-47.36	-74.89	-77.67	3.87	4.77	0.965	no	13
56after-12before	-86.57	-74.38	-66.40	-76.18	-52.53	281.33	248.95	-32.09	11.71	52.81	-60.31	61.20	-51.9	16.36	0.175	no	13
78after-12before			-43.11	-16.98	61.63	171.49	89.12	-49.51	-81.52	-71.72	-52.43	57.57	55.89	6.14	0.803	no	11

Table 3.5b. buffers

	13	16	855	858	891	895	905	985	993	998	1002	1004	1099	X2	P	sign?	n
12after-12before	-40.48	-32.54	-48.61	-44.56	-38.39	16.17	166.99	-17.04	6.27	96.77	468.41	89.96	29.41	69.00	<10-6	yes	13
34after-12before	50.27	41.49	-44.93	-48.81	-30.27	44.55	85.82	-48.06	-60.37	26.49	34.30	-62.79	22.35	30.98	0.002	yes	13
56after-12before	-79.23	-75.91	-60.31	-32.59	-60.66	151.64	250.29	-8.12	-22.54	357.82	277.18	55.15	-30.70	169.19	<10-6	yes	13
78after-12before			-36.55	-13.41	8.45	59.74	158.89	-58.32	-83.97	5.12	242.33	10.29	151.50	68.11	<10-6	yes	11

Table 3.5c. controls

"Fire yr" / control	1988 1	1988 2	1988 3	1990 1	1990 2	1990 3	1991 1	1991 2	1991 3	1993 1	1993 2	1993 3
12after-12before	-33.85	-41.92	-68.31	6.94	-45.04	-9.81	-78	-32	-37	-11	3	-40
34after-12before	-65.84	-62.71	-77.29	15.28	-78.33	-84.41	-105	-33	-57	27	132	233
56after-12before	-63.17	-85.29	-96.07	29.29	54.08	192.12	-85	48	139	-14	75	23
78after-12before	-58.70	4.56	-26.45	-26.06	-48.02	23.70	-106	12	-11			



Table 3.6. Extracted data of lightning strike densities (lightning per unit area) within the burn scars, buffers, and control areas from Fig. 3.5.

Lightning Strikes per Area	Control	Scars	Buffers
above 15	2	10	11
below 15	10	3	2
total	12	13	13
%above 15	17	77	85

Table 3.7. The AVHRR post-fire temperature differences were significantly different from the pre-fire temperatures ( $p < 0.0001$ ). The Landsat post-fire temperature differences were also significantly different from the pre-fire temperatures ( $p = 0.0016$ ).

Data set	Time period	Mean radiant temperature difference (scar-buffer) [EC]	Standard deviation [EC]
AVHRR	pre-fire	-0.03	0.37
AVHRR	post-fire (3-7 yrs)	1.06	0.69
Landsat	pre-fire	0.17	0.55
Landsat	post-fire(7-13 yrs)	1.86	1.39

Table 3.8. Multiple linear regression results for lightning changes in burn scars. Only the variables that entered the model are included in the table. The variables “in” or “out” refers to the overlap with older burn scars in the scar and buffers, respectively.

dependent	independent	p_value	adj r2	std err est	std err intercept	beta(1)	intercept	n	F	sign?
scar lightning	meanrad	0.044	0.26	72.76	51.31	0.566	-88.10	13	5.18	yes
	lightning									
	scarConifer	0.330	0.0032	84.35	63.99	-0.290	79.94	13	1.04	no
	scarDeciduous	0.085	0.18	76.67	59.05	0.495	-84.84	13	3.57	no
	All	0.0026	0.98	11.77	45.06	see below	-524.27	13	68.36	yes
	meanrad					1.240				yes
	scarDeciduous					0.321				yes
	scar size					-0.950				no
	scar-std (ndvi std)					2.110				no
	buffer-std (ndvi-std)					-1.900				no
	scarConifer					0.843				no
	bufferDeciduous					-0.200				no
	buffer size					0.301				no
	in1980-89%					0.078				no

Table 3.9. Multiple linear regression results for lightning changes in buffers. Only the variables that entered the model are included in the table. The variables “in” or “out” refers to the overlap with older burn scars in the scar and buffer, respectively.

dependent	independent	p-value	adj r2	std err est	std err	beta(1)	intercept	n	F	sign?
buffer	scar size	0.32	0.008	150.91	64.43	-0.300	106.71	13	1.09	no
	Mean elevation	0.277	0.025	149.57	195.11	0.326	-162.6	13	1.31	no
lightning	in1970-79%	0.104	0.150	139.55	95.31	-0.470	95.31	13	3.14	no
	out1970-79%	0.11	0.144	140.12	59.51	0.464	-22.85	13	3.025	no
	out1980-89%	0.121	0.132	141.14	55.55	0.452	-10.69	13	2.82	no
	scar-std (ndvi std)	0.34	0.0012	151.39	149.19	-0.290	199.76	13	1.015	no
	buffer-std (ndvi-std)	0.21	0.059	146.91	184.10	-0.370	293.63	13	1.759	no
	All variables	0.042	0.997	8.62	11519.39	see below	-156201	13	336.62	yes
	in1970-79%					-1.500				yes
	Year of fire					0.927				yes
	bufferDeciduous					-0.270				no
	buffer-std (ndvi-std)					-1.400				no
	buffersize					2.040				no
	scarConifer					0.343				no
	bufferConifer					-0.150				no
	scar size					-1.300				no
	scar-std (ndvi std)					1.610				no
scarDeciduous					-0.400				no	
out1970-79%					0.051				no	

## Chapter 4<sup>5</sup>. Thunderstorm Activity in Interior Alaska for the Summer of 2001

### Abstract

We compiled thunderstorm statistics for the summer 2001 season in Alaska by examining the links between the thunderstorm potential as represented by Convective Available Potential Energy (CAPE) and Lifted Index (LI), surface characteristics, as represented by forest coverage and elevation, thundercloud occurrence and lightning strike frequency. In general, the spatial relationships between CAPE, LI, thunderclouds and lightning match well. Thunderstorm potential, as described by CAPE shifts from east towards the western part of the study area through the season. LI was a slightly better than CAPE in predicting lightning strike frequency and occurrence in Alaska. CAPE and LI values were smaller than values typical for lower latitudes. The use of vegetation and elevation information with the indices improved diagnostic skill for all longitude zones and for both thundercloud and lightning strike frequency by about 9% on average. The amount of explained variation in lightning strike activity and thundercloud occurrences in many cases was more than 30% larger on airmass than on synoptic days, suggesting that the underlying surface has more of an influence on thunderstorm development on days with airmass storms than on days with synoptic storms.

---

5

This paper was prepared as a manuscript to be submitted to the Journal of Applied Meteorology under the same title by Dorte Dissing, Peter Q. Olsson, and Dave Verbyla

#### 4.1. Introduction

General Circulation Models predict that the largest climatic changes will occur at high latitudes (IPCC, 1996). Recent observations support these predictions (Serreze *et al.*, 2000). This had led to predictions of increased fire frequency in the boreal forest as the climate warms (Kasischke *et al.*, 1995; Li *et al.*, 2000). In many areas of the boreal forest, lightning strikes are the primary cause of large wildfires (Kasischke *et al.*, In Press).

Most publications on lightning and thunderstorms in the U.S. do not even mention Alaska or include the state on their storm distribution maps (Court and Griffiths, 1992; Price and Rind, 1994; Schneider, 1996). However, lightning is responsible for more area burned in Alaska annually than in any other state in the U.S. This is because most forest fires result from lightning activity, occur in remote areas that are difficult to access, have a low priority for fire suppression, and are very expensive to control (Chapin *et al.*, 2003). In Alaska, little research has been done on the relationships between lightning strike activity, thundercloud development and the effectiveness of convective indices. This study sets out to examine these relationships.

In general, thunderstorm formation requires a conditionally unstable airmass, sufficient moisture<sup>6</sup> in the lower atmosphere (<3km), and a triggering mechanism to initiate convective activity (Henderson-Sellers and Robinson, 1986; Schneider, 1997; Huntrieser *et al.*, 1997). The unstable airmass ensures that an air parcel, if lifted sufficiently, will become positively buoyant and continue to rise to its equilibrium level (EL). The moisture provides the thunderstorm with energy through the release of latent heat after the air parcel is raised to its lifted condensation level or LCL (Grice and Comisky, 1976; Schneider, 1996). Some triggering mechanism often initiates and focuses the lifting and is usually caused by one or more of: (i) surface heterogeneities (in the case of a convective boundary layer), (ii) mesoscale forcing (orographic or frontal), (iii) low-level convergence (Schroeder and Buck, 1970), or (iv) upper-level short waves.

---

<sup>6</sup> The amount of moisture (to be "sufficient") will depend upon the strength of convection (whether it is deep enough to reach the lifting condensation level) and the vertical profile of virtual potential temperature (which dictates how much latent heating is required before free convection starts, and what the vertical extent will be) (Stull, 1988).

In this study, we group thunderstorms into two broad categories; “localized air-mass” and “widespread synoptic” events. Air-mass<sup>7</sup> thunderstorms form as isolated storms in confined areas and often result from air-mass interactions with the underlying surface. For example, topography and vegetation distribution influence the development and location of thunderstorms and lightning strikes (Byers and Braham, 1949; Hane *et al.*, 1997; Sturtevant, 1995; Dissing and Verbyla, 2003; Burrows *et al.*, 2002). In contrast, synoptic thunderstorms are typically formed by lifting associated with fronts (Biswas and Jayaweera, 1976). Air-mass thunderstorms are classified as either convective or orographic, although these lifting processes often work in combination with each other (Schroeder and Buck, 1970). In Interior Alaska, low-level advection of marine air masses inland provides the moisture that fuels air-mass thunderstorms, since boundary layer moisture sources in the Interior are relatively limited. Dry air-mass thunderstorms (Schroeder and Buck, 1970), are especially important as wildfire starters since their high cloud-base often results in little accompanying precipitation (less than 0.25cm, <http://www.spc.noaa.gov/>). The lack of moisture in these storms increases the probability of ignition (Rorig and Ferguson, 1999).

Throughout a thunderstorm season, most days with recorded lightning in Alaska are due to air-mass storms formed in the absence of significant large-scale circulation (Biswas and Jayaweera, 1976; Henry, 1978). These air-mass thunderstorms start most of the lightning-caused fires in Interior Alaska (Henry, 1978). However, most of the total number of lightning strikes in Interior Alaska are due to synoptic events (Fig. 4.1). For example, during summer of 1999 more than 20% of the total annual lightning strikes were due to lightning from a single day.

In Alaska, thunderstorms have been studied using satellite imagery (Biswas and Jayaweera, 1976), and inferred from analyzing lightning strike data (Reap, 1991; Dissing and Verbyla, 2003). An alternative way to examine thunderstorm development, and the approach we implement here, is by diagnostic indices of atmospheric instability and thunderstorm potential.

---

<sup>7</sup> An air-mass is defined as any widespread body of air that is approximately homogeneous in its horizontal extent, particularly with reference to temperature and moisture distribution; in addition, the vertical temperature and moisture variations are approximately the same over its horizontal extent (Huschke, 1959).

#### 4.1.a. Background

Static stability is related to the existence and severity of convective activity as conditionally unstable air provides a higher potential for the upward motion needed for convective storms; the faster the upward motion, the greater the potential severity of the storm. In general, indices of atmospheric instability and thunderstorm potential combine factors important for convective activity, such as thermal and moisture properties and wind shear in the lower atmosphere (Blanchard, 1998). These indices summarize the potential convective state of the atmosphere with one number.

The Lifted Index (LI) (Galway, 1956) represents a combined measure of the temperature and moisture conditions important for thunderstorm development. LI is calculated by subtracting the observed temperature at 500mb from the temperature of a parcel (with the mean potential temperature and mixing ratio in some arbitrarily layer, typically near the surface) lifted pseudo-adiabatically to that pressure level. This provides a measure of the “excess” temperature (Galway, 1956), with negative values signifying positively buoyant parcels, and the most unstable soundings yielding large negative LI (Table 4.1). Modifications of the LI exist, such as the Best Lifted Index and the Model Lifted Index (Doswell et al, 1991). Solomon and Baker (1994) found LI to be poorly correlated with lightning occurrence in New Mexico. They found that air at the cloud base levels came from the 700-800mb layer, not the surface level as assumed when calculating LI, suggesting that LI by itself may not be an adequate tool for predicting or diagnosing lightning activity.

Convective Available Potential Energy (CAPE) has been described as the ultimate index of latent instability (Darkow, 1992), because it is based on data from entire atmospheric soundings as opposed to most other instability indexes (Doswell *et al.*, 1991). CAPE was first introduced by Moncrieff and Miller (1976) and has roots in basic thermodynamic concepts.

Graphically, CAPE (usually expressed in units of  $\text{Jkg}^{-1}$ ) is proportional to the positive area on a true thermodynamic diagram (e.g., skew-T, log-P Hess) between the ambient temperature profile and the thermodynamic trajectory of a lifted parcel (Fig. 4.2). It represents the potential buoyant energy of an air



parcel lifted to the level of free convection (LFC). The lifting agent could be a front, a jet streak, forced upslope flow over terrain, or buoyancy resulting from solar heating. Energy is released by latent heat of condensation from the air as the parcel rises above its LCL. Thunderstorm development is possible if the parcel rises to its LFC. High CAPE values correspond to potentially severe convective activity (Table 4.2).

Correlations between CAPE and LI will reveal the fraction of the CAPE variation that is due to instability. The remaining part of the CAPE variation is caused by factors such as the depth and distribution of CAPE in the layer between the LFC and EL, as viewed on a skew-T diagram (Blanchard, 1998). In a study from high thunderstorm frequency areas of the contiguous U.S., almost 50% of the variation in CAPE was shown to be due to stability (Blanchard, 1998).

Important factors influencing the size of CAPE are the temperature and mixing ratio of the lifted parcel, and the environmental temperature above the LFC. Boundary layer depth, temperature and moisture, are a function of entrainment from above and sensible and latent heat fluxes from below (Garrett, 1982). The surface fluxes in turn depend on surface characteristics such as vegetation cover, stomatal resistance, soil moisture and roughness length (Garrett, 1982; Oke, 1987).

The shape of the positive area can provide information about the nature of the potential convection. The positive area tends to be tall and narrow for oceanic environments and short and wide for continental environments (Blanchard 1998). Oceanic convection has weaker updrafts than continental convection at similar CAPE values (Wicker and Cantrell, 1996).

Several studies have found high CAPE values correspond to high lightning frequencies for continental air masses, and low CAPE values corresponded to low lightning frequencies for maritime air masses (Williams *et al.*, 1992; Rutledge *et al.*, 1992). However, other studies, conducted both in the tropics and in Alberta, Canada, found weak to no positive correlations between cloud-to ground lightning frequency and CAPE (Molinié and Pontikis, 1995; Petersen *et al.*, 1996; Anderson, 1991). To our knowledge, a CAPE climatology of Interior Alaska has never been synthesized.

In this paper we examine three factors that potentially influence thunderstorm development in Interior Alaska: meteorology, elevation, and vegetation. The objective is to understand the relative contribution of each potential factor, not to develop a new forecasting tool. The two main objectives of this paper are: (1) to develop a thunderstorm climatology for the summer season of 2001 by examining the spatial distribution of CAPE, LI, thundercloud occurrences and lightning strikes and their relationships to the underlying surface and, (2) to evaluate CAPE and LI as diagnostic indicators of convective and lightning activity in Interior Alaska under various meteorological conditions.

#### 4.2. Study area

This study focused on Interior Alaska (Fig. 4.3), a region where most thunderstorms develop without the influence of synoptic-scale weather systems (Biswas and Jayaweera 1976; Henry 1978). Almost 90% of all recorded lightning strikes in Alaska occur in the Interior, defined as the region bounded in the north by the Brooks Range and in the south by the Alaska Range (Fig. 4.3). It is largely restricted to a single water source for atmospheric moisture - the Bering Sea- because of the barriers provided by the bounding mountain ranges to the north and south, and the relative aridity of interior N. Canada. Maritime moisture is transported from west to east across the region by large-scale advection (Reap 1991; Sullivan 1963). Boreal forest is the dominant biome in the Interior region, covering 63% of the total area (Labau and VanHess, 1990). The dominant vegetation changes from boreal forest to tundra with increasing proximity to the coast as a result of the west-east moisture and temperature gradients. The central and eastern regions of the Interior experience large annual temperature extremes, with relatively hot summers (Hammond and Yarie 1996). Despite the low moisture gradient, there is generally sufficient moisture available throughout the Interior to fuel thunderstorms.

Since airmass thunderstorms are speculated to be strongly influenced by the underlying surface, we used a physiographic classification of Interior Alaska, based primarily on physical landscape features such as relief and proximity to major rivers (Fig. 4.3), as a spatial reference for discussion in this study. In this

way, we can link thunderstorm potential and activity regions to the physical features of the surface. There is an east-west climate gradient (from maritime to continental) across the study region. We therefore divided the study region into east-west longitudinal sectors of  $4^\circ$  width (Fig. 4.4). Here, we shall refer to each longitudinal sector by its eastern longitude. For example "zone 144" refers to the sector spanning 144-148°W. The furthest east zone is only  $3^\circ$  wide, due to lack of data on the Canadian side of the Canada-Alaska border (longitude 141°W). Each zone is 50,000-150,000km<sup>2</sup> in area, representing the upper end of the mesoscale.

### 4.3. Methods

#### 4.3.a. Lightning data

Lightning data from 2001 were used as a primary indicator of thunderstorm development, though not all convection produces lightning. The data were obtained from an automated network of cloud-to-ground lightning sensors, operated by the Bureau of Land Management Alaska Fire Service (Reap, 1991). This network consists of nine stations in Alaska and three in the Yukon Territory. It was implemented for fire management purposes and therefore explicitly records cloud-to-ground (CG) lightning strikes. The lightning strike data within the interior region are assumed to have a positional accuracy of 0.5 - 4km and a detection efficiency of 60-80% in Interior Alaska (Global Atmospheric, Inc, written communication).

The position of a lightning strike is estimated by triangulation. Consequently, a strike is recorded only if it is detected by more than one sensor. Positional accuracy of estimated lightning strike locations vary with the number of detectors sensing the strike, and with detector location geometry (Hiscox *et al.*, 1984). The data recorded for each detected strike include time, estimated location (x, y coordinates), and the positional accuracy of the strike. Studies concerning detection efficiency and location accuracy have not been done in Alaska. However, Idone *et al.* (1998a,b) did a performance evaluation comparing the network lightning data with video-derived locations of cloud-to-ground lightning and found a median location accuracy of two to four km, and a detection efficiency of 67-86% in eastern New York. Throughout this

paper, a “lightning strike” refers to a recorded CG lightning discharge as detected by the network sensors. Nothing is inferred about whether a particular strike causes ignition, and no other lightning strikes than CG are included.

#### *4.3.b. Satellite data*

As an independent measure of thunderstorm activity, satellite images were used to map probable thunderclouds based on cloud-top temperatures. Radiant temperatures were derived from NOAA Advanced Very High Resolution Radiometer (AVHRR) data. AVHRR were available for every afternoon during the Alaskan thunderstorm season of 2001 (May-August). Radiant temperatures were derived from the thermal channel four data, which have a spatial resolution at nadir of one km. The data were obtained from the NOAA Satellite Active Archive website (<http://www.saa.noaa.gov>). The daily AVHRR data were sought as close to the hour of maximum lightning activity (Fig. 4.5) in Alaska as possible.

#### *4.3.c. Elevation and vegetation data*

Terrain height / relief and vegetation have been shown to influence the development and location of thunderstorms and lightning strikes (Byers and Braham, 1949; Hane *et al.*, 1997; Sturtevant, 1995; Dissing and Verbyla, 2003; Burrows *et al.*, 2002). We obtained spatial terrain height (hereafter referred to as “elevation”) and vegetation data from the Alaska Geodata Clearinghouse ([www.agdc.usgs.gov](http://www.agdc.usgs.gov)). An elevation grid at 1km cellsize was derived from United States Geological Survey 1:250,000 series digital elevation models, and for this study aggregated as a 45km mean elevation grid.

We used a vegetation grid produced by Markon *et al.* (1995) at 1km cellsize. The vegetation classes were produced using an unsupervised classification of 1991 multi-temporal AVHRR Normalized Difference Vegetation Index data (NDVI, Markon *et al.* 1995). Forest coverage may be an important vegetational factor for predicting areas of thunderstorm / lightning activity (Dissing and Verbyla, 2003). In this study we aggregated the 1km vegetation grid into a 45km areal coverage [%] forest grid (Fig. 4.4).

#### *4.3.d. Meteorological data*

The meteorological potential for thunderstorm development was assessed using two convective indices: CAPE and LI. Indices are ideally based on the observed data from atmospheric soundings. However, operational soundings are taken at only two locations in Interior Alaska (Fairbanks and McGrath). Therefore, since the observations needed to construct maps of the spatial distribution of CAPE and LI are not available, we have used gridded data from the National Centers for Environmental Prediction (NCEP) / NOAA Eta model. Data output from the model were archived at the International Arctic Research Center (IARC) in Fairbanks, Alaska for the summer of 2001. The Alaska data is from the Eta 216 grid at 45km resolution. The data spans most of the thunderstorm season (May-August) of 2001 (Table 4.3). The Eta data of interest to us for this study is not typically archived for this grid. Fortunately, 216 grid data was archived for 2001 only and represents a rare opportunity for us to utilize this data in a region with very sparse observations.

The Eta initial objective analysis was derived from atmospheric soundings, surface observations, satellite data, flight data and several other sources. The spatial scale of the native Eta grid cells is 22 km square in the horizontal dimension, with 50 vertical levels. The vertical layers are more closely spaced in the planetary boundary layer and near the upper level jet (~ 250hPa) to more accurately resolve these regions (Chuang and Manikin, 2001). The special Eta coordinate system incorporates a smoothed elevation component to account for mesoscale phenomena in mountainous areas. The elevation is represented as a step function, which is rounded off to the nearest pressure level.

Since the data used in this study does represent a modeled surface, we decided to compare data from the original two afternoon soundings from Fairbanks and McGrath (Fig. 4.3) with data from the two corresponding 45km by 45km grid cells in the Eta model. The sounding data is archived by the Dept. of Atmospheric Science University of Wyoming in Laramie.

### 1) CAPE

CAPE calculations are very sensitive to the thermodynamic properties (temperature and mixing ratio) of the parcel being lifted. No standard method exists as to which parcel to lift, nor to the depth of the layer within which this parcel would be found (Doswell and Rasmussen, 1994). The Eta post-integration analysis software selects the parcel with the warmest equivalent potential temperature in the lowest 70mb above the model surface (Zhang and McFarlane, 1991). The parcel is then lifted from its LFC to its EL (Fig. 4.2). As the parcel is lifted, the positive area within each layer is accumulated as CAPE (Chuang and Manikin, 2001).

### 2) LI

All LI from the Eta model output are computed as the temperature difference between a lifted parcel and the ambient temperature at 500mb. The LI used in this study is the “Best (4 layer) Lifted Index”. This is obtained by using the most negative LI from lifting parcels in several constant layers (Chuang and Manikin, 2001).

#### *4.3.e. CAPE and LI climatology*

To produce a spatial climatology of thunderstorm indices and their seasonal variations, daily maps of CAPE and LI were produced for two-week time periods over the 2001 summer. An isodata clustering algorithm (Ball and Hall, 1965) was used to group cells with similar daily values in the n-dimensional space. This way we could determine areas that tended to have high CAPE (or low LI) versus areas that tended to have lower CAPE (or higher LI) values, thus giving information about the persistence of the thunderstorm potential. In addition, we tabulated the mean CAPE and LI values for each cluster. The maps of the two-week clusters were visually compared with the thundercloud and lightning strike spatial distributions.

The isodata algorithm is based on a migrating means technique often used as a base for unsupervised classifications, which here produced 3 classes. The maps produced with the resulting unsupervised classification were used for the visual subjective comparisons.

#### 4.3.f. *Thundercloud analysis*

An afternoon AVHRR satellite image was acquired for every day throughout the season as close to mean peak lightning activity and hour of CAPE / LI fields as possible. Thunderclouds were mapped based on a channel 4 radiant temperature threshold value for the cloud tops of  $-25^{\circ}\text{C}$ . Physically, this threshold value coincides with the formation of graupel (Zajac and Weaver, 2002), which by several studies have been found to correlate with the initial electrification process in a cloud (Dye *et al.*, 1986). Biswas and Jayaweera (1976) used a threshold temperature for cloud tops colder than  $-28^{\circ}\text{C}$  as their definition of thunderclouds in Alaska. It is generally agreed that the anvil portion of the thundercloud is colder than  $-40^{\circ}\text{C}$  (Uman, 1984; Henderson-Sellers and Robinson, 1991; Wallace and Hobbs, 1977) depending on the height of the tropopause.

A threshold value of  $-25^{\circ}\text{C}$  means that high-level clouds and towering cumulus clouds may have been mapped in the thundercloud category. As the images included in this study represent an instantaneous snapshot, convective clouds developing earlier or later in the day would be missed. Therefore, we chose to include too many, rather than too few clouds with our threshold value and to call the category “thunderclouds”, as opposed to Cumulonimbus (Cb) clouds. High level stratus clouds, which would be misclassified as thunderclouds in this scheme, were assumed to be fairly rare over Interior Alaska during the summer.

Maps of thundercloud occurrences were used to compare, verify and evaluate the utility of the convective indices. These maps were grouped into two-week segments. The total number of daily thundercloud presences derived from AVHRR cloud top temperatures were summed up to produce

thunderstorm frequency maps for each two-week segment and each 45km grid cell. The spatial and temporal scales were the same as the CAPE and LI grids to allow for easy comparisons.

#### *4.3.g. Lightning strike climatology*

As a further verification and evaluation of the convective indices, maps of lightning strike data were produced. The daily lightning data complements the satellite data by directly measuring electrical activity in convective systems not captured by an afternoon satellite image. The total lightning for each two-week period was summed to produce spatial distribution maps for each 45km grid cell, corresponding to the CAPE and LI gridded data.

#### *4.3.h. Statistical analysis*

Most of air-mass thunderstorms in Alaska were expected to be influenced by the underlying surface. We therefore examined the effects of surface properties (elevation and areal coverage of forest) on the convective indices. These relationships were studied along a climatological transect from continental to maritime, represented by longitudinal 4° wide sectors from the eastern Interior west to the Seward Peninsula. The relationships were studied for the entire period, as well as for two separate data sets representing the airmass and synoptic thunderstorm days. Days with more than 1000 strikes were classified as synoptic, and days with less than 1000 strikes were classified as airmass days.

The data sets were constructed as follows (Fig. 4.6). For each day and longitudinal transect, all variables (CAPE, LI, number of thundercloud occurrences, lightning strike count, mean elevation, and percentage of each cell covered by forest) were recorded for every 45km cell. Within each longitudinal zone, data for all the days over the season (May - August) were summarized by averaging the changing independent variables (CAPE, LI, and thundercloud occurrence) for cells with similar lightning strike frequency. For the variables which remained constant throughout the season (elevation and forest coverage), we instead summarized lightning frequency and thundercloud occurrences for each cell and used that as a



base for the regression analysis. Each data point was weighted within the analysis based on the number of cells it represented. This procedure was repeated for each longitude zone (six zones), by thunderstorm “mode” (all days, airmass days, and synoptic days), resulting in 18 data sets.

Stepwise multiple regression of each of these data sets was used to evaluate both the relationships between the thunderstorm potential and the underlying surface, and the usefulness of CAPE and LI as thunderstorm and lightning indicators for Alaska. This was done by regressing lightning as a function of vegetation, elevation, CAPE, LI, (CAPE, vegetation and elevation), (LI, vegetation and elevation), and thundercloud occurrences. Thundercloud occurrences were regressed as a function of the same variables.

Additionally, some data verification and representativeness of the 2001 summer was tested. The CAPE and LI data from the Eta initialization grid was compared to CAPE and LI values calculated from the sounding data at the two sites at Fairbanks and McGrath. The 2001 data on lightning, temperature and precipitation was compared to existing longer term data sets to assess the representativeness of the 2001 summer.

#### **4.4. Results**

##### *4.4.a. Seasonal variations in CAPE and LI*

The isodata clustering grouped cells that had similar temporal CAPE and LI patterns and allows us to easily determine the spatial variation in high thunderstorm potential for each two-week segment. However, the cluster analysis does not seek to make the mean CAPE value of each cluster the same between the time periods. The maximum CAPE value for any of the clustered groups this season,  $1373\text{Jkg}^{-1}$ , was obtained during the July\_2 time period (Table 4.4). Generally, the highest values were found during the two time segments in July. The CAPE groups are classified as 3 clusters, based on spatial distributions in the two-week segments (eight segments). The clusters with the highest numeral have the largest mean CAPE values (Table 4.4). Some time periods did not have enough data for the classification (2<sup>nd</sup> 2 weeks of June, all of August).

In general, the continental (eastern) half of the study area had higher CAPE values than the maritime (western) half (Figs. 4.7a, b), in agreement with the tendency for higher maximum diurnal temperatures in this region. As the season progressed, the high CAPE values tended to migrate towards the western half. Thus, for the first time period of May\_1, a high convective potential appears in the southeastern Interior, whereas the highest thunderstorm potential appeared in the southwestern part of the area for the August\_2 time period. This time segment shows the largest area of high thunderstorm potential, extending throughout the entire region.

The cluster analysis of 2-week segments for LI is organized in a like manner to the CAPE cluster analysis. The lowest LI values have the highest cluster numeral. Thus the least stable cells, which will have low LI values, have the higher cluster numeral. LI values in general are high (Table 4.5), as compared to the values from Table 4.2. The minimum LI for any cluster were not always below 0°C. This shows that, just as is the case for CAPE, values for Alaska differ relative to lower latitudes (Table 4.1, 4.2). The mean values of maximum CAPE and minimum LI for 5 days with "Alaska severe" (synoptic thunderstorms) and 4 days of "Alaska not severe" (air-mass thunderstorms) are not significantly different from each other, but the maximum and minimum values were (Table 4.6).

To further illustrate this point, we used the results from the multiple regression analysis, and produced CAPE and LI values corresponding to lightning strike frequencies for weak, moderate and strong convective activity based on Alaskan values (Tables 4.7 and 4.8). These computed LI values are very low (Table 4.7). In fact, the values are lower than the "very unstable" category of Table 4.1 already at weak to moderate convective activity, and such low values as in the "very strong convective activity" case do not occur in the data we analyzed.

The computed CAPE values were similarly low (Table 4.8), and were almost as incompatible with the values of severe conditions in the contiguous United States (Table 4.2) as the LI values were. Indeed, the CAPE values were so low, that even for the very severe Alaska days, the CAPE values are not above the "little to none" convective potential values shown in Table 4.2.

The least stable air (cluster 3, low LI values) was in the eastern (continental) half of the study area, and these values did not vary appreciably through the season (Figs. 4.8a, b). Data for LI were unavailable for the month of July. In general, the areas of least stable air as predicted by LI were less widespread than the areas of high thunderstorm potential as predicted by the CAPE index, and the index never reached negative values the furthest west and northwestern areas of the study region.

#### *4.4.b. Seasonal variation in thundercloud occurrence*

The most frequent cold cloud top occurrences are concentrated in the southeastern quarter of the study area (Figs. 4.9a, b), in the regions of White Mountains, Kantishna River, Tanana and Tetlin Flats. In general, there is a fairly good agreement between the spatial distribution of thunderclouds and the lightning strikes throughout the season. However, there is a surprising lack of cold cloud tops in the images analyzed for the June\_2 period; a period with relatively frequent thunderstorms in Interior Alaska, as supported by the lightning strike data. Given the great length of the heating period at these high latitudes, we speculate that the thunderstorms occurred later on in the day, causing the images, centered around 4pm ADT, to miss the thunderclouds. May, July, and August show more cold cloud tops than June. During late July and August, colder cloud tops appear further west, in the Kuskokwim Mountains, Nulato Hills and on the Seward Peninsula.

#### *4.4.c. Seasonal variation in lightning strike distribution*

In accordance with the thermodynamic indices, lightning strike activity is concentrated in the eastern part of the study area (Figs. 4.10a, b). The thunderstorm season starts in May, where few lightning strikes occurred during 2001 (Table 4.9). During June, scattered lightning “hot spots” appear in the Ray and White Mountains, and in the Yukon and Kantishna River Flats. During July the regions of high lightning activity stay fairly concentrated in the White Mountains, Yukon Uplands and Kantishna River Flats. Typically the end of July to early August begins the rainy season, characterized by nonconvective stratiform

precipitation, ending the fire season. The low lightning strike activity in the August\_1 time period illustrates this. However, lightning strike activity increases again in the late August time segment. However, more than 50% of the lightning within the August\_2 time period was due to lightning from just two days of strong convection.

#### *4.4.d. Regression analysis*

Regressions predicting thundercloud occurrences had higher  $r^2$  than regressions predicting lightning strike frequency (Fig. 4.11). LI is a better predictor of both thundercloud occurrence and lightning strike frequency than CAPE at all longitudes (Fig. 4.11), with the exception of the very extreme continental and maritime zones (140 and 160). This trend is clear on airmass days, but not on synoptic days.

To understand the impact of land surface characteristics, the underlying surface was parameterized by two variables - percent forest, and mean elevation. Individually, vegetation and elevation can explain up to 36% (mean value 12%) and 48% (mean value 8%), respectively, of the variation in lightning strike frequency and thundercloud occurrences (Table 4.10). When vegetation and elevation was added to LI or CAPE as the explaining (independent) variables, the amount of explainable variation increased (Fig. 4.11). This was true for all longitude zones and for both thundercloud and lightning strike frequencies.

For the continental longitude zones of 140 - 152, the independent variables CAPE and LI with the additional vegetation and elevation information result in higher  $r^2$ -values for airmass days than for synoptic days. The daily temporal distribution of lightning activity showed that most of the lightning in all six zones occurred between 1pm and 6pm ADT (Fig.4.12), which is the time window most favorable for surface heating and thus airmass thunderstorms. However, in the maritime zone 160, almost 50% of the total seasonal lightning occurred outside this time period (Fig. 4.12f).

The largest differences in  $r^2$  values between airmass and synoptic days were found in zones 144, 152 and 160 (Figs. 4.11c, e). In many cases the explained variation was more than 30% larger on airmass days than on synoptic days. There were mostly minor differences in zones 140 and 156, and in these two

zones, the predictions were generally better on synoptic days than on airmass days. Regression  $r^2$ -values generally increase from the continental to the maritime zones, for all days, airmass and synoptic days. The largest variation across the longitudinal transects between the  $r^2$  values occur on the synoptic days.

There was a seasonal variation in lightning strike frequency between the longitudinal zones. In the two most continental zones (140, and 144) most of the lightning (all days) occurred in the month of July (Fig. 4.14). In zone 152, most lightning occurred in June, whereas for the two western zones (156 and 160), most lightning happened in August (Fig. 4.14). Zone 148 shows a transition from July to June lightning, with approximately 40% of the registered lightning in each of those two months. The number of lightning strikes within each zones decreases rapidly towards the western zones, and the seasonal lightning statistics for these zones are therefore heavily influenced by the two days of severe storm activity August 26-27. Thus whatever mechanisms inhibiting convection in the two most continental zones was not preventing it in zones 148 and 152. The number of lightning strikes within each zone decreases rapidly towards the western zones, and the seasonal lightning statistics for these zones are therefore heavily influenced by the two days of severe storm activity August 26-27. Evidence of the storm activity from these two days can be seen in Fig. 4.10b.

Thundercloud occurrences and lightning strike frequency are not perfectly correlated. Frequently, CAPE and LI are better predictors for lightning strike frequency than thunderclouds, especially on synoptic days (Fig. 4.11e). We tested the correlation between CAPE and LI, similarly to Blanchard (1998) and found comparatively very high  $r^2$ -values, ranging from 0.92 in zone 140 to 0.61 in zone 148 (Table 4.11).

A comparison between the appropriate cells of the modeled Eta data for CAPE and LI and CAPE and LI calculated for the soundings at Fairbanks and McGrath had correlations up to 0.9 (Table 4.12).

Since our data for this study only spans one summer, it is important to test the representativeness of this summer in relation to the “normal” conditions in Interior Alaska. The temporal distribution of the 2001 summer lightning strike data diverts from a typical Alaska season, as defined by the mean values for the 1986-99 period, with less lightning strikes in the July\_1 and August\_1 periods, and more strikes in the

August\_2 period (Fig. 4.15). We compared climatological data for eight Interior Alaska stations for the summer 2001 with a mean value for the 1950-2002 time period (Fig. 4.12). The temperature and precipitation data were judged “normal” if they fell within  $\pm 1$  standard deviation of the long-term mean value. The data shows a generally cool May with normal precipitation in Interior Alaska (Fig. 4.12). June was within normal warm, but drier than normal, July temperatures were within normal cool, but wetter than normal, and August had normal temperatures, but was on the dry side of normal.

#### 4.5. Discussion

In general, the spatial relationships between CAPE, LI, thundercloud occurrence and lightning match well. There was a discrepancy between the indices and the thundercloud and lightning strike spatial distribution data for the 2-week periods where high instability, as indicated by CAPE, LI, and areas of high thundercloud occurrence, extend further to the northwest into Selawik Flats and Seward Peninsula than do the lightning strike data. This suggests that while the convective potential exists in the northwestern Alaska region (e.g., cold mid and upper-tropospheric temperatures), the inhibiting factors (e.g., low insolation due to low-level stratiform cloud cover) are too large for the instability to be realized.

The area of high lightning strike activity extended further north into the Yukon Flats and Uplands, and northern White Mountains than do the thundercloud occurrence and high CAPE values (Figs. 4.7, 4.8, 4.10). Since the AVHRR images used here are for the mean hour of maximum activity for the entire state, thunderclouds occurring much later or earlier than 4pm ADT would not be detected by the images. A closer look at the hours of lightning activity happening north of the Arctic Circle ( $\sim 66^\circ\text{N}$ ) reveals that more lightning strikes occur earlier in the day (1-2pm) than for the state as a whole (Fig. 4.5).

The months of May and June showed some disagreement between the convective indices, thundercloud occurrences, and lightning strike activity (Figs. 4.7, 4.8, 4.9, 4.10). However, the temperature records for May 2001 reveals a relatively cool month in the Interior (Fig. 4.13). During early May, much of

Interior Alaska may have snow on the ground. Thus, surface heating probably was insufficient to develop a deep convective boundary layer conducive to air mass thunderstorm development.

We tested the correlation between thundercloud occurrences and lightning strike frequency for all the longitudinal zones, and found that the two variables are not perfectly correlated (Fig. 4.11). Just as frequently, CAPE and LI are better predictors of lightning strike frequency than thundercloud occurrence (as we have defined it) (Fig. 4.11). Several factors are important here, as not all thunderclouds produce lightning and not all lightning is registered by the detection network, only CG lightning. Additionally, the thundercloud occurrences are a snapshot for a given day, coincident with the thunderstorm indices and the mean hour of maximum lightning strike activity, whereas the lightning data are included for the entire day.

There was a good correlation between CAPE and LI for all longitudinal zones ( $r^2$ -values of 0.61-0.92). According to Blanchard (1998), these correlations show that 60-90% of the variation in CAPE is due to instability, the rest is due to factors like the vertical distribution of CAPE. The  $r^2$ -values of the CAPE - LI relationship found in this study were higher than the ones reported by Blanchard (1998), which were typically around 50%. Blanchard's study was based on data from the contiguous United States, which typically has more deeply penetrating convection. In Alaska the CAPE is confined to lower atmospheric levels, thus limiting the variation in vertical CAPE distribution that were observed in Blanchard's study.

The relationship between the convective activity and the underlying surface was examined by the use of two variables, percent forest and mean elevation within each 45km cell, in addition to the thermodynamic indices and observed convective activity variables. Individually, vegetation and elevation typically explain about 10% (mean value) of the variation in daily lightning strike frequency and thundercloud occurrences (Table 4.10). The addition of vegetation and elevation information increased the regression adjusted  $r^2$  of the convective indices for all longitude zones and for both thundercloud and lightning strike frequency predictions by ~9%

We found that the days classified as air mass were more similar to the general scenario as characterized by all the days in the study than were the days classified as synoptic (Figs. 4.11a,c,e) with

respect to lightning strike frequency. Few days are classified as synoptic, though the large spread in  $r^2$ -values which occur within these days could be due to a large variation in thunderstorm development processes on these days. A large fraction of the annual lightning is due to thunderstorms on the days we have classified as synoptic. This has a large effect on the maritime zones, which receive less lightning than the continental zone. Maybe this is why the diagnostic indices capture more of the variation in lightning strike frequency in the maritime than in the continental zones (Fig. 4.11), explaining the general trend towards higher  $r^2$ -values in the maritime zones.

The high  $r^2$ -values encountered when adding elevation and vegetation to the diagnostic equations suggest these factors provide additional information about factors influencing thunderstorm development that is not incorporated into the Eta initialization grids. We also found that the amount of explained variation in lightning strike activity and thundercloud occurrences in many cases were more than 30% larger on airmass than on synoptic days (Fig. 4.11). This agrees with earlier studies (Garrett, 1982; O'Neal, 1996; Dissing and Verbyla, 2003) which suggested that the underlying surface has more of an influence on convective development on days with airmass storms than on days with synoptic storms. The daily temporal distribution of lightning activity supports this argument. Most lightning occurred between 1pm and 6pm ADT (Fig. 4.12); the time window most favorable for diurnal surface heating and consequent airmass thunderstorms. In the maritime zone however, almost half of the total seasonal lightning did not occur in this time period.

For the maritime zone, airmass thunderstorms are not as common, and most lightning strikes are likely due to synoptic conditions. Therefore, surface properties such as vegetation and elevation would not have as great an influence on the lightning strike distribution as in the continental climate regimes. This is also supported by the fact the vegetation and elevation is negatively correlated with lightning strike frequency and thundercloud occurrence in zones 156 and 160, whereas mostly positive correlations occur in the continental zones.



In evaluating CAPE and LI as convective activity and lightning strike frequency indicators, we found that LI was a better indicator of both thundercloud occurrence and lightning strike frequency than CAPE at all longitudes, except for the very extreme continental and maritime zones (140 and 160) where the predictive strengths of the two indices were essentially equal (Fig. 4.11). CAPE and LI at all longitude zones were better predictors of thundercloud occurrences than of lightning strike frequency. It is important to note that not all thunderstorms produce CG lightning, explaining in part why a variable can be a good index for convective cloud occurrences, but not necessarily for lightning strike frequency.

CAPE incorporates the degree of instability and the amount of moisture present, thus portraying two factors that are necessary for development of thunderstorms. In the tropics, CAPE values for severe storms can be 1000-6000  $\text{Jkg}^{-1}$  for deep, moist convective storms (Molinié and Pontikis, 1995). In Alaska, relatively intense thunderstorm days can be found at CAPE values as low as 300-400  $\text{Jkg}^{-1}$ . This could be due to the relatively high number of high-based dry thunderstorms, which exists because of the relatively dry boundary layer and consequent high LCL seen in Interior Alaska. For these high based storms, relatively little moisture is involved, and the vertical and horizontal extent of these storms is fairly small and little CG lightning is produced. However, since they are per definition accompanied by very little precipitation (less than 2,5mm; Rorig and Ferguson, 2002), they are an important factor in wildfire ignition (Henry, 1978; Rorig and Ferguson, 1999). By contrast, "wet" convective storms occur when there is abundant lower-level moisture and only moderately conditionally unstable conditions are needed (Rorig and Ferguson, 1999), as associated fronts often supply the lifting mechanism needed to realize the instability. The nature of the dry thunderstorms means that convective indices may correctly indicate a lesser probability for thunderstorms (low CAPE due to little available moisture), but the corresponding fire starting danger for these storms is very severe.

As noted above a complete data set for this study was available for one summer only. To get an idea of the representativeness of the summer of 2001, we compared lightning strike, and climatological data from 2001 with annual and monthly means. We found that the weather of the summer of 2001 deviated

slightly from an average Alaskan summer with respect to temperature, precipitation, and temporal lightning strike distribution (Fig. 4.13), but was fairly representative of a typical season.

The comparison between the modeled CAPE and LI data from the Eta initialization fields and the calculated CAPE values from the sounding data at Fairbanks and McGrath showed  $r^2$ -values of 0.59 and 0.91 with only one value below 0.75 (Table 4.12). These differences are within reason of error, given how sensitive both CAPE and LI are to the selection mechanism for the parcel to be lifted, which is likely to have been different between the two calculation methods. Also, the model probably performs some smoothing operation for the large 45km grid cells, whereas the sounding calculations represent a point value. Thus we found a fairly good agreement, suggesting it safe to conclude that the relationships we have found between thunderstorm activity and CAPE/LI are real, and not just an artefact found between thunderstorm activity and the eta model's forecasts of CAPE/LI.

#### 4.6. Summary

Here we have analyzed thunderstorm activity and related parameters for the summer 2001 season in Interior Alaska. We have examined the links between the thunderstorm potential as represented by CAPE and LI, surface characteristics, as represented by forest coverage and elevation, and thunderclouds and lightning strikes. We have found that :

\* Most of the lightning strike activity in Alaska takes place in the eastern part of the Interior (Fig.4.10). This agrees well with previous studies in the area (Biswas and Jayaweera, 1976; Reap, 1991).

\* In general, the spatial relationships between CAPE, LI, thunderclouds and lightning match well (Figs.4.7-4.10).

\* Thunderstorm potential, as described by CAPE shifts from east towards the western part of the study area through the season.

\* Use of vegetation and elevation information with the convective indices increased the diagnostic skill for all longitude zones and for both thunderstorms and lightning strike frequency predictions by on average about 9%. The amount of explained variation in lightning strike activity and thundercloud occurrences in many cases were more than 30% larger on airmass than on synoptic days, when the vegetation and elevation information was added to the predictive indices. This agrees with earlier studies (Garrett, 1982; O'Neal, 1996; Dissing and Verbyla, 2003) and suggests that the underlying surface has more of an influence on convective development on days with airmass storms than on days with synoptic storms. This is to be expected considering the nature of lifting mechanisms involved with the two classes of storms.

\* In evaluating CAPE and LI as convective activity and lightning strike frequency predictors, we found that LI in most cases is a slightly better predictor of both thundercloud occurrence and lightning strike frequency than CAPE. All the variables at all longitude zones were better indicators of thundercloud occurrences than of lightning strike frequency. This agrees with earlier findings (Anderson, 1991) that it is easier to diagnose the occurrence of lightning than its frequency.

\* The extreme (max, min) variation in the two indices does capture the difference between very electrically active and inactive storms in Alaska, but there was too much variation in the indices to do reversibly defined lightning occurrence thresholds.

\* Typical midlatitude and tropical values of CAPE and LI given in other studies are not illustrative for the Alaska case. In Alaska, electrically intense thunderstorms can be found at CAPE values as low as 300-400

$\text{Jkg}^{-1}$ . This could be due to the relatively high number of high based (dry) thunderstorms that result from the relatively dry boundary layer typical of Interior Alaska.

Climate warming is a factor making future predictions of the Alaskan thunderstorm and fire regimes difficult. However, even for present conditions, the links between climate, vegetation and fire are very important for the boreal environment, but still poorly defined (Campbell and Flannigan, 2000). Thus a better understanding of the processes involved is necessary. This study represents a first view of some of the existing links using the available data.

#### **4.7. Acknowledgements**

The Authors wish to thank Jonathan Henkelman, UAF, Nazila Merati, PMEL, and Bob Bolton, UAF for programming assistance and to Craig Searcy and Eric Stevens, NWS for information about the NCEP Eta model. Further thanks to the University of Alaska Center for Global Change, and to the Bonanza Creek Long Term Ecological Research (LTER) site for generously providing funding. Support was also provided through University of Alaska Anchorage funding for the Alaska Experimental Forecast Facility. Finally, thanks to John Yarie, John Fox, and Terry Chapin, and the anonymous reviewers for suggestions to improve this paper.

#### **4.8. References**

Anderson, K.R., 1991: Models to Predict Lightning Occurrence and Frequency Over Alberta. M.S. thesis, University of Alberta, 91pp.

Ball, G.H. and D.J. Hall, 1965: ISODATA - *A novel method of data analysis and pattern classification*. Tech. Report AD 699616, Stanford Research Institute, California.

Biswas, A.K., and K.O.L.F. Jayaweera, 1976: NOAA-3 Satellite Observations of Thunderstorms in Alaska.

*Mon. Wea. Rev.*, **104**, 292-297.

Blanchard, D.O., 1998: Assessing the vertical distribution of Convective Available Potential Energy. *Wea.*

*Forecasting*, **13**: 870-877.

Burrows, W.R., P. King, P.J. Lewis, B. Kochtubajda, B. Snyder, and V. Turcotte, 2002: Lightning

occurrence patterns over Canada and adjacent United States from lightning detection network observations.

*Atmos.-Ocean*, **40** (10): 59-81.

Byers, H.R. and R.R. Braham, 1949: The thunderstorm. U.S. Weather Bureau, U.S. Department of

Commerce Technical Report, 287pp.

Campbell, I.D. and M.D. Flannigan, 2000: Long-term perspectives on fire-climate-vegetation relationships

in the North American boreal forest. *Fire, climate change and carbon cycling in the boreal forest*, E.S.

Kasischke and B.J. Stocks, Eds., *Ecol. Stud.* 138, Springer Verlag, 151-172.

Chapin, F.S., T.S. Rupp, A.M. Starfield, L. DeWilde, E.S. Zavaleta, N. Fresco, J. Henkelman, and A.D.

McGuire, 2003: Planning for resilience: modeling change in human-fire interactions in the Alaska boreal

forest. *Frontier Ecol. Environ.*, **1** (5): 255-261.

Chuang, H.-Y. and G. Manikin, 2001: The NCEP meso Eta model post processor: a documentation.

U.S. Department of Commerce, National Weather Service (NWS), National Centers for Environmental

Prediction (NCEP), Office Note 438, 23 pp.

Court, A. and J.F. Griffiths, 1992: Thunderstorm climatology. *Thunderstorm Morphology and Dynamics*, Vol.2, E. Kessler, Ed., University of Oklahoma Press, 9-40.

Darkow, G.L., 1992: Basic Thunderstorm Energetics and Thermodynamics. *Thunderstorm Morphology and Dynamics*, Vol.2, E. Kessler, Ed., University of Oklahoma Press, 59-74.

Dissing, D. and D.L. Verbyla, 2003: Spatial Patterns of Lightning Strikes in Interior Alaska and their Relations to Elevation and Vegetation. *Can. J. Forest Res.*, **33**, 770-782.

Doswell, III C.A., and E.N. Rasmussen, 1994: The effect of neglecting the virtual temperature correction on CAPE calculations. *Wea. and Forecasting*, **9**, 625-629.

\_\_\_\_\_, L.C. Anderson, and D.A. Imy, 1991: Basic convection - I. A Review of Atmospheric Thermodynamics. NOAA - NWS. OTB Module 3, Norman, Oklahoma, 71 pp.

Dye, J.E., J.J. Jones, W.P. Winn, T.A. Cerni, B. Gardiner, D. Lamb, R.L. Ritter, J. Ha;ett, and C.P.R. Saunders, 1986: Aerly electrification and precipitation developoment in a small isolated Montana cmulonimbus. *J. Geophys. Res.*, **91**, 1231-1247.

Galway, J.G., 1956: The Lifted Index as a predictor of latent instability. *Bull. Amer. Meteor. Soc.*, **37** (10), 528-529.

Garrett, A.J., 1982: A parameter study of interactions between convective clouds, the convective boundary layer and a forested surface. *Mon. Wea. Rev.*, **110**, 1041-1059.

Global Atmospheric, Inc. Written comm. from Global Atmospheric to AFS containing estimated lightning strike detection efficiency and location accuracy of the ALDF and IMPACT sensors. Letters dated May 18, and September 7, 1995.

Grice, G.K, and A.L. Comisky, 1976: Thunderstorm climatology of Alaska. NOAA Tech. Memorandum NWS AR-14, 36pp.

Hammond, T. and J. Yarie, 1996: Spatial prediction of climatic state factor regions in Alaska. *Ecoscience*, 3, 490-501.

Hane, C.E., H.B. Bluestein, T.M. Crawford, M.E. Baldwin, and R.M. Rabin, 1997: Severe thunderstorm development in relation to along-dryline variability: a case study. *Mon. Wea. Rev.*, 125, 231-251.

Henderson-Sellers, A. and P.J. Robinson, 1986: *Contemporary Climatology*. Longman Scientific and Technical / Wiley and Sons, 439 pp.

Henry, D.M., 1978: Fire occurrence using 500mb map correlation. NOAA Tech. Memorandum, NWS AR-21, 31 pp.

Hiscox, W.L., E.P. Krider, A.E. Pifer, and M.A. Uman, 1984: A systematic method for identifying and correcting site errors in a network of magnetic direction-finders. *Proc., Int. Aerospace and Ground Conf. on Lightning and Static Electricity*, Orlando, Florida, 7-1 - 7-15.

Huntrieser, H., H.H. Schiesser, W. Schmid, and A. Waldvogel, 1997: Comparison of traditional and newly developed thunderstorm indices for Switzerland. *Wea. and Forecasting*, 12, 108-125.

Huschke, R.E. 1959. *Glossary of Meteorology*. Amer. Meteor. Soc., Boston. 638 pp.

Idone, V.P., D.A. Davis, P.K. Moore, Y. Wang, R.W. Henderson, M. Ries, and P.F. Jamason, 1998a: Performance evaluation of the U.S. National Lightning Detection Network in eastern New York. 1. Detection efficiency. *J. Geophys. Res.*, **103D**: 9045-9055.

\_\_\_\_\_, \_\_\_\_\_, \_\_\_\_\_, \_\_\_\_\_, \_\_\_\_\_, \_\_\_\_\_, and \_\_\_\_\_, 1998b: Performance evaluation of the U.S. National Lightning Detection Network in eastern New York. 2. Location accuracy. *J. Geophys. Res.*, **103D**: 9057-9069.

Intergovernmental Panel on Climate Change (IPCC) (1996) *Climate change 1995 - the science of climate change*. Cambridge, Cambridge University Press, 572 pp.

Janjic, Z.I., 1994: The step-mountain Eta Coordinate Model : further development of the convection viscous sublayer and turbulence closure schemes. *Mon. Wea. Rev.*, **122**, 927-945.

Kasischke, E.S., N.L. Christensen, and B.J. Stocks, 1995: Fire, global warming, and the carbon balance of boreal forests. *Ecol. Applications*, **5**, 437-451.

\_\_\_\_\_, T.S. Rupp, and D.L. Verbyla, In Press: Fire trends in the Alaskan boreal forest. *Alaska's changing boreal forest*, F.S. Chapin, J. Yarie, K. Van Cleve, Eds., Oxford, UK, Oxford University Press.

Labau, V.J., and W. Van Hess, 1990: An inventory of Alaska's boreal forests: their extent, condition, and potential use. *Proc., Int. Symp. Boreal Forests: Condition, Dynamics, Anthropogenic Effects*, Archangel, Russia. State Committee of USSR on Forests, part 6, Moscow, 30-39.



Li, C., M.D. Flannigan, and I.G.W. Corns, 2000: Influence of potential climate change on forest landscape dynamics on West-Central Alberta. *Can. J. Forest Res.*, **30**, 1905-1912.

Markon, C.J., M.D. Fleming, and E.F. Binnian, 1995: Characteristics of vegetation phenology over the Alaskan landscape using AVHRR time series data. *Polar Rec.*, **31**, 179-191.

Molinié, J. and C.A. Pontikis, 1995: A climatological study of tropical thunderstorm clouds and lightning frequencies on the French Guyana coast. *Geophys. Res. Lett.*, **22** (9): 1085-1088.

Moncrieff, M.W. and M.J. Miller, 1976: the dynamics and simulation of tropical cumulonimbus and squall lines. *Quart. J. Roy. Meteor. Soc.*, **102**, 373-394.

Oke, T.R., 1987: *Boundary Layer Climates*, 2nd ed. Routledge, 435 pp.

O'Neal, M., 1996: Interactions between land cover and convective cloud cover over Midwestern North America detected from GOES satellite data. *Int. J. Remote Sens.*, **17** (6), 1149-1181.

Petersen, W.A., S.A. Rutledge, and R.E. Orville, 1996: cloud-to-ground lightning observations from TOGA COARE: selected results and lightning location algorithms. *Mon. Wea. Rev.*, **124**, 602-620.

Price, C. and D. Rind, 1994: Modeling global lightning distributions in a general circulation model. *Mon. Wea. Rev.*, **22**, 1930-1939.

Reap, R.M. 1991: Climatological Characteristics and Objective Prediction of Thunderstorms in Alaska. *Wea. Forecasting*, **6**, 309-319.

Renno, N.O. and A.P. Ingersoll, 1996: Natural convection as a heat engine: a theory for CAPE. *J. Atmos. Sci.*, **53** (4), 572-585.

Rorig, M.L. and S.A. Ferguson, 1999: Characteristics of lightning and wildland fire ignition in the Pacific Northwest. *J. Appl. Meteor.*, **38**, 1565-1575.

\_\_\_\_\_ and \_\_\_\_\_, 2002: The 2000 fire season: lightning-caused fires. *J. Appl. Meteor.*, **41**, 786-791.

Rutledge, S.A., E.R. Williams, and T.D. Keenan, 1992: The Down Under Doppler Radar Experiment (DUNDEE) : overview and preliminary results. *Bull. Amer. Meteor. Soc.*, **73**, 3-16.

Serreze, M.C., J.E. Walsh, F.S. Chapin, T. Osterkamp, M. Dyurgerov, V. Romanovsky, W.C. Oechel, J. Morison, T. Zhang, and R.G. Barry, 2000: Observational evidence of recent change in the northern high-latitude environment. *Climatic Change*, **46**, 159-207.

Schneider, S.H. (Ed.), 1996: *Encyclopedia of Climate and Weather*. Oxford University Press, 929 pp.

Schroeder, M.J. and C.C. Buck, 1970: Fire weather. Agriculture Handbook 360, U.S. Department of Agriculture, Forest Service, 229 pp.

Solomon, R. and M. Baker, 1994: Electrification of New Mexico thunderstorms. *Mon. Wea. Rev.*, **122**, 1878-1886.

Stull, R.B. 1988: *An Introduction to Boundary Layer Meteorology*. Kluwer Academic Publishers, 670 pp.

- Sturtevant, J.S., 1995: *The severe local storm forecasting primer*. Weather Scratch Meteorological Services, 197 pp.
- Sullivan, W.G., 1963: Low-level convergence and thunderstorms in Alaska. *Mon. Wea. Rev.*, **91**, 89-92.
- Uman, M.A., 1984: *Lightning*. Dover Publications, 298 pp.
- Wallace, J.M. and P.V. Hobbs, 1977: *Atmospheric Science. An introductory survey*. Academic Press, 467 pp.
- Wicker, L.J. and L. Cantrell, 1996: The role of vertical buoyancy distributions in miniature supercells. Preprints, *18<sup>th</sup> Conf. on Severe Local Storms*, San Francisco, CA, Amer. Meteor. Soc., 225-229.
- Williams, E.R., S.A. Rutledge, S.G. Geotis, N. Renno, E. Rasmussen, and T. Tickenback, 1992: A radar and electrical study of tropical "Hot Towers". *J. Atmos. Sci.*, **49**, 1386-1395.
- Zajac, B.A. and J.F. Weaver, 2002: Lightning meteorology I: an introductory course on forecasting with lightning data. *Preprints, Symp. On the Advanced Weather Interactive Processing System (AWIPS)*, Orlando, FL, Amer. Meteor. Soc.
- Zhang, G.J. and N.A. McFarlane, 1991: Convective stabilization in Mid-latitudes. *Mon. Wea. Rev.*, **119**, 1915-1928.

# Lightning in Interior Alaska

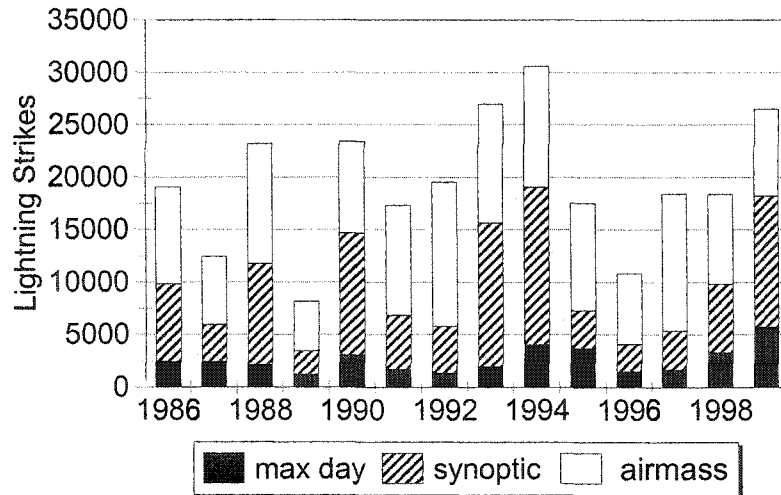


Figure 4.1. Annual lightning variation in Interior Alaska. Max day is the lightning on the day with the most recorded strikes. Synoptic lightning is the sum of all days with more than 1000 recorded strikes. Note that synoptic events contribute a large part of the total annual strikes.

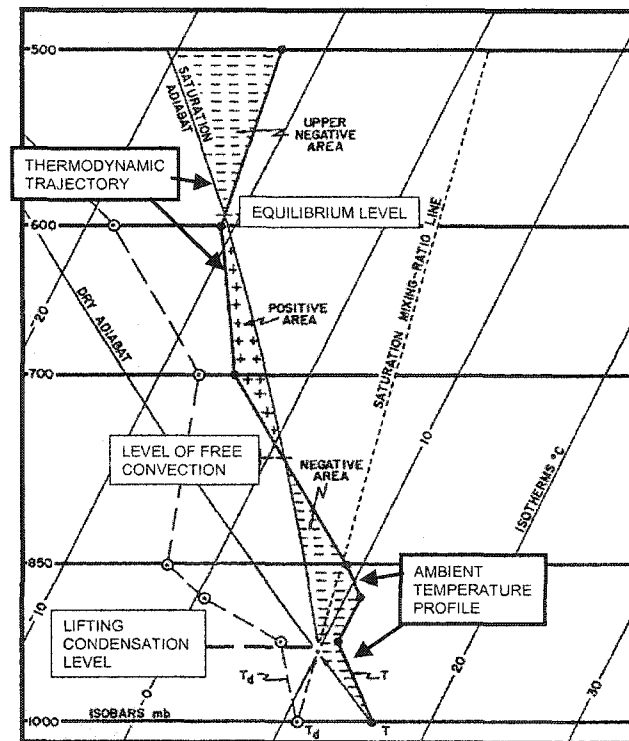


Figure 4.2 Atmospheric sounding shown on a skew-T diagram. CAPE is represented by the above positive area, which is bound downwards by the level of free convection and upwards by the equilibrium level. After Doswell *et al.* (1991).

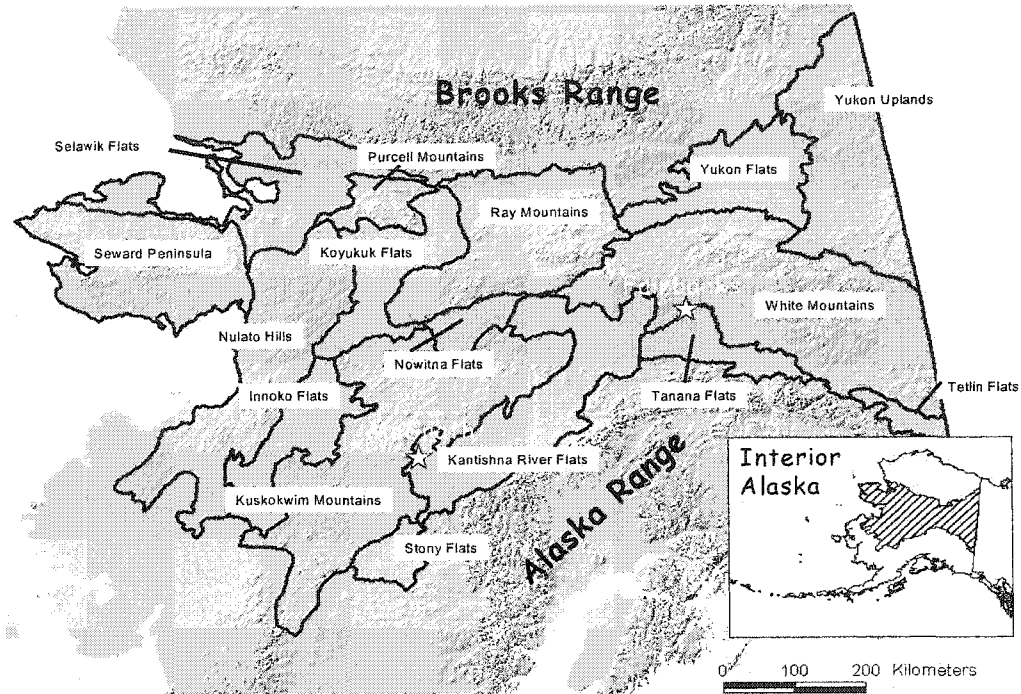


Figure 4.3. The Alaska study area, including the physiographic regions used for geographical reference purposes.

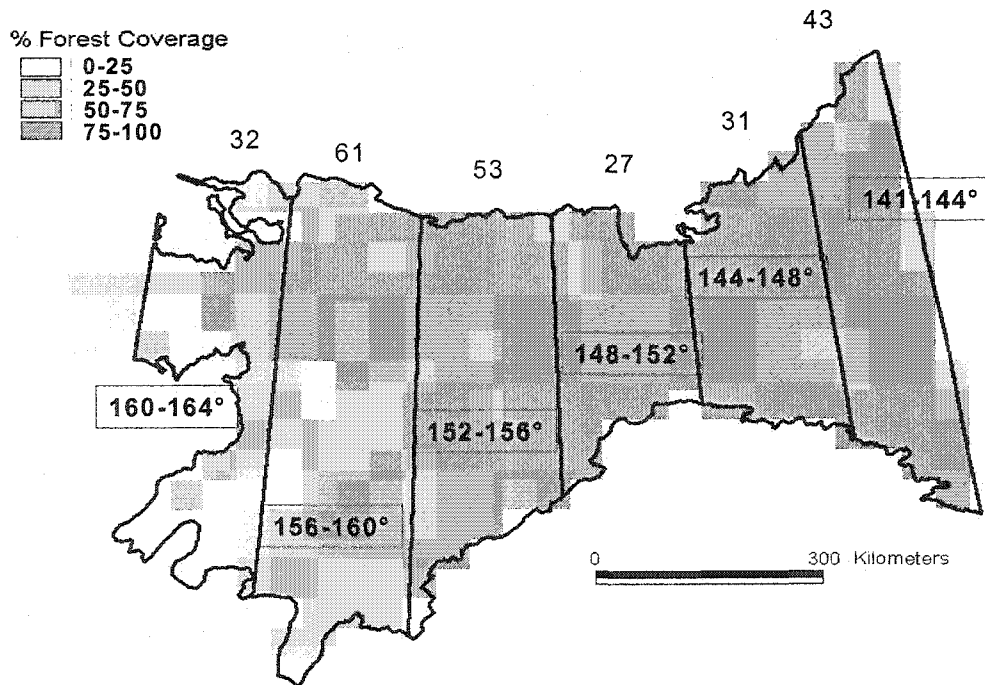


Figure 4.4 The analysis was conducted for six longitudinal sectors, which follow a climatological gradient from continental to maritime.

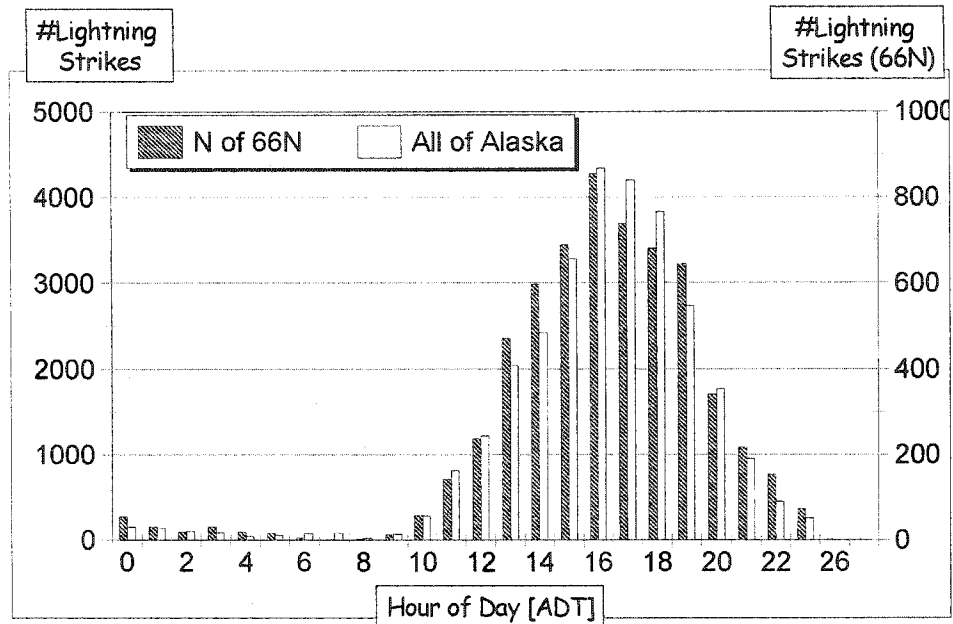
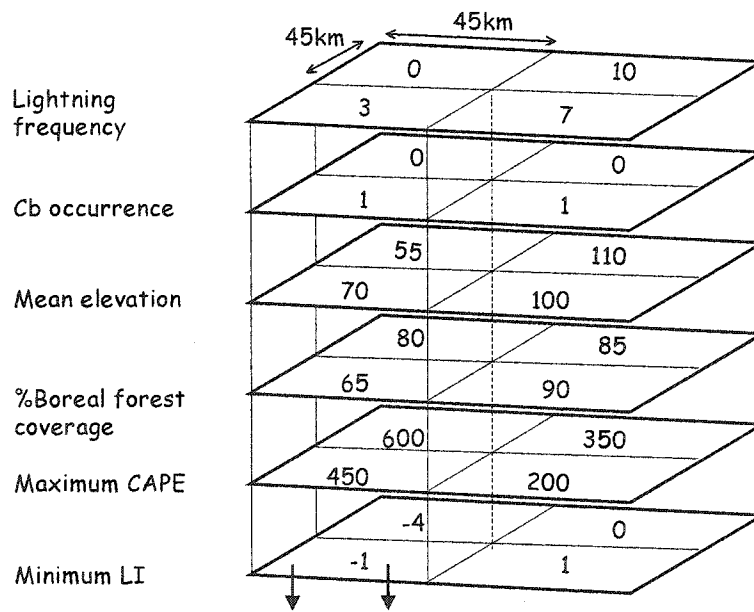


Figure 4.5. The hour of maximum lightning activity for the 2001 season in Alaska and north of the Arctic Circle (66°N). Most of the lightning strikes hit between 4pm and 6pm ADT. All the lightning strikes for the 2001 season are included.



Cell output:({3, 1, 70, 65, 450, -1} day1),({daily layer values} day2)...({daily layer values} day n)

Figure 4.6. Construction of data sets used for linear regression. For each cell (45km by 45km) of each longitudinal transect, values for the six variables (CAPE, LI, # of thundercloud occurrences, # of lightning strikes, mean elevation, and % of each cell covered by forest) were written to an output file. The file contained cell data for the whole season, thus we created 18 files. One for each longitudinal transect (6), and one for each meteorological condition (all days, synoptic days, airmass days).

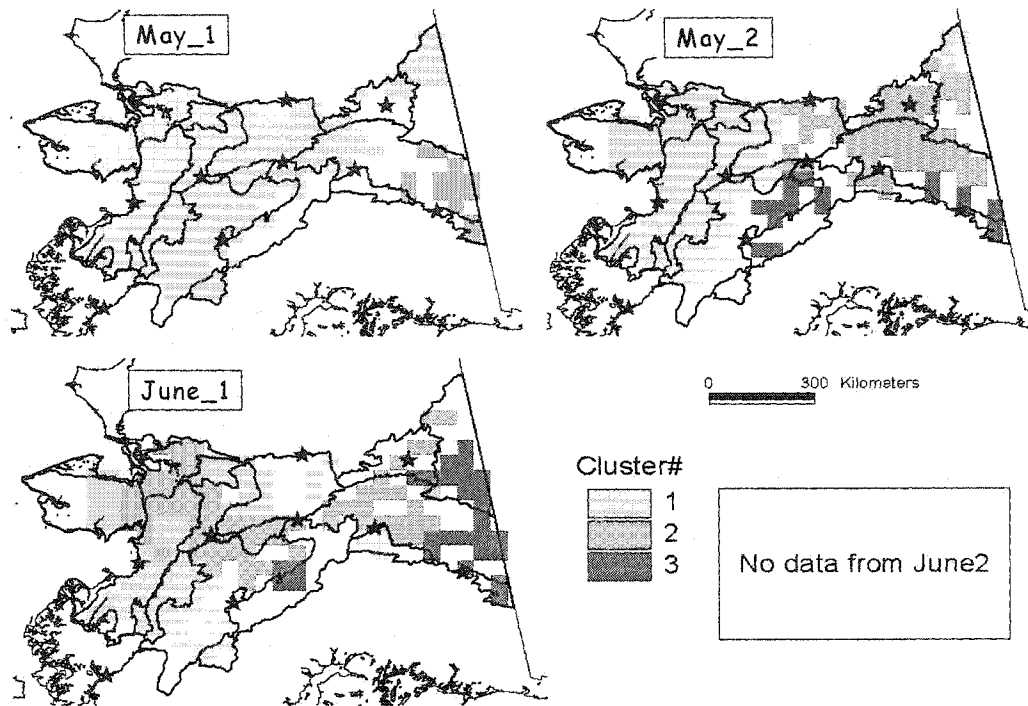


Figure 4.7a. Seasonal spatial distribution of CAPE for the summer of 2001, divided into two-week time segments. Data was insufficient for the cluster analysis for the second period of May and all of August.

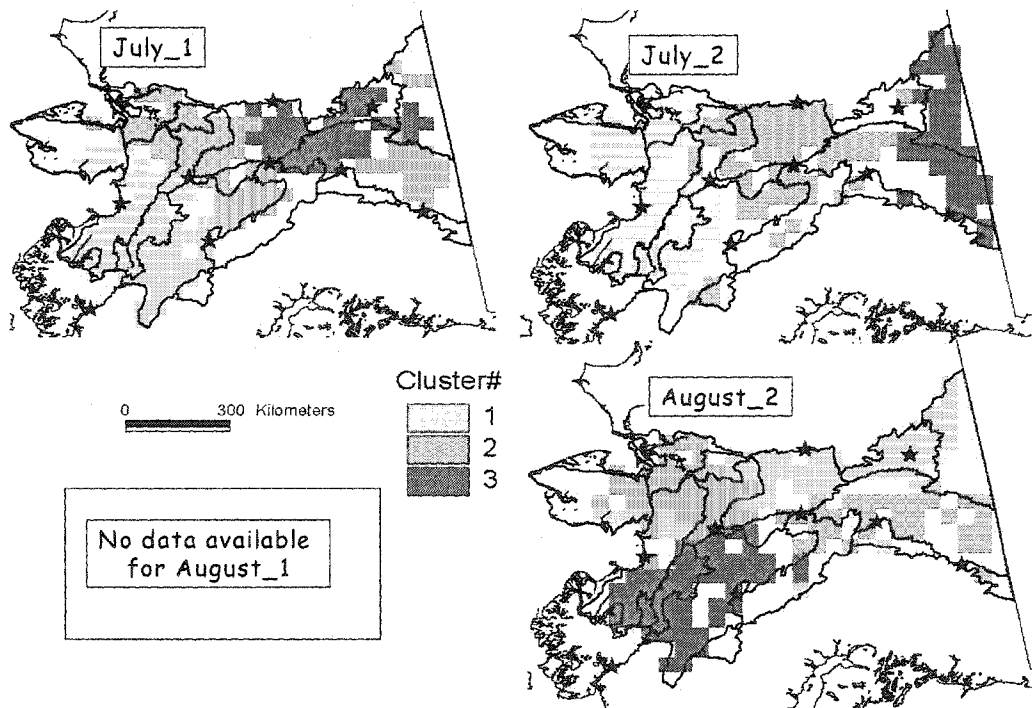


Figure 4.7b. Seasonal spatial distribution of CAPE for the summer of 2001, divided into two-week time segments. Data was insufficient for the cluster analysis for the second period of May and all of August.

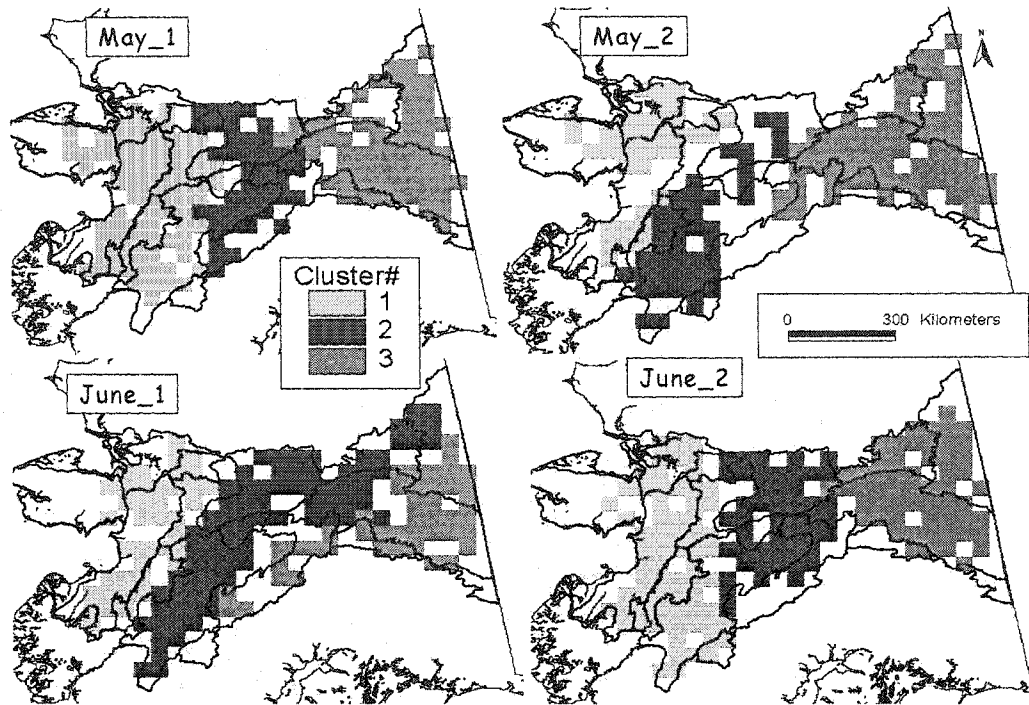


Figure 4.8a. Seasonal spatial distribution of LI for the summer of 2001, divided into two-week time segments. Data was unavailable for all of July.

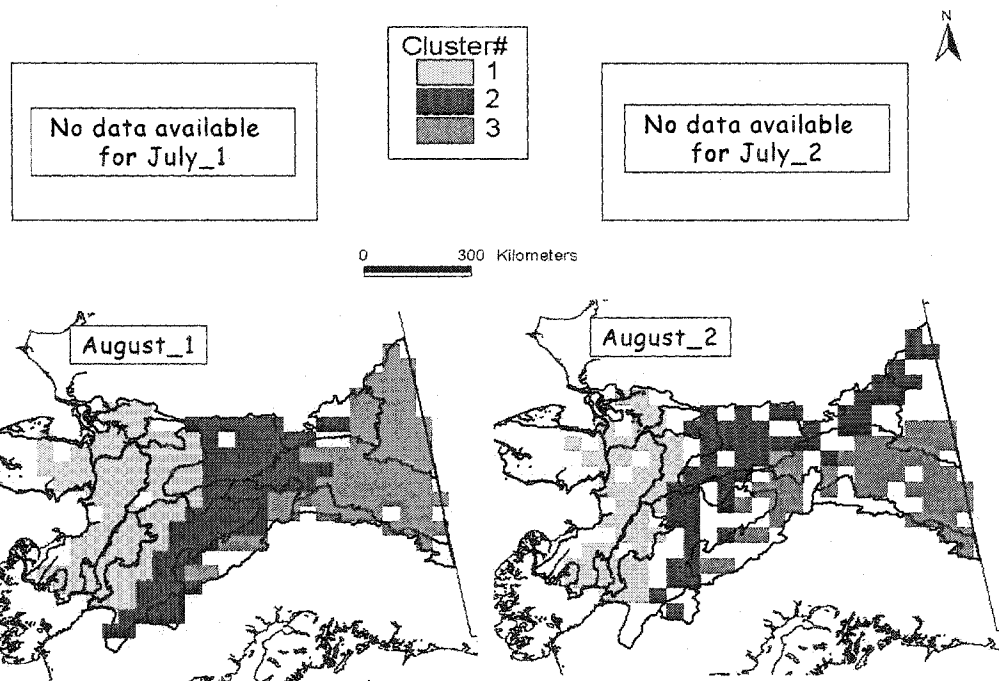


Figure 4.8b. Seasonal spatial distribution of LI for the summer of 2001, divided into two-week time segments. Data was unavailable for all of July.



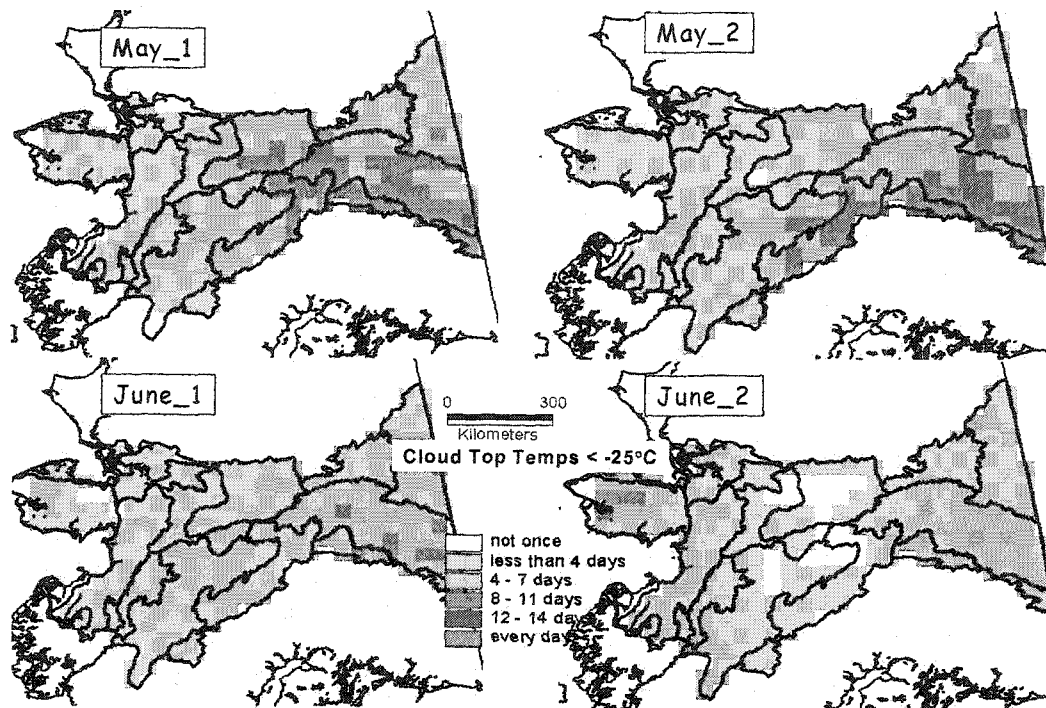


Figure 4.9a. Seasonal spatial distribution of Cb occurrences for the summer of 2001, divided into two-week time segments. The classification is based on a cloud top temperature of  $-25^{\circ}\text{C}$ .

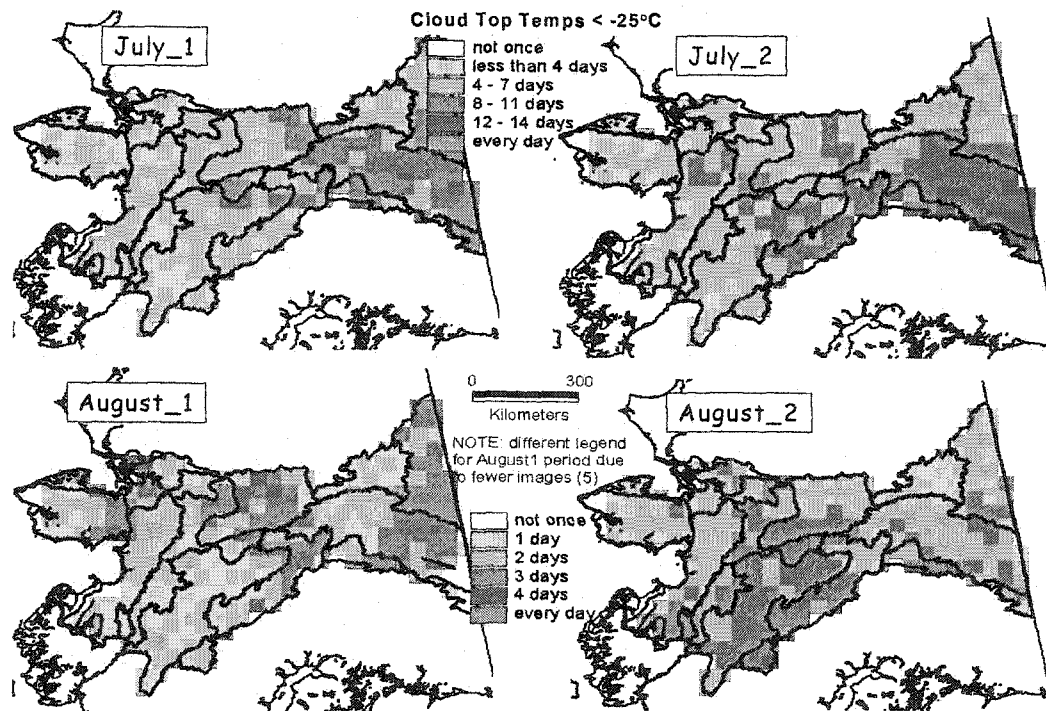


Figure 4.9b. Seasonal spatial distribution of Cb occurrences for the summer of 2001, divided into two-week time segments. The classification is based on a cloud top temperature of  $-25^{\circ}\text{C}$ .

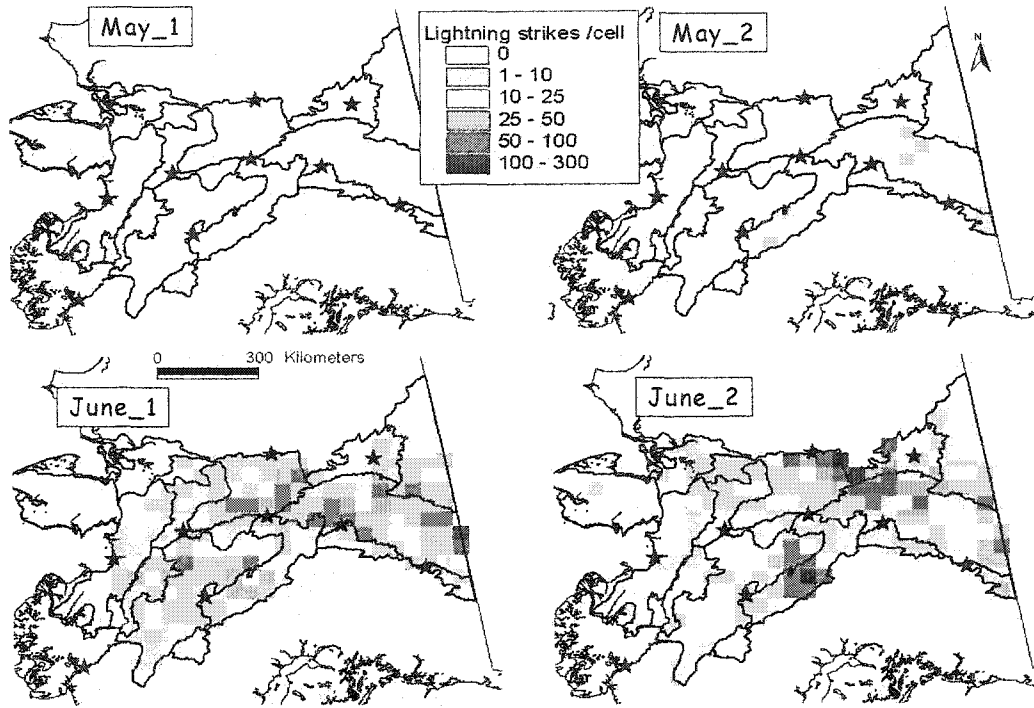


Figure 4.10a. Seasonal spatial distribution of lightning strikes for the summer of 2001, divided into two-week time segments. For each time period, the total number of lightning strikes within each grid cell were summed up.

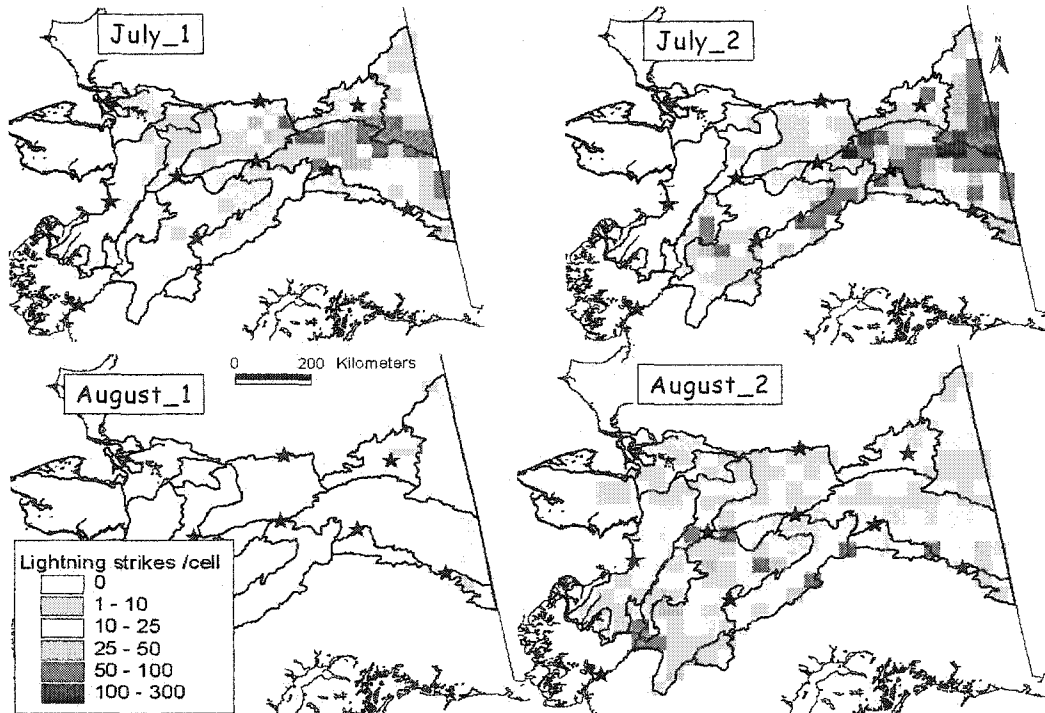


Figure 4.10b. Seasonal spatial distribution of lightning strikes for the summer of 2001, divided into two-week time segments. For each time period, the total number of lightning strikes within each grid cell were summed up.

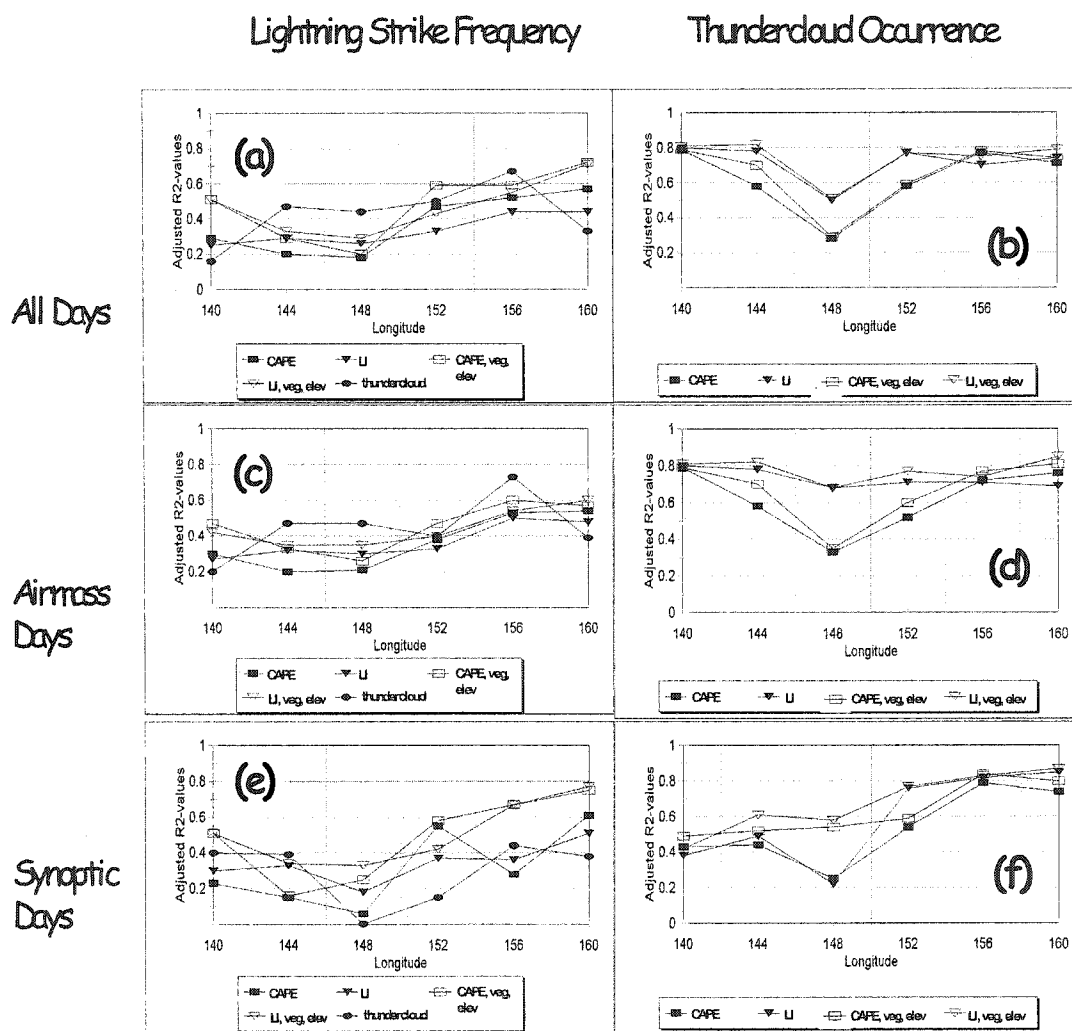


Figure 4.11 a-f. Coefficient of determination ( $r^2$ ) results from the multiple regression analysis. Each analysis was run with lightning strike frequency and convective activity (thundercloud occurrence) as the dependent variation. The data is classified as either all days in the season, airmass days, or synoptic days.

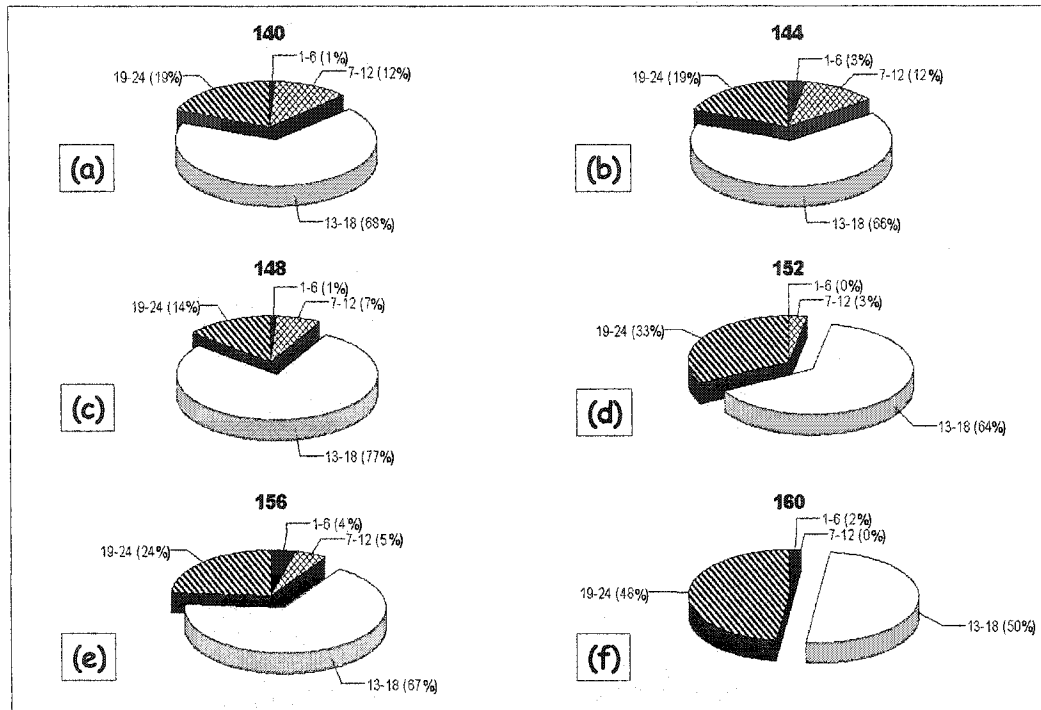


Figure 4.12a-f. Lightning strike distribution by 6-hour periods for the 2001 lightning season. The values are the hours, and the percentages represent the fraction of the total annual lightning, which occurred in that time period for each longitudinal zone.

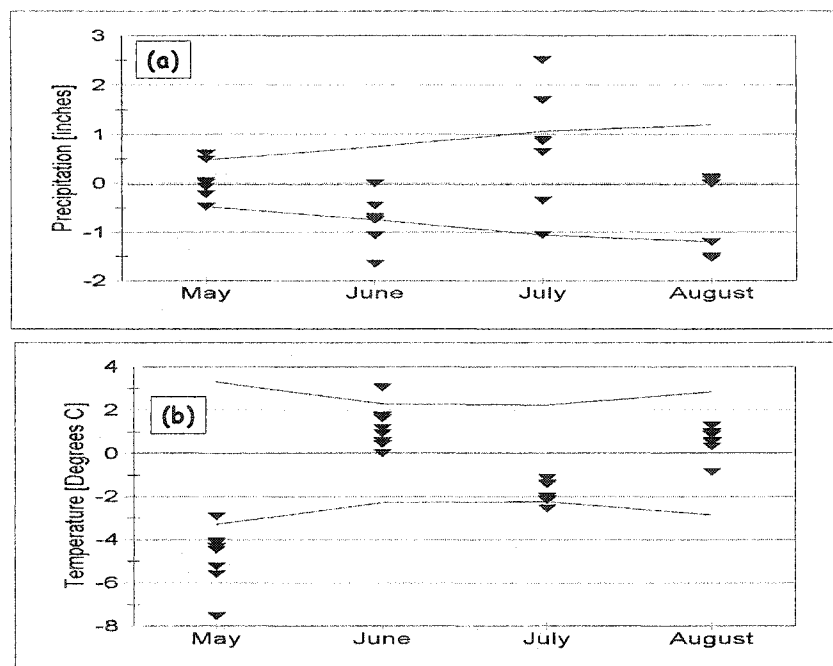


Figure 4.13. Precipitation (a) and temperature (b) data from 8 Interior Alaska stations in 2001. The values represent the difference from the mean values for the 1950-2002 time period, and the lines represent  $\pm 1$  standard deviation from the mean.

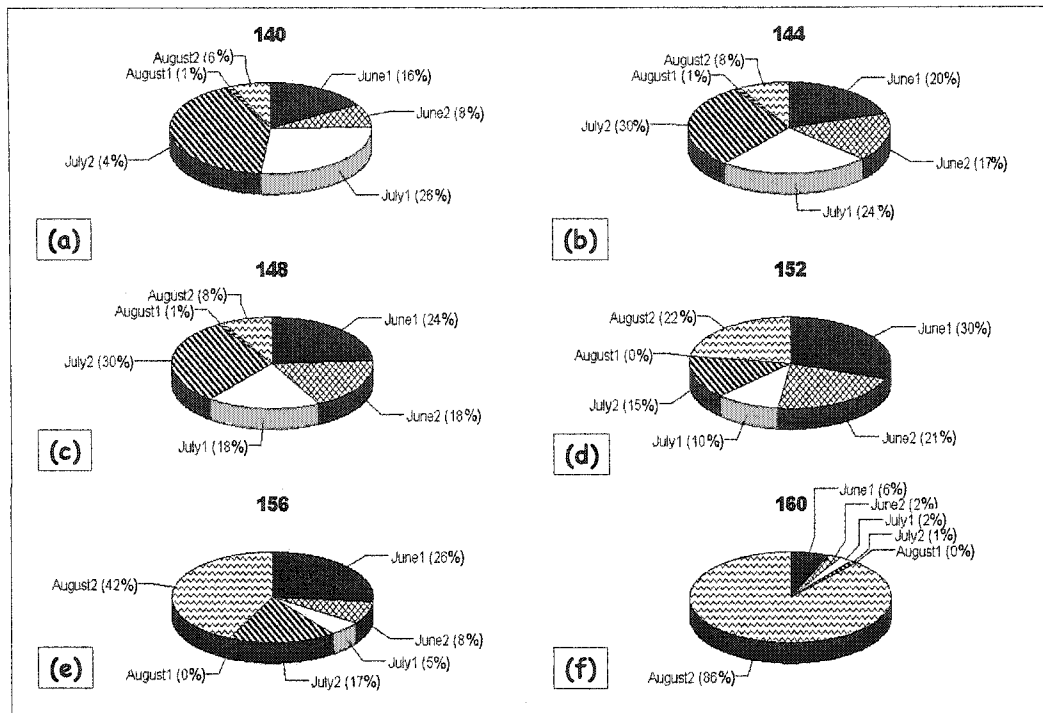


Figure 4.14a-f. Seasonal lightning strike distribution by two-week period for the six longitudinal transects. The percentages represent the fraction of the total annual lightning, which occurred in that two-week period for each longitudinal zone.

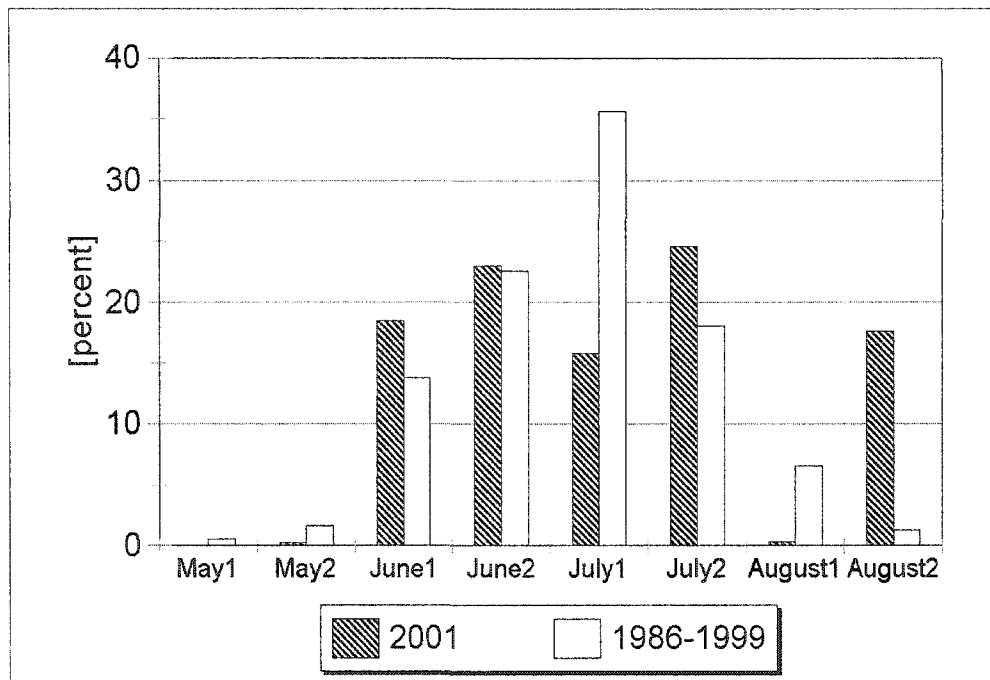


Figure 4.15. Seasonal distribution of lightning strikes in Interior Alaska for two-week periods. Comparison between the average (1986-99) year and 2001.

Table 4.1 Typical values of LI (from Sturtevant, 1995 ).

LI [K]	Possibility of Thunderstorm
> 0	unlikely
0 - -2	possible, good trigger needed
-3 - -5	unstable / thunderstorm probable
< -5	very unstable / heavy to strong thunderstorm potential.

Table 4.2. Typical CAPE values (from Sturtevant, 1995).

CAPE [Jkg-1 or m2s-2]	Convective Potential
300-1000	weak
1000-2500	moderate
2500-3000	strong

Table 4.3 Temporal coverage of meteorological data for summer 2001.

Index	Time Coverage (Julian Days)	Number of Days
CAPE	121-176, 178-221, 229-243	114
LI	121-176, 178-181, 213-221, 229-243	84

Table 4.4 Statistics for the two-week segment clustering algorithm of CAPE. Values of mean, standard deviation, maximum and minimum values for each clustered group. See figure 4.7a-b for spatial representation of the clustered groups.

two_week	segment	cluster#	#of days	#cells in cluster	mean	std.dev	max	min
May_1	1	15	225	14.8	10.6	41.0	0.8	
May_1	2	15	27	140.7	111.1	371.9	4.4	
May_1	3	15	-	-	-	-	-	
May_2	1	16	140	12.5	13.5	49.6	1	
May_2	2	16	79	50.8	38.5	126.3	5.6	
May_2	3	16	33	121.0	71.3	300.5	30	
June_1	1	15	108	45.1	49.6	200	3.72	
June_1	2	15	104	11.2	146.1	499.8	5.8	
June_1	3	15	40	276.0	310.4	1023	20.3	
July_1	1	15	90	41.9	18.0	73.8	14.9	
July_1	2	15	113	157.4	100.9	383.7	39.3	
July_1	3	15	49	322.6	301.3	1009.4	18.8	
July_2	1	16	95	35.5	20.0	80.0	9.1	
July_2	2	16	103	185.1	175.2	567.2	15.5	
July_2	3	16	54	259.7	324.3	1372.6	36.3	
Aug_2	1	15	75	41.8	38.5	148.6	7.5	
Aug_2	2	15	109	89.0	68.6	246.1	6.1	
Aug_2	3	15	68	120.4	109.9	380.0	1.5	

Table 4.5 Statistics for the two-week segment clustering algorithm of LI. Values of mean, standard deviation, maximum and minimum values for each clustered group. See figure 4.8 for spatial representation of the clustered groups.

two_week segment	cluster#	#of days	#cells in cluster	mean	std.dev	max	Min
may1	1	14	107	10.7	3.5	16.8	5.5
may1	2	14	54	7.1	3.1	12.0	2.3
may1	3	14	91	3.3	2.3	7.9	0.9
may2	1	16	66	9.2	2.1	13.9	6.2
may2	2	16	72	5.4	1.9	8.3	2.3
may2	3	16	114	2.9	2.2	8.4	0.2
june1	1	15	70	4.5	3.5	11.9	-0.6
june1	2	15	115	2.4	2.2	6.9	-0.6
june1	3	15	67	1.0	1.9	3.9	-2.1
june2	1	14	96	4.7	2.8	9.4	0.4
june2	2	14	70	2.4	2.3	6.4	-0.3
june2	3	14	86	1.4	1.9	5.2	-0.6
august1	1	9	96	10.2	1.9	11.4	7.4
august1	2	9	72	7.4	1.7	10.1	3.8
august1	3	9	84	4.5	1.4	6.5	2.5
august2	1	15	77	4.4	4.1	12.2	-0.1
august2	2	15	87	2.8	2.5	7.4	0.2
august2	3	15	88	1.5	1.9	4.6	-0.6



Table 4.6. Comparison of 5 intense lightning days (synoptic storms, lightning strikes  $> 700\text{day}^{-1}$ ) with 4 non-intense lightning days (air-mass storms, lightning strikes  $100\text{-}200\text{day}^{-1}$ ).

Lightning intensity	# of lightning strikes	Mean CAPE	Max. CAPE	Mean LI	Min. LI	# of days
A) Intense (synoptic)	$>700$	133.9	2600	1.2	-6.0	5
B) Not intense (air-mass)	100-200	135.8	720	2.7	-2.0	4
p-value (A vs B)	-	0.955	0.0023	0.1186	0.035	-

Table 4.7. Predicted values of LI for set numbers of lightning strikes per 45km by 45km cell, using the results of the multiple regression analysis for two of the longitudinal zones (140 and 160), showing extreme continental and extreme maritime conditions.

Lightning per cell	convective activity	140 (synoptic)	140 (airmass)	160 (synoptic)	160 (airmass)
0	none	5.1	7.8	6.0	7.3
5	weak	-3.9	-1.8	-0.9	0.2
10	moderate	-13.0	-11.4	-7.9	-7.0
15	moderate	-22.1	-21.0	-14.8	-14.1
100	very strong	-176.7	-184.5	-132.9	-135.6

Table 4.8. Predicted values of CAPE for set numbers of lightning strikes per 45km by 45km cell, using the results of the multiple regression analysis for two of the longitudinal zones (140 and 160), showing extreme continental and extreme maritime conditions.

Lightning per cell	convective activity	140 (synoptic)	140 (airmass)	160 (synoptic)	160 (airmass)
0	none	2.0	3.5	0.6	0.7
5	weak	12.4	12.5	7.0	7.6
10	moderate	22.9	21.6	13.4	41.4
15	moderate	33.3	30.7	19.8	21.3
100	very strong	210.4	185.3	128.8	137.7

Table 4.9. Temporal lightning strike distribution over the 2-week periods of summer season 2001. The last column represents an average temporal lightning strike distribution for Interior Alaska, based on lightning data from the 1986-99 period.

Julian day	Dates	Time period	total strikes in period	%strikes in period	% mean strikes 1986-99
121-135	May 1 - 15	May_1	0	0	0.52
136-151	May 16 - 31	May_2	73	0.27	1.65
152-166	June 1 -15	June_1	4949	18.47	13.73
167-181	June 16 - 30	June_2	6151	22.95	22.54
182-196	July 1 - 15	July_1	4237	15.81	35.65
197-212	July 16 - 31	July_2	6579	24.55	18.01
213-227	August 1 - 15	August_1	86	0.32	6.59
228-243	August 16 - 31	August_2	4722	17.62	1.22

Table 4.10. Results of the regression analysis modeling lightning strike frequency as a function of vegetation and elevation. The table shows significant  $r^2$ -values for the regression for each longitudinal zone.

Dependent variable	longitude	Independent variable	All days	Airmass days	Synoptic days
Lightning	140	%Forest cover	0.02	0.03	-
Lightning		Elevation	0.35	0.31	0.35
Thunderclouds		%Forest cover	0.06	0.06	0.08
Thunderclouds		Elevation	0.36	0.34	0.34
Lightning	144	%Forest cover	0.08	0.08	0.02
Lightning		Elevation	0.14	0.16	0.01
Thunderclouds		%Forest cover	0.01	0.01	0.01
Thunderclouds		Elevation	0.36	0.36	0.36
Lightning	148	%Forest cover	-	-	0.16
Lightning		Elevation	0.08	0.09	0.003
Thunderclouds		%Forest cover	0.20	0.20	0.20
Thunderclouds		Elevation	-	-	-
Lightning	152	%Forest cover	0.02	0.01	0.004
Lightning		Elevation	0.04	0.02	0.05
Thunderclouds		%Forest cover	0.004	0.004	0.004
Thunderclouds		Elevation	0.06	0.06	0.06
Lightning	156	%Forest cover	0.03	0.09	0.003
Lightning		Elevation	0.07	0.03	0.05
Thunderclouds		%Forest cover	0.02	0.05	0.02
Thunderclouds		Elevation	0.02	0.02	0.01
Lightning	160	%Forest cover	0.003	0.06	0.14
Lightning		Elevation	0.003	-	0.004
Thunderclouds		%Forest cover	0.11	0.48	0.48
Thunderclouds		Elevation	-	-	-

Table 4.11. Correlations between CAPE and LI, similar to Blanchard (1998).

Longitude	Adjusted $r^2$ -values
140	0.92
144	0.70
148	0.61
152	0.84
156	0.86
160	0.82

Table 4.12. Comparison ( $r^2$ -values) between the 45km by 45km cells of modeled Eta CAPE and LI and CAPE and LI calculated from the raw sounding data from Fairbanks and McGrath.

	CAPE	LI
Fairbanks	0.75	0.77
McGrath	0.59	0.91

## Chapter 5. General Conclusions

This dissertation has focused on the development of thunderstorms and lightning strike activity in a boreal forest region in Interior Alaska and on how the underlying surface can influence their development. I have examined the distributions and correlations between lightning strikes, thunderclouds, thunderstorm indices (CAPE and LI), elevation, and vegetation variables in Alaska. The relationships were examined at scales ranging from the Interior region of the state to individual wildfire burn scars, and at temporal scales ranging from annual to daily. The objective is to understand the influential factors and processes responsible for thunderstorm development in Alaska, such that we may produce well-founded predictions on future thunderstorm regimes caused by a changing climate.

### 5.1. A hierarchy of spatial scales

At the regional scale (interior Alaska, 630,000km<sup>2</sup>) we found that forest coverage and elevation were important factors for determining lightning strike densities. Within the region, lightning strike density was consistently higher in boreal forest than in tundra or shrub vegetation (figure 2.7). The interaction between increasing boreal forest area and elevation was correlated with increasing lightning strike density, providing explanation for 66% of the variation in the lightning strike densities at this scale (table 2.1). Boreal forest, due to its high sensible heat fluxes, may enhance convective activity of *air-mass* thunderstorms (Harding et al, 2001). Another explanation is that the boreal forest biome exists in a climatic region that sustains the convective activity. Our data suggest that both explanations are important.

The areas of highest lightning strike densities seemed to be located within 10-25km on either side of the boundary between boreal forest and tundra (figures 2.5 and 2.6), suggesting that the boreal forest-tundra boundary (treeline) has an impact on thunderstorm development. This is similar to suggestions by Pielke and Vidale (1995) who proposed that the northern boreal forest to tundra transition through its differences in surface heat fluxes influenced the position of the polar front. Conversely, other studies argue

that the position of the northern treeline represents a response to, rather than a forcing on, the summer position of the Arctic front (Serreze et al., 2001, Beringer et al., 2001). However, the authors conclude that the differences in energy partitioning between tundra and boreal forest could be significant enough to drive local-scale circulations of ecological importance (Beringer et al., 2001). This has strong implications for future climate change scenarios, with speculations about extension of treeline (Wilmking, 2003).

Consistent with the observed trend for the regional scale, the mesoscale showed higher lightning strike densities within the boreal forest, followed by shrubs and tundra (figure 2.7). The effect was more pronounced in the continental than in the maritime climate. The combination of boreal forest areal coverage, elevation, and a continentality factor explained for ~57% of the variation in the lightning strike density (table 2.2).

The mesoscale (longitudinal transects, ~100,000km<sup>2</sup>) is important for airmass thunderstorm development, and some of this research has focused on the distinction between the airmass and thunderstorm days. I found that the amount of explained variation in lightning strike activity and thundercloud occurrences in many cases was more than 30% greater on airmass than on synoptic days, when the vegetation and elevation information was added to the predictive indices. This agrees with earlier studies (Garrett, 1982; O'Neal, 1996) and suggests that the underlying surface has more of an influence on convective development on days with airmass storms than on days with synoptic storms. This is to be expected considering the nature of lifting mechanisms involved with the two classes of storms. In Alaska, electrically intense thunderstorms can be found at CAPE values as low as 300-400 Jkg<sup>-1</sup>. This could be due to the relatively high number of high based (dry) thunderstorms that result from the relatively dry boundary layer typical of Interior Alaska.

In general, the thunderstorm indices of CAPE and LI explain larger fractions of the variation in lightning strike frequencies than did the forest cover or elevation variables individually. I found that the presence of thunderclouds, as determined by an afternoon AVHRR image, was not consistently the best



predictor of lightning frequency. This is different from Anderson (1991), who concluded that convection was the best indicator of lightning occurrence.

At the local scale (physiographic sub-regions, 50,000km<sup>2</sup>) I found that more than half of the sub-regions showed the highest lightning strike densities within boreal forest. Elevation and forest coverage did not provide as good an explanation for the variability in lightning strike data as at the meso- or regional scales. However, the best model for explaining lightning strike density was still the combined model of elevation and areal forest coverage. The combined effects of boreal forest and elevation on increased lightning strike activity was found in the larger scales (regional and mesoscale), but was less prevalent at the smallest scale (local). The zones at the local scale that were examined were delineated based on physiographic features such as proximity to major rivers, or mountainous areas. Possibly not all of these delineations were appropriate for showing the above effects, thus I only saw trends similar to the larger scales at some zones, whereas the statistical analysis, incorporating all the zones, did not show as strong a pattern. Likewise, the study of high lightning strike density pixels in relation to the boreal forest-tundra boundary did not portray a consistent pattern at the patch scale (regardless of size).

At smallest scale (200 - 2200km<sup>2</sup>) , lightning strike activity was examined with respect to individual wildfire burn scars in the Yukon Flats. I looked for evidence in support of a wildfire feedback mechanism as suggested by modeling studies (Knowles, 1991) around 13 fire scars within the boreal forest of the Yukon Flats region, Interior Alaska. I found two satellite images where convective cloud development could be associated with burn scars. In one of these cases, thunderstorm and lightning activity developed in the immediate area, suggesting a possible burn scar induced circulation. We found that in general, relative lightning activity decrease in the burned areas as well as the control areas following a fire. In some areas, however, lightning activity increased in the surrounding unburned areas. In the four cases of positive lightning activity changes in buffers and some scars the positive lightning activity changes seemed to be concentrated in 2-3 geographical areas. Were these local circulation patterns related to the presence of the wildfire burn scars, or were they related to local topography and small-scale meteorology?

In examining factors with a possible influence on these local convective patterns, I discovered that the changes in lightning strike activity were tied closer to parameters describing fire severity, such as difference in radiant temperatures between the burns and surrounding buffers and deciduous vegetation within the burn scars, than to environmental variables such as slope and elevation.

The predominant result from this study however, was that the Yukon Flats is a vegetation mosaic heavily influenced by the areas active wildfire history, making it difficult to detect a feedback mechanism. Additionally, a given burn scar would rarely represent a single severity class, rather a patchwork of severity. This is likely to result in some mixed signals of factors important for lightning activity within the burn scars. We have found some evidence in support of the existence of the feedback mechanism, but not enough to make any strong statements about it.

These scale-related studies show that both processes and important variables for development of thunderstorms and lightning activity vary both within and between the scales. It appears that on the larger scales, the combined effects of boreal forest and elevation on increased lightning strike activity were more prevalent than at the smallest scale (local). When the scale gets very small, bordering the scales were surface properties no longer appears to have a strong influence on the boundary layer (<10km; Shuttleworth, 1988; Blyth et al. 1994; Pielke et al. 1998), the burn scar study showed that it gets exceedingly difficult to isolate influential signals and factors. Chapter 4 correlated lightning strike frequencies within the mesoscale, but each cell represented a 45 by 45km area. The results suggested that the underlying surface (in the form of areal forest coverage and vegetation) has more of an influence on convective development on days with airmass storms than on days with synoptic storms.

## 5.2. Assumptions

The distinction between synoptic and airmass thunderstorms have several interpretations. This project used the scenario as described by Biswas and Jayaweera (1976) where Alaskan thunderstorms are grouped into two general categories; localized air-mass and widespread synoptic. Thus, air-mass

thunderstorms form as isolated storms in confined areas, and result from air-mass interactions with the underlying surface. Synoptic thunderstorms are typically formed by frontal activity. Most days with recorded lightning in Alaska are due to air-mass storms formed in the absence of significant large-scale circulation, but most lightning occurs on the few days with synoptic storms (Biswas and Jayaweera, 1976; Henry, 1978). A study of summer convection over the Mackenzie River basin classified most of the lightning as resulting from airmass thunderstorms (Kochtubajda et al., 2002). Air-mass thunderstorms start most of the lightning-caused fires in Interior Alaska (Henry, 1978).

The most correct and thorough distinction between the two types of thunderstorms would be based on the meteorological conditions as determined by synoptic weather maps. However, this method would be both time-consuming and somewhat subjective. We therefore chose to keep the very conceptually simplistic distinction based on Biswas and Jayaweera's study. When quantitative distinctions had to be applied (i.e. was this a synoptic or an airmass day), we used a somewhat arbitrary threshold at 1000 strikes. In the Mackenzie River study, Kochtubajda et al. (2002) used a threshold of 2000 strikes to distinguish between extreme and moderate lightning events. For an average Alaska thunderstorm season, use of this threshold would have reduced the number of days classified as synoptic from 5-10 per year to 2-3, which does not adequately illustrate the meteorological conditions. If we assume that our threshold of 1000 strikes is an appropriate distinction value, a change to 2000 strikes should not change the synoptic categories mentionably but would likely make some large changes to the airmass category.

Other thresholds or methods of separating the two thunderstorm types could certainly be applied. One possibility would be to base the distinction on the time of day where the thunderstorm / lightning strikes occurred. The most favorable time for airmass thunderstorm development would likely be associated with the diurnal heating cycle and fall in the noon-4pm time frame. Table 5.1 shows that these two approaches would yield rather similar results, using the 2001 lightning data set (Chapter 4 data) as an example.

Table 5.1. Distribution of lightning strikes for days classified as airmass days based on two different distinction methods.

Distinction Method (airmass thunderstorms)	% of total annual lightning (Interior Alaska region)
< 1000 strikes per day (Alaska region)	51.7
noon-4PM (ADT)	45.6

### 5.3. Alaska lightning strike climatology

The Alaskan thunderstorm season goes from May-September with very few exceptions. The hours of most lightning activity are 4-6PM (ADT), and 80% of the total strikes occur between 1PM and 8PM (ADT). Almost 60% of the total annual lightning strikes are recorded in the last half of June or first half of July, typically coinciding with the highest summer temperatures in the Interior (Fairbanks). However, correlations between total annual lightning and Fairbanks mean temperatures (May-August) are low, ranging from less than 0.01 to 0.13, highest for the month of July because most the strikes are associated with synoptic rather than airmass storms. At Mackenzie River, Kochtubajda et al. (2002) found that the days with extreme lightning events occurred on days slightly warmer (+1.9°C) than the more moderate lightning days.

It is difficult to say if the number of total annual lightning strikes has increased in Alaska due to several factors. First, the lightning detection network has been updated, making comparisons difficult. Second, a data set of 17 years is not much to base such predictions on. However, in comparing the seasonal distribution of lightning from 2001 and 2002 with the 1986-99 average, it appears that a higher fraction of lightning strikes are recorded earlier and later in the season in the last few years (figure 5.1).

Most days with recorded lightning are due to airmass thunderstorms (according to our classifications), but a large fraction of the total annual lightning occurs over just a few days. On average the day with the highest number of recorded lightning strikes compose 13 percent of the total annual lightning strikes.

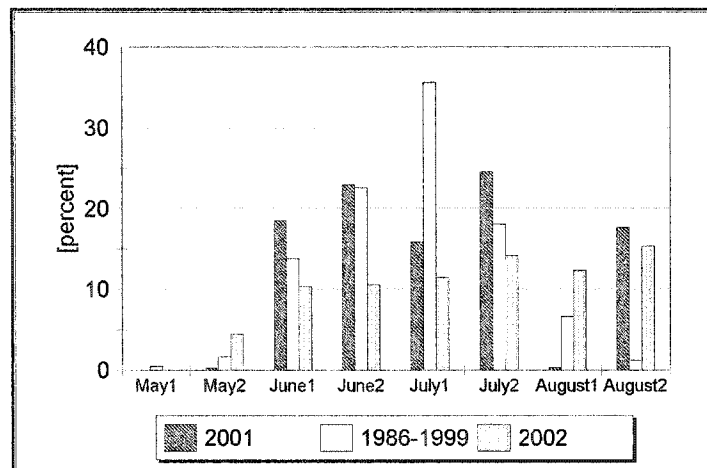


Figure 5.1 Seasonal distribution of lightning strikes in Interior Alaska, two-week periods.

The areas with the most recorded lightning are all located in the eastern to central part of the Interior. Continental Alaska has more lightning than the maritime parts, which have a milder climate with more stable air masses, less surface heating, and warmer air aloft, inhibiting extensive convective activity. Our study found that areas of high lightning strike density were not limited to mountainous regions, but also occurred at river flats such as the Tetlin, Yukon and Tanana Flats. This agrees with findings from northern Saskatchewan (Burrows et al., 2002), but disagrees with Biswas and Jayaweera's (1976) study of Alaskan thunderstorms, where only the Tanana Flats were found to have any significant lightning activity.

#### 5.4. Future under a changing climate

Climate warming is a factor making future predictions of the Alaskan thunderstorm and fire regimes difficult. However, even for present conditions, the links between climate, vegetation and fire are very important for the boreal environment, but still poorly defined (Campbell and Flannigan, 2000). Thus a better understanding of the processes involved is necessary. This study represents a first view of the some of the existing links using the available data.

The objective of this project was to find influential factors and processes responsible for thunderstorm development in Alaska, and, using those, attempt to produce well-founded predictions on future thunderstorm regimes caused by a changing climate. In the following section, we will list the factors we have “identified” as important for thunderstorm and lightning activity in Interior Alaska, and comment on their likely response to climate change.

#### 5.4.1. CAPE

Renno and Ingersoll (1996) predict that the average global CAPE value should be larger in a warmer and moister climate regime and smaller in a colder climate regime than the presently observed value. Ye et al. (1998) suggests that since climate sensitivity of CAPE to surface temperature is only  $\sim 50\text{--}100\text{JKg}^{-1}\text{C}^{-1}$  it is unlikely that climate warming induced changes are significant enough to be detected in the global electric circuit. Lightning occurrence is a very nonlinear function of convection intensity. Solomon and Baker (1994) report a reversibly defined threshold for lightning occurrence of about  $400\text{JKg}^{-1}$  for New Mexico. However, Ye et al. (1998) concludes that it is difficult to state that increased lightning will necessarily accompany global warming. However, if  $100\text{JKg}^{-1}$  of CAPE due to a  $2^\circ\text{C}$  increase in sea surface temperature is added to that of the current climate, then the barrier for the occurrence of lightning can more frequently be overcome to introduce a jump in lightning frequency. In Alaska, CAPE values are lower than for the southern U.S. and tropics (Chapter 4), and the projected temperature changes are higher. This could lead to a significant increase in lightning occurrence.

Biswas (1976) finds in his one season study of Alaska thunderstorms that 34% of thunderstorms were associated with the Arctic front. Thus any changes in the position or behavior of the Arctic front could have a measurable influence on the Interior Alaska thunderstorm activity and preferred locations.

#### 5.4.2. Treeline expansion

Scenarios based on four GCM 2xCO<sub>2</sub>-scenarios suggest a polewards shift of the forested zones, causing boreal forest to move into the current tundra region (Smith et al, 1992). This region would then likely see increasing fire frequency (Kasischke et al, 1995). Of the regions presently covered by boreal forests, only 28% would remain boreal forest, whereas 72% would shift to temperate, mixed deciduous forests, and likely see a decrease in fire frequency.

Brubaker et al.(1995) speculates that deciduous trees or shrubs, rather than evergreens, would expand as a result of future warmer conditions. If post-fire vegetation would regrow as deciduous forests, a cooler, more moist, less flammable summer fire fuel scenario would result. The shift from coniferous to more deciduous forest would thus result in a decrease in fire frequency, because deciduous forest is less flammable than coniferous forest. Conversely, if the warmer summers would also be drier, moisture-stressed, highly flammable trees may be the consequence and therefore an increased fire frequency. It is also possible that an increase in fire frequency, resulting in large wildfires around the northern extent of the boreal forest, could influence the position of the Polar Front (Pielke and Vidale, 1995). A southward movement of the polar front in the summer would bring colder air down, bringing south the 13 °C isotherm which is currently thought to influence (and be influenced by) the northern extent of the boreal forest .

Permafrost is a strong factor in the northern ecosystems. Climatic warming is already resulting in melting of the permafrost layer. Melting of the permafrost takes a large amount of the available energy at tundra ecosystems, leaving less for sensible heat fluxes and surface temperatures. The existence of permafrost thus act as a temporary buffer against rapid increases in surface temperatures and sensible heat fluxes (Eugster et al., 2000). However, the more permafrost that melts, the less this buffer mechanism will be in effect, allowing further temperature increases.

Large fractions of lightning in Interior Alaska at present are due to synoptic events often happening in a few consecutive days. A typical example is summer 1999 where we had a few days with ~ 5000 strikes. Average annual lightning strikes in Interior Alaska is about 25,000. The predicted summer warming,

potentially influencing both the composition and distribution of vegetation types and permafrost, could cause a further increase in surface temperatures due to vegetation feedback mechanisms. This could enhance the Interior Alaska thermal through, which is a strong factor in thunderstorm development and low-level moisture advection (Biswas, 1976), thus increasing the potential for lightning. If more deciduous vegetation was to result from a climatic warming, we might see cooler, more moist summers with a decreased thunderstorm activity, because the deciduous vegetation transpire more, has higher albedo, and smaller sensible heat fluxes than do coniferous vegetation. Conversely, if the redistribution of vegetation or the climatic warming would influence the behavior and average position of the polar front, where more synoptic thunderstorms dominated a generally wetter summer pattern. Such a scenario may bring more lightning strikes to Interior Alaska, although due to their often wet nature fewer fires are likely to result.

#### **5.4.3. Fire severity**

Several studies predict increases in fire frequency in the boreal forest zone as a result of climate warming (Clark, 1988; Chapin et al., 2003). Price and Rind (1994) predict an increase in U.S. lightning fire ignitions by 78%. For Canada, Flannigan and Van Wagner (1991) suggest that the fire seasonal severity rating may increase by 46%. An increase in fire severity within the boreal zone has potential impact on the forest composition, possibility of migration of new species into the region, and for the elusive feedback mechanism between (probably especially severe) wildfire burn scars and convective activity.

Interestingly enough, studies of paleoecology have shown that frequent small fires are correlated with a warm, dry climate, and widespread fires are correlated with a cool, wet climate (Li et al., 2000; Lynch et al., 2003). Thus we cannot simply equate global warming with larger, more widespread fires.

#### **5.4.4. Length of fire season**

Flannigan and Van Wagner (1991) estimated that warmer, drier conditions should result in a 40% increase in annual area burned in Canada. As a possible response to the current climate warming, the annual



area burned in North America has almost doubled over the last two decades (Murphy et al., 2000). The area burned is affected by the length of the fire season, which is also predicted to lengthen. Wotton and Flannigan (1993) estimated that the warmer climate would increase the length of the fire season by 28-29 days and thus result in a 20% increase in annual area burned in the Canadian boreal forest.

The seasonal distribution of lightning strikes in Interior Alaska (figure 5.1) suggests a possible shift towards more lightning in late August than has previously been the case. This could be associated with or cause a longer fire season, depending on the amount of accompanying precipitation and the state of the flammable materials.

### 5.5. Suggestions for future work

- \* Produce a dry thunderstorm climatology for Interior Alaska, similar to the work of Rorig and Ferguson (1999, 2001) in Washington state.
- \* Concentrating on high lightning strike accuracy areas, make correlations with topography, patch sizes (and shapes) and focus on burn scar analysis and treeline proximity study (Chapter 2).
- \* Compare fire starts (ignition) and lightning data (weather data). Anderson (2001) has produced a model for this.
- \* The wildfire burn scar feedback mechanism study would benefit from field measurements of fire severity, wind direction and strength and sensible and latent heat fluxes at the scars.

### 5.6. Literature cited

Anderson, K.R., 1991: Models to Predict Lightning Occurrence and Frequency Over Alberta. M.S. thesis, University of Alberta, 91pp.

Anderson, K.R., 2001: A model to predict lightning-caused fire occurrences. Preprints, Fourth Symposium on Fire and Forest Meteorology. Reno, NV, 13-15. Nov, 2001. American Meteorological Society, 206-212

- Beringer, J., Tapper, N.J., McHugh, I., Chapin, F.S., Lynch, A.H., Serreze, M.C., and Slater, A. 2001. Impact of Arctic treeline on synoptic climate. *Geophysical Research Letters*, **28**, 4247-4250.
- Biswas, A.K. 1976. Climatology of Thunderstorms in Alaska. M.S. thesis, University of Alaska Fairbanks. 75 p.
- Biswas, A.K. and Jayaweera, K.O.L.F. 1976: NOAA-3 Satellite Observations of Thunderstorms in Alaska. *Monthly Weather Review*, **104**, 292-297.
- Blyth, E.M., Dolman, A.J. and Noilhan, J., 1994: The effect of forest on mesoscale rainfall: an example from HAPEX-MOBILHY. *Journal of Applied Meteorology*, **33**, 445-454.
- Brubaker, L.B., Anderson, P.M., and Hu, F.S., 1995: Arctic Tundra Biodiversity: A Temporal Perspective from Late Quaternary Pollen Records. In: Chapin, F.S.III and Körner, C.(Eds): *Arctic and Alpine Biodiversity: Patterns, Causes and Ecosystem Consequences*. Ecological Studies 113, Springer Verlag Berlin Heidelberg.
- Burrows, W.R., King, P.J., Lewis, B., Kochtubajda, B., Snyder, and V. Turcotte, 2002: Lightning occurrence patterns over Canada and adjacent United States from lightning detection network observations. *Atmos.-Ocean*, **40** (10), 59-81.
- Campbell, I.D. and Flannigan, M.D., 2000: Long-term perspectives on fire-climate-vegetation relationships in the North American boreal forest. In: Kasischke, E.S. and Stocks, B.J. (Eds): *Fire, Climate Change, and Carbon Cycling in the Boreal Forest*. Ecological Studies 138, Springer Verlag, New York, 151-172.

Chapin III, F.S., Eugster, W., McFadden, J.P., Lynch, A.H., and Walker, D.A. 2000. Summer Differences among Arctic Ecosystems in Regional Climate Forcing. *Journal of Climate* **13**: 2002–2010.

Chapin, F.S., Rupp, T.S., Starfield, A.M., DeWilde, L., Zavaleta, E.S., Fresco, N., Henkelman, J. and McGuire, A.D., 2003: Planning for resilience: modeling change in human-fire interactions in the Alaska boreal forest. *Frontiers in Ecology and the Environment*, 1 (5), 255-261.

Clark, J.S., 1988: Effect of climate change on fire regimes in northwestern Minnesota. *Nature*, **334**, 233-235.

Eugster W., Rouse W.R., Pielke R.A., McFadden J.P., Baldocchi D.D., Kittel T.G.F., Chapin F.S. III, Liston G.L., Vidale P.L., Vaganov E., and Chambers S.D. 2000. Land-atmosphere energy exchange in Arctic tundra and boreal forest: available data and feedbacks to climate. *Global Change Biology*, **6** (suppl.1), 84-115.

Flannigan, M.D. and Van Wagner, C.E., 1991: Climate change and wildfire in Canada. *Canadian Journal of Forest Research*, **21**, 66-72.

Garrett, A.J., 1982: A parameter study of interactions between convective clouds, the convective boundary layer and a forested surface. *Monthly Weather Review*, **110**, 1041-1059.

Harding, R.J., Gryning, S.-E., Halldin, S. and Lloyd, C.R., 2001: Progress in understanding of land surface-atmosphere exchanges at high latitudes. *Theoretical and Applied Climatology*, **50**, 5-18.

Henry, D.M, 1978: Fire occurrence using 500 mb map correlation. NOAA Technical Memorandum, NWS AR-21, 31 pp.

Kasischke, E.S. Christiansen, N.L.,and Stocks, 1995: Fire, Global Warming, and Carbon Balance of Boreal Forests. *Ecological Applications*, 5 (2), 437-451.

Knowles, J.B., 1993; M.S. Thesis: The influence of forest fire induced albedo differences on the generation of mesoscale circulations. Department of Atmospheric Science, Colorado State University, 86 pp.

Kochtubajda, B., Stewart, R.E., Gyakum, J.R. and Flannigan, M.D., 2002: Summer convection and lightning over the Mackenzie River Basin and their impact during 1994 and 1995. *Atmosphere-Ocean*, 40 (2), 199-220.

Li, C., Flannigan, M.D. and Corns, I.G.W., 2000: Influence of potential climate change on forest landscape dynamics on West-Central Alberta. *Canadian Journal of Forest Research*, 30, 1905-1912.

Lynch, J.A., Clark, J.S., Bigelow, N.H., Edwards, M.E. and Finney, B.P., 2003: Geographic and temporal variation in fire history in boreal ecosystems of Alaska. *Journal of Geophysical Research*, 108 (D1), 8152, doi:10.1029/2001JD000332.

Murphy, P.J., Mudd, J.P., Stocks, B.J., Kasischke, E.S., Barry, D., Alexander, M.E. and French, N.H.F., 2000: Historical fire records in the North American boreal forest. In: Kasischke, E.S. and Stocks, B.J. (Eds): *Fire, Climate Change, and Carbon Cycling in the Boreal Forest*. Ecological Studies 138, Springer Verlag, New York, 274-288.

O'Neal, M. 1996. Interactions between land cover and convective cloud cover over Midwestern North America detected from GOES satellite data. *International Journal of Remote Sensing*, **17**: 1149-1181.

Pielke, R.A., Avissar, R., Raupach, M., Dolman, H., Zeng, X. and Denning, S., 1998: Interactions between the atmosphere and terrestrial ecosystems: Influence on weather and climate. *Global Change Biology*, **4**, 461-475.

Pielke, R.A. and Vidale, P.L. 1995. The Boreal Forest and the Polar Front. *Journal of Geophysical Research*. **100D**: 25,755-25,758.

Price, C. and Rind, 1994: Modeling global lightning distributions in a general circulation model. *Monthly Weather Review*, **22**, 1930-1939.

Renno, N.O. and A.P. Ingersoll, 1996: Natural convection as a heat engine: a theory for CAPE. *Journal of the Atmospheric Sciences*, **53** (4), 572-585.

Rorig, M.L. and Ferguson, S.A., 1999: Characteristics of lightning and wildland fire ignition in the Pacific Northwest. *Journal of Applied Meteorology*, **38**, 1565-1575.

Rorig, M.L. and Ferguson, S.A., 2002: The 2000 fire season: lightning-caused fires. *Journal of Applied Meteorology*, **41**, 786-791.

Serreze, M.C., Lynch, A.H., and Clark, M.P. 2001. The Arctic Frontal Zone as seen in the NCEP-NCAR Reanalysis. *Journal of Climate*, **14**: 1550-1567.

Shuttleworth WJ (1988) Macrohydrology: the new challenge for process hydrology. *Journal of Hydrology* **100**, 31-56.

Smith, T.M., Leemans, R., and Shugart, H.H., 1992: Sensitivity of terrestrial carbon storage to CO<sub>2</sub>-induced climate change: comparison of four scenarios based on general circulation models. *Climatic Change*, **21**, 367-384.

Solomon, R. and Baker, M., 1994: Electrification of New Mexico thunderstorms. *Monthly Weather Review*, **122**, 1878-1886.

Wilmking, M., 2003: The Treeline Ecotone in Interior Alaska - From theory to application and the ecology in between. Dissertation, University of Alaska Fairbanks.

Wotton, B.M. and Flannigan, M.D., 1993: Length of the fire season in a changing climate. *Forest Chronicles*, **69**, 187-192.

Ye, B., Del Genio, A.D. and Lo, K.K-W., 1998: CAPE variations in the current climate and in a climate change. *Journal of Climate*, **11**, 1997-2015.